Université d'Ottawa · University of Ottawa

Université d'Ottawa · University of Ottawa

FACULTÉ DES ÉTUDES SUPÉRIEURES ET POSTDOCTORALES

FACULTY OF GRADUATE AND POSTDOCTORAL STUDIES

Marc LAPLANTE

AUTEUR DE LA THÈSE - AUTHOR OF THESIS

M. A. Sc. (Chemical Engineering)

GRADE - DEGREE

Department of Chemical Engineering

FACULTÉ, ÉCOLE, DÉPARTEMENT - FACULTY, SCHOOL, DEPARTMENT

TITRE DE LA THÈSE - TITLE OF THE THESIS

A Java™-Based Model for Multi-Component Free-Radical Bulk and Solution Polymerizations

M.A. Dubé

DIRECTEUR DE LA THÈSE - THESIS SUPERVISOR

D. Taylor

CO-DIRECTEUR DE LA THÈSE - THESIS CO-SUPERVISOR

EXAMINATEURS DE LA THÈSE - THESIS EXAMINERS

C. Lan

H. Zezel

J.-M. De Koninck, Ph.D.

LE DOYEN DE LA FACULTÉ DES ÉTUDES SUPÉRIEURES ET POSTDOCTORALES

DEAN OF THE FACULTY OF GRADUATE AND POSTDOCTORAL STUDIES

A Java™-Based Model for Multi-Component Free-Radical Bulk and Solution Polymerizations

by
Marc Laplante

A thesis submitted to the Faculty of Graduate and Post-Doctoral Studies in partial fulfillment of the requirements for the degree of

Master of Applied Science
Chemical Engineering

Department of Chemical Engineering
University of Ottawa

© Marc Laplante 2004

Library and Archives Canada

Published Heritage Branch

395 Wellington Street
Ottawa ON K1A 0N4
Canada

Bibliothèque et Archives Canada

Direction du Patrimoine de l'édition

395, rue Wellington
Ottawa ON K1A 0N4
Canada

Your file Votre référence
ISBN: 0-494-01521-7
Our file Notre référence
ISBN: 0-494-01521-7

NOTICE:
The author has granted a non-exclusive license allowing Library and Archives Canada to reproduce, publish, archive, preserve, conserve, communicate to the public by telecommunication or on the Internet, loan, distribute and sell theses worldwide, for commercial or non-commercial purposes, in microform, paper, electronic and/or any other formats.

The author retains copyright ownership and moral rights in this thesis. Neither the thesis nor substantial extracts from it may be printed or otherwise reproduced without the author's permission.

AVIS:
L'auteur a accordé une licence non exclusive permettant à la Bibliothèque et Archives Canada de reproduire, publier, archiver, sauvegarder, conserver, transmettre au public par télécommunication ou par l'Internet, prêter, distribuer et vendre des thèses partout dans le monde, à des fins commerciales ou autres, sur support microforme, papier, électronique et/ou autres formats.

L'auteur conserve la propriété du droit d'auteur et des droits moraux qui protège cette thèse. Ni la thèse ni des extraits substantiels de celle-ci ne doivent être imprimés ou autrement reproduits sans son autorisation.

In compliance with the Canadian Privacy Act some supporting forms may have been removed from this thesis.

While these forms may be included in the document page count, their removal does not represent any loss of content from the thesis.

Conformément à la loi canadienne sur la protection de la vie privée, quelques formulaires secondaires ont été enlevés de cette thèse.

Bien que ces formulaires aient inclus dans la pagination, il n'y aura aucun contenu manquant.

Canada

Statement of Contributions of Collaborators

I hereby declare that I am the sole author of this thesis. My supervisor, Dr. Marc A. Dubé, provided editorial comments to my written work, as well as guidance throughout the duration of the project.

I am also the sole software developer for the Java™-based simulator, with the exception of the Bulirsch-Stoer ODE solver, which was adapted from the code generated for Chris Badeen's M.A.Sc. thesis. Values for the simulator database were taken with consent from the University of Waterloo's WATPOLY database, some of which were modified over the years within the "Polymer Group" in the Department of Chemical Engineering at the University of Ottawa.

I have conducted no experimental work for the purposes of this thesis, only simulation and interpretation of readily available data. The people who collected the experimental data are credited appropriately in each chapter's acknowledgement section, and are listed here: Renata Jovanovic, Hong Hua, Jean-Philippe St-Pierre, Melissa Dorval and Cathy Goubko.

Marc Laplante	25 November 2004
Signature	**Date**

Abstract

Modelling and simulation play an essential role in developing, optimizing and understanding the steps involved in the production of polymers. A simulator was designed in order to model free-radical bulk and solution homopolymerizations, as well as multi-component polymerizations. Several optional models were incorporated in to the simulator, such as several glass transition temperature models, and the penultimate model. Java™ was selected as the programming language because of its object-oriented nature, providing high flexibility and ensuring easy extension of the code. Once the simulator was validated against experimental data and another simulator, it was used to model three systems: butyl acrylate/vinyl acetate (BA/VAc), styrene/butyl acrylate (Sty/BA), and butyl acrylate/methyl methacrylate/vinyl acetate (BA/MMA/VAc).

The solvent effect of toluene on the BA and VAc homopolymerizations and copolymerizations was investigated, by varying the lumped kinetic constant, $k_p/k_t^{0.5}$. Data were collected at different solvent concentrations, as well as a variety of BA:VAc ratios in the case of the BA/VAc copolymer. The lumped kinetic constant decreased with an increase in toluene concentration, resulting in significant improvements in predicting conversion data, which proves the solvent affects the termination reaction. In addition, preliminary results suggest the presence of slight solvent effects on monomer reactivity ratios. There appears to be a solvent effect on both the propagation and termination reactions, but further targeted runs need to be performed before a definite claim can be made.

Sty and BA homopolymerizations and copolymerizations were carried out in toluene as solvent. Copolymer data were collected at two different solvent concentrations, and four Sty:BA ratios were run for each of those two sets. Conversion and cumulative copolymer composition are well predicted by the simulator. Although cumulative weight-average molecular weight data of the same magnitude as the model, more accurate estimates of the transfer parameters would provide better fits to the data. The change in amount of solvent did not significantly affect the conversion or the cumulative copolymer composition data, but the cumulative weight-average molecular

weight was noticeably greater at lower toluene concentrations. The glass transition temperature model study proved to be inconclusive due to excessive amounts of solvent present in the reaction medium. Diffusion control only took place in two of the runs, and occurred toward the end of the polymerization.

The terpolymerization of BA/MMA/VAc was examined, as well as the copolymerization of MMA/VAc. The terpolymerizations behaved similarly to the MMA/VAc copolymerization, i.e. a double rate phenomenon was observed. In the early stages of the reaction, there was practically a solution copolymerization of BA and MMA monomers, with the vinyl acetate acting as the solvent. Once the acrylic monomers were virtually depleted, the remaining vinyl acetate polymerized and exhibited its own auto-acceleration. The homopolymer database, as well as the copolymerization reactivity ratios, provided good model predictions. The simulator showed good agreement with the experimental data at low conversions, but it halted once the auto-acceleration began. The ODE solver was unable to cope with the excessive stiffness of the system.

Résumé

La modélisation et la simulation jouent un rôle important dans le développement, l'optimisation et la compréhension des étapes impliquées dans la production de polymères. Un simulateur a été conçu afin de modéliser des homopolymérisations à radicaux libres en « bulk » et en solution, ainsi que des polymérisations à composantes multiples. Plusieurs modèles optionnels ont été incorporés dans le simulateur, tels que quelques modèles pour la température de transition de verre et le modèle pénultième. Le langage de programmation Java™ a été choisi puisqu'il est polyvalent et il permet une extension facile du programme. Un fois que le simulateur fut validé à l'aide de données expérimentales ainsi qu'un autre simulateur, il a été utilisé afin de modéliser trois systèmes : acrylate de butyle/acétate de vinyle (BA/VAc), styrène/acrylate de butyle (Sty/BA), en plus de acrylate de butyle/méthacrylate de méthyle/acétate de vinyle (BA/MMA/VAc).

L'effet de solvant du toluène sur les homopolymérisations et les copolymérisations de BA et de VAc fut investigué en variant la constante cinétique, $k_p/k_t^{0.5}$. Des données ont été rassemblées à différentes concentrations de solvant, ainsi qu'à des ratios de BA:VAc variés dans le cas du copolymère BA/VAc. La constant cinétique a diminué suite à un augmentation de la concentration de toluène, résultant en une amélioration importante pour la prédiction de la conversion, ce qui prouve que le solvant affecte la réaction de terminaison. De plus, des résultats préliminaires suggèrent la présence d'effets de solvant légers sur les ratios de réactivité des monomères. Il semble que le solvant affecte à la fois les réactions de propagation et de terminaison, mais d'autres expériences stratégiquement conçues seront nécessaires avant que ceci soit affirmé avec certitude.

Des homopolymérisations et des copolymérisations en solution de Sty et de BA ont été effectuées dans du toluène. Dans le cas du copolymère, des données ont été rassemblées à deux différentes concentrations de solvant, et quatre ratios de Sty:BA ont été effectués pour chacun d'eux. Le simulateur a bien prédit les conversions et les compositions de copolymère cumulatives. Les valeurs de masse moléculaire cumulatives

obtenues à l'aide du modèle étaient du même ordre que les données expérimentales; par contre, des valeurs plus précises pour les paramètres de transfert permettraient de meilleures prédictions de modèle. Le changement de la quantité de solvant n'a pas affecté de façon significative les conversions ni les compositions de copolymère cumulatives, mais les masses moléculaires cumulatives étaient supérieures aux concentrations de toluène plus basses. L'étude des modèles de température de transition de verre fut peu concluante due aux quantités excessives de solvant présent dans le mélange de réaction. Le contrôle à diffusion a seulement eu lieu dans deux cas, et ceci vers la fin de la polymérisation.

La terpolymérisation de BA/MMA/VAc a été examinée, ainsi copolymérisation de MMA/VAc. Les terpolymérisations se sont comportées de façon semblables à la copolymérisation de MMA/VAc, i.e. un phénomène de taux double fut observé. Au début de la réaction, c'était à toute fin pratique une copolymérisation en solution de BA et de MMA, le VAc agissant comme solvant. Une fois que les monomères acryliques furent pratiquement épuisés, le VAc restant s'est polymérisé et a démontré sa propre auto-accélération. La base de données d'homopolymérisation, ainsi que les ratios de réactivité de copolymérisation, ont produit de bonnes prédictions de modèle. Le simulateur a démontré un bon accord avec les données expérimentales à de basses conversions, mais le début de l'auto-accélération a immobilisé la simulation. Le solutionneur d'équations différentielles était incapable de supporter la rigidité numérique excessive du système.

Quotes

It was the best of times, it was the worst of times, it was the age of wisdom, it was the age of foolishness, it was the epoch of belief, it was the epoch of incredulity, it was the season of Light, it was the season of Darkness, it was the spring of hope, it was the winter of despair, we had everything before us, we had nothing before us [...]

Charles Dickens, *A Tale of Two Cities*

All that hard work will soon pay off.

Fortune Cookie

Acknowledgements

I must admit I didn't fully comprehend or appreciate what I was getting myself into when I first decided to pursue a Master's degree. It proved to be the most difficult and trying times of my life. But the last few years have also been my most challenging and rewarding experience to date. I would like to acknowledge the help of many people, without whom I never would have achieved this endeavour.

First and foremost, I would like to extend my deepest gratitude to my supervisor, Dr. Marc A. Dubé. He conceived this project, and without him, it never would have come to fruition. His organization and structure via weekly meetings and periodic "big picture" reassessments were key in maintaining a steady rhythm. I also appreciated his patience and understanding during the first three quarters of the thesis, when I was building the sizeable simulator from the ground up. Perhaps most importantly, Dr. Dubé taught me to value the three kinds of people involved in the simulation of experimental data: the ones who collect the experimental data, the ones who build the simulator, and the ones who model the data by running simulations... none of which truly appreciate the work performed by the other two!

With that thought in mind, I would like to express gratitude to Renata, Hong, Jean-Philippe, Melissa and Cathy for having acquired a variety of experimental data over the years. Without their countless hours in the lab, there would be no data, and hence no thesis.

I would also like to thank my co-supervisor, Dr. David G. Taylor for his input and his financial support.

I gratefully acknowledge the financial support provided by the Ontario Graduate Scholarship in Science and Technology (OGSST), made possible by donations from Mr. David McLimont.

I would like to thank my parents for their unconditional love, support and pride, not only throughout my graduate years, but all my life. I have truly been blessed. Also, I have had the good fortune of having two younger (although all grown up now!) sisters, who have both in their own unique ways been instrumental in this achievement. It will never be forgotten.

I am also very appreciative of my friends who have been extremely supportive and patient throughout this journey. Their encouragement and loyalty made the difficult times easier to bear, and they were often the first people I turned to share my successes. More specifically, I would like to thank Eric for his patience and understanding; Dino, for his unyielding support, and his insights into the human psyche, which helped me recognize the often overlooked human element involved in projects of this magnitude; Yves, well, let's just say we are kindred spirits; Joanne, despite the miles (not km... she moved to the U.S.) that separate us, she remains a true friend; Michel, my longest friend, who I had the honour of being his Best Man during this journey; Mike, who started off as my roommate at the onset of my thesis, but grew to be a kind, considerate friend; Hayley and Salvador, who started out as officemates, but ended up as good friends, and often seemed to be the only ones who could truly appreciate this journey; and all of the graduate students and staff in the department of chemical engineering, who were welcoming and made it worthwhile and rewarding to organize social events.

And last but certainly not least, endless thanks go out to Mitchell, who appeared in the last leg of this journey. Initially a welcome distraction, he quickly became my biggest supporter and helped me to regain my motivation. This thesis would never have been completed without him. He gave me a sense of purpose, and a reason to smile, and for that, I will be forever in his debt.

Table of Contents

List of Figures

List of Tables

Nomenclature

$[X]$	total concentration of component (X) in the particles [mol L^{-1}]
a	root-mean-square end-to-end distance per square root of the number of monomer units [dm]
A	adjustable free volume theory parameter [L]
A_i	parameter for temperature-dependent density for component i [g L^{-1}]
A_{jacket}	jacket heat transfer area [m^2]
B_i	parameter for temperature-dependent density for component i [g L^{-1} °C^{-1}]
B_j	free volume theory parameter for diffusion-controlled propagation [L]
c	mass concentration of accumulated polymer in reaction mixture [g L^{-1}]
$C_{p,i}$	specific heat capacity of component i [cal g^{-1} K^{-1}]
$\Delta C_{p,i}$	difference in specific heat capacity for component i above and below its glass transition temperature [cal g^{-1} K^{-1}]
C_i	exponential parameter for initiator efficiency i [L]
D	reaction-diffusion control coefficient [—]
$dcpFactor_j$	diffusion-controlled propagation factor associated with monomer j [—]
$eff_{0,i}$	initial efficiency factor for initiator i [—]
eff_i	efficiency factor for initiator i [—]
$f_{X,i}$	mole fraction of component (X) i in reaction mixture [—]
F_i	molar flow rate of component i [mol min^{-1}]
$F_{inst,i}$	instantaneous copolymer composition (mole fraction of monomer i bound in the polymer) [—]
$F_{cumul,i}$	cumulative copolymer composition (mole fraction of monomer i bound in the copolymer) [—]
$\Delta H_{p,i}$	heat of polymerization of monomer i [cal mol^{-1}]
j_c	entanglement spacing of pure polymer [—]
$k_{d,i}$	decomposition rate constant of initiator i [min^{-1}]
$k_{f,X}$	overall rate constant for transfer to component (X) [L mol^{-1} min^{-1}]
$k_{f,X,j}$	rate constant for transfer to component (X) j, weighted with monomer mole fractions [L mol^{-1} min^{-1}]
$k_{f,X,ij}$	rate constant for transfer from radical ending in monomer i to component (X) j [L mol^{-1} min^{-1}]

k_{MSI}	overall rate constant for reaction between radical and monomer soluble impurity [L mol^{-1} min^{-1}]
$k_{MSI,j}$	rate constant for reaction between radicals and monomer soluble impurity j [L mol^{-1} min^{-1}]
$k_{MSI,ij}$	rate constant for reaction between radical ending in repeat unit i and monomer soluble impurity j [L mol^{-1} min^{-1}]
$k_{p,ij}$	propagation rate constant for radical ending in repeat unit i, adding monomer j, accounting for diffusion-controlled propagation [L mol^{-1} min^{-1}]
$k_{p,0,ij}$	chemically-controlled propagation rate constant for radical ending in repeat unit i, adding monomer j [L mol^{-1} min^{-1}]
$k_{p,overall}$	overall pseudo-kinetic propagation rate constant [L mol^{-1} min^{-1}]
k_{pidb}	overall pseudo-kinetic rate constant for reaction with internal double bonds [L mol^{-1} min^{-1}]
$k_{pidb,ij}$	rate constant for reaction with internal double bonds (transfer from radical ending in monomer j to repeat unit i) [L mol^{-1} min^{-1}]
k_{ptdb}	overall pseudo-kinetic rate constant for reaction with terminal double bonds [L mol^{-1} min^{-1}]
$k_{ptdb,ij}$	rate constant for reaction with terminal double bonds (transfer from radical ending in monomer j to repeat unit i) [L mol^{-1} min^{-1}]
k_t	overall termination rate constant [L mol^{-1} min^{-1}]
$k_{t,0,ij}$	rate constant for termination between radicals ending in components i and j, at zero polymer concentration [L mol^{-1} min^{-1}]
$k_{t,0,overall}$	overall pseudo-kinetic termination rate constant at zero polymer concentration [L mol^{-1} min^{-1}]
$k_{t,comb}$	rate constant for termination by combination [L mol^{-1} min^{-1}]
$k_{t,crit}$	critical termination rate constant [L mol^{-1} min^{-1}]
$k_{t,disp}$	rate constant for termination by disproportionation [L mol^{-1} min^{-1}]
$k_{t,rd}$	reaction diffusion-controlled termination rate constant [L mol^{-1} min^{-1}]
$k_{t,seg}$	segmental diffusion-controlled termination rate constant [L mol^{-1} min^{-1}]
$k_{t,tr}$	translational diffusion-controlled termination rate constant [L mol^{-1} min^{-1}]
$k_{t,residual}$	"residual" reaction-diffusion control termination constant [L mol^{-1} min^{-1}]
K_3	free volume theory parameter [(g mol^{-1})^m]
K_3^*	flag for onset of translational diffusion-controlled termination [(g mol^{-1})^m]
l_0	length of a monomer unit [dm]
m	adjustable free volume theory parameter [—]

m	adjustable free volume theory parameter [—]
$\overline{M}_n$	cumulative number-average molecular weight [g mol^{-1}]
$\overline{M}_w$	cumulative weight-average molecular weight [g mol^{-1}]
$\overline{M}_{w,crit}$	critical weight-average molecular weight [g mol^{-1}]
$M_{w,eff}$	effective molecular weight of copolymer [g mol^{-1}]
MW_i	molecular weight of component i [g mol^{-1}]
n	adjustable free volume theory parameter [—]
n_i	number of components of type i [—]
$n_{M\ in\ P}$	number of monomer units per polymer chain segment [—]
n_{TOT}	total number of components [—]
N_{Av}	Avogadro's number [molecule mol^{-1}]
N_i	moles of component i [mol]
P_{ij}	probability of sequence ij occurring in the copolymer [—]
Q_0, Q_1, Q_2	zeroeth, first, second moments of the molecular weight distribution [mol L^{-1}]
Q_{jac}	heat loss from the cooling jacket [cal min^{-1}]
Q_R	heat loss from the reactor [cal min^{-1}]
r_{ij}	reactivity ratio for monomer j adding to radical ending in repeat unit i [L mol^{-1} min^{-1}]
R_I	overall rate of initiation [mol L^{-1} min^{-1}]
$R_{I,i}$	rate of initiation of initiator i [mol L^{-1} min^{-1}]
$R_{p,i}$	rate of polymerization of monomer i [mol L^{-1} min^{-1}]
t	time [min]
T	temperature [K]
T_{ref}	reference temperature [K]
T_g	glass transition temperature of the copolymer [K]
$T_{g,AB}$	glass transition temperature of the alternating copolymer [K]
$T_{g,i}$	glass transition temperature of component i [K]
U	overall heat transfer coefficient [cal min^{-1} K^{-1} m^{-2}]
V_i	volume of component i [L]
V_F	free volume [L]
$V_{F,0,i}$	base value for free volume for component i [L]
$V_{F,crit,t}$	critical free volume of translational diffusion-control [L]

$V_{F,crit,f,i}$	critical free volume for efficiency of initiator i [L]
$V_{F,crit,p,j}$	critical free volume for propagation of monomer j [L]
$\dot{V}_{in}$	inlet volumetric flow rate [L min^{-1}]
V_m	molar volume [L mol^{-1}]
$\dot{V}_{out}$	outlet volumetric flow rate [L min^{-1}]
V_T	total volume of reaction mixture [L]
W_i	weight fraction of monomer i in copolymer [—]
x	overall mass conversion of monomer [mass fraction]
Y_o	total concentration of free radicals [mol L^{-1}]

Greek Letters

α_i	difference in thermal expansion coefficients for component i above and below its glass transition temperature [L K^{-1}]
γ	fraction of termination by disproportionation [—]
δ	segmental diffusion parameter [L g^{-1}]
δ_{rr}	reaction radius [dm]
θ_{ij}	cross-termination factor for termination between radicals ending in components i and j [—]
ρ_i	density of component i [g L^{-1}]
σ	Lennard-Jones diameter [dm]
ϕ_i	mole fraction of radicals ending in monomer i [—]
ψ_i	intermediate variable used to calculate ϕ_i [L mol^{-1} min^{-1}]

Subscripts

in	inlet, entering the reactor
jacket	cooling jacket around the reactor
min	minimum value, lower limit
max	maximum value, upper limit
out	outlet, exiting the reactor

Abbreviations and Acronyms

AIBN	2,2'-azobisisobutyronitrile
BA	butyl acrylate
BPO	benzoyl peroxide
CTA	chain transfer agent
I	initiator
M	monomer
MMA	methyl methacrylate
MSI	monomer soluble impurity
P	polymer, or monomer bound in the copolymer
S	solvent
Sty	styrene
THF	tetrahydrofuran
VAc	vinyl acetate

Chapter 1: Introduction

Polymers are macromolecules constructed using much smaller molecules, repeating within the chain, known as monomers. In free-radical polymerizations, monomers are rapidly added one by one until the chain terminates. Although these polymerizations require only one monomer to produce a polymer (known as a homopolymer), they can be carried out with mixtures of more than one monomer to form products with several different structures in the polymer chain. This latter type of process is called multi-component polymerization. The amount of each monomer within the copolymer depends on their relative concentrations and reactivities. Multi-component polymerization reactions are useful for studying the effects of chemical structure on reactivity, and, from a technological viewpoint, greatly increase the ability of the polymer scientist to customize a polymer product to exhibit desired properties.

Polymers take many forms (e.g. plastics, synthetic textiles, rubbers) and numerous applications have evolved from cheap substitutes for metal and other materials into a material of choice for many applications, for example packaging, building materials, automobile and electrical components, paints and adhesives. Their adaptable properties and ability to be moulded to almost any shape further increase their suitability to a wide range of applications.

Modelling and simulation play an important role in developing these processes. They are key for conducting research or for designing polymerization reactors — batch, semi-batch or continuous — for commercial applications. Mathematical modelling of polymerizations provides many benefits. Gao and Penlidis[1] discuss the numerous benefits of modelling; a summary is provided here.

1. Models help to direct further research by expanding the process understanding.
2. Models are useful for process design, parameter estimation, sensitivity analysis, and process simulation.
3. Models can be used for process optimization and process control.
4. Models are useful for safety purposes, to anticipate worst-case scenarios.
5. Interactive models (simulators) can be used to educate and train personnel.

1.1 Justification and Objectives

Several objectives were established at the onset of this work. First, a simulator was to be created, making use of an existing mechanistic model for free-radical polymerization. The complexity of the model, combined with the anticipation of future work, required that the following features be integrated into the simulator.

1. The simulator must be capable of modelling bulk and solution homopolymerization as well as multi-component reactions.
2. An object-oriented language (Java™ was used) should be used to provide high flexibility and to ensure easy extension.
3. The addition of several optional models (e.g. glass transition temperature models, penultimate model) would allow the testing of various systems.

Subsequently, the simulator had to be validated against experimental data and other simulators. Once complete, the simulator had to be used for three systems: butyl acrylate/vinyl acetate, styrene/butyl acrylate, and butyl acrylate/methyl methacrylate/vinyl acetate.

1.2 Thesis Structure

Chapter 2 provides a brief yet complete overview of the complex polymerization model, which is the foundation of this thesis. The equations used are enumerated, along with some theoretical background. The simulator design is also described, including an analysis of programming languages and the use of Java™, and a review of ordinary differential equation solvers.

In Chapter 3, the validity of the simulator is substantiated with comparisons to experimental data.

Chapters 4-5 consist of two independent papers, which will be submitted for publication in different journals. Chapter 4 studies the effects of solvent and chain-transfer agent on the butyl acrylate and vinyl acetate homopolymers as well their copolymers. Chapter 5 investigates the styrene/butyl acrylate system and the use of glass transition temperature models.

In Chapter 6, the simulator is shown to be able to model the butyl acrylate/methyl methacrylate/vinyl acetate terpolymer.

Finally, Chapter 7 provides a general discussion of the results from the papers. Conclusions drawn, as well as direction for future work, are also listed.

References

1. Gao, J.; Penlidis, A. *J. Macromol. Sci. – Rev. Macromol. Chem. Phys.*, **36**(2), 199 (1996).

Chapter 2: Literature Review and Model Development

2.1 Polymerization kinetics

The model presented in this section includes a set of differential and algebraic equations that describe the underlying physical and chemical phenomena of free-radical polymerizations. One of the simplest and most widely used models is the *terminal* (or *Mayo-Lewis*) model, which assumes that the reactivity of the polymer radical chains is a function of its terminal unit and the type of monomer to be added. The equations developed in this section are based on the terminal model. In section 2.3, alternative models are enumerated and discussed briefly. In section 2.3.1, one of these models, the *penultimate* model, is examined in more detail.

2.1.1 Introduction

For the purposes of this thesis, only bulk and solution polymerizations will be presented. *Bulk polymerization* is often favoured over other methods due to its simplicity and minimal product contamination. However, a keen understanding of the physics and kinetics is required to manage the extremely exothermic reaction, as well as the highly viscous medium, both of which rendering temperature control challenging. *Solution polymerization* circumvents the important drawbacks of bulk polymerization because the solvent improves heat transfer and reduces the viscosity of the reaction medium, which facilitates stirring. However, a solvent must be carefully selected to prevent interactions with the growing polymer chain. In addition, polymer purity may be compromised if the solvent removal proves to be difficult. For details on extending the model to encompass emulsion polymerizations, the reader is referred to [2,3].

The model equations were developed for a *multi-component* system, but the model collapses to a homopolymerization when only one monomer is present in the system. For multi-component systems, the pseudo-kinetic rate constant method was used, which allows a weighted average of kinetic rate constants. The validity of this approach has been examined and demonstrated by Tobita and Hamielec,[4] and Xie and Hamielec.[5,6]

Most of the experimental work conducted for the purposes of research is performed in *batch* and *semi-batch* modes; however, in the interests of flexibility and

broadness, the model is presented in *continuous* mode. The inflow and/or outflow terms are simply set to zero when the reactor is operated in batch or semi-batch mode.

Six different types of ingredients are considered in the model. *Monomers* (M) are the foundation of polymerizations, and *polymers* (P) are their end-result. In free-radical polymerizations, an *initiator* (I) is required to start the process. A s*olvent* (S) can be used to improve the physical properties of the reaction medium, resulting in a solution polymerization. A c*hain-transfer agent* (CTA) allows control of the average molecular weight of the resulting polymer. Finally, *monomer-soluble impurities* (MSI), which may or may not be intentionally present in the system, slow down and/or delay the polymerization process. The impact of solvent addition is addressed in section 2.1.2, and CTAs and MSIs are discussed briefly in section 2.1.6.

For a free-radical polymerization to take place, three reactions must occur: initiation, propagation and termination. Depending on the system, other reactions may arise, such as transfer reactions, branching reactions, and reactions with impurities. However, before discussing the various reactions associated with a polymerization, some physical phenomena related to the process are addressed.

2.1.2 Physical Considerations

During the course of a polymerization, the physical properties of the reaction medium evolve, which can have a significant impact on the kinetic parameters of the reaction, as well as the heat transfer parameters. Therefore, when modelling polymerization reactions, one must take into consideration both the chemical reactions occurring as well as the impact of physical changes on these parameters.

A physical phenomenon having a considerable effect in polymerizations is *diffusion control*. As the polymer chains increase in length, the free volume between the chains, V_F, decreases. As a result, the viscosity increases and the various ingredients have more difficulty moving within the reaction mixture. Once V_F decreases below a certain critical free volume, diffusion control is said to occur. An *auto-acceleration*, also known as the Trommsdorff or *gel effect*[7,8], occurs when the free volume hinders the chains' ability to terminate due to diffusional limitations, which increases the overall rate of

polymerization. Various types of diffusion control can arise; these are addressed in more detail in sections 2.1.3-2.1.5.

The free volume of the reaction mixture can be calculated as follows:

$$V_F = \sum_{i=1}^{n_M+n_P+n_S} \left[\left(V_{F0,i} + \alpha_i \left(T - T_{g,i} \right) \right) \frac{V_i}{V_T} \right] \tag{2.1}$$

where n_M, n_P and n_S are the number of monomers, polymers and solvents present in the system, respectively. In equation (2.1), $n_P = 1$ even when $n_M > 1$, since a model is used to obtain a weighted average for the copolymer glass transition temperature, $T_{g,P}$. Details for T_g are included in section 2.2. The contribution of component i is only present when $T > T_{g,i}$. $V_{F0,i}$ is the base value for the free volume for component i, α_i is the difference in thermal expansion coefficients for component i above and below its glass transition temperature, $T_{g,i}$ is the glass transition temperature of component i, and V_i is the volume occupied by component i. The latter is simply obtained from the individual components' physical properties

$$V_i = \frac{N_i MW_i}{\rho_i} \tag{2.2}$$

where N_i is the number of moles of component i, MW_i is its molecular weight, and ρ_i is its density. The density varies with temperature according to the following relation

$$\rho_i = A_i - B_i T \tag{2.3}$$

where A_i and B_i are constants that depend on component i, and T is the temperature (°C).

The term "rate constant" is somewhat of a misnomer since it varies with temperature. As is common practice, this terminology will be adopted throughout the text, signalling when a "constant" is temperature-dependent. Unless otherwise stated, the expression "temperature-dependent" refers to a parameter (rate constant or otherwise), which has a temperature dependency that follows an Arrhenius-type relationship.

Addition of solvent can have an effect on the reaction medium as well as the kinetics. Aside from the obvious decrease in monomer concentration, the solvent also decreases the viscosity of the medium and lessens the gel effect by increasing the free

volume. The solvent effect on the propagation (section 2.1.4) and termination (section 2.1.5) rate constants, has been discussed considerably in the literature[9]. Ongoing research is conducted to elucidate the exact nature of the solvent effect on both reactions. Chain transfer reactions, examined in section 2.1.6, can also be affected by the presence of a solvent.

2.1.3 *Initiation*

To instigate a free-radical polymerization reaction, a highly reactive species is required. Initiator molecules, I_2, decompose to form extremely reactive free radicals. A variety of thermal, photochemical and redox techniques are available to initiate this decomposition[10,11]. The initiator radical requires an electron to become stable. An electron from the double-bond in a molecule, e.g. a vinyl monomer, can easily be captured by the initiator radical. This electron pair forms a new chemical bond between the initiator radical and one of the double-bond carbons. The double bond is therefore reduced to a single bond, and the second electron from the double bond associates itself with the other vinyl carbon, forming a monomer radical.

Initiation involves a two-step reaction. First, the initiator decomposition occurs, as shown by reaction (2.4). Then in reaction (2.5), the initiator radicals, $R_{IN}^{\bullet}$, react quickly with monomer molecules, M, to produce *primary radicals*, $R_1^{\bullet}$.

$$I_2 \longrightarrow 2R_{IN}^{\bullet} \tag{2.4}$$

$$R_{IN}^{\bullet} + M \longrightarrow R_1^{\bullet} \tag{2.5}$$

The rate of initiation for initiator i is given by the expression

$$R_{I,i} = 2\,eff_i\,k_{d,i}\left(\frac{N_{I,i}}{V_T}\right) \tag{2.6}$$

where $k_{d,i}$ is the initiator decomposition rate constant, $N_{I,i}$ is the number of moles of initiator i, and V_T is the total volume of the reaction mixture. The initiator efficiency, eff_i, is defined as the fraction of radicals obtained through decomposition that produce a primary radical. Usually $eff_i \leq 1$ to account for *wastage reactions* and *induced*

decomposition of initiator. Wastage reactions refer to initiator radicals reacting to form neutral molecules, while induced decomposition refers to propagating radicals attacking an initiator before it decomposes. Although the latter does not reduce the number of radicals in the system, an initiator molecule has been decomposed without a corresponding increase of two radicals, which does in effect reduce the initiator efficiency. However, wastage reactions are usually considered exclusively when reporting literature values of eff_i[12]. The quantitative effects of induced decomposition are handled later, in section 2.1.6.

Initiation diffusion-control reduces the initiator efficiency as conversion increases. The following semi-empirical equation has been used to describe the changing initiator efficiency when V_F becomes less than the critical free volume for initiator efficiency, $V_{F,crit,f,i}$.

$$eff_i = eff_{0,i} \exp\left(-C_i\left(\frac{1}{V_F} - \frac{1}{V_{F,crit,f,i}}\right)\right) \tag{2.7}$$

where $eff_{0,i}$ is the initial initiator efficiency for initiator i, and C_i is the free volume theory exponential parameter for diffusion-controlled initiation.

In equations (2.6) and (2.7), C_i is a constant, while $k_{d,i}$, $eff_{0,i}$ and $V_{F,crit,f,i}$ are temperature-dependent parameters. All four parameters depend on both the initiator and the monomer(s) used in the system. If more than one monomer is present, these values are weighted over the various monomers using their respective mole fractions in the mixture at time t. For example, for C_i,

$$C_i = \sum_{j=1}^{n_M} C_{ij} f_{M,j} \tag{2.8}$$

where $f_{M,j}$ is the mole fraction of monomer j.

2.1.4 Propagation

Following initiation, monomers are added to the primary radicals in rapid succession. The reaction in which the radical of chain length r, $R_r^\bullet$, grows by the addition of monomer is known as the propagation reaction.

$$R_r^\bullet + M \longrightarrow R_{r+1}^\bullet \tag{2.9}$$

The rate of propagation for monomer j is given by

$$R_{p,j} = Y_o \frac{N_{M,j}}{V_T} \sum_{i=1}^{n_M} k_{p,ij} \phi_i \tag{2.10}$$

where Y_o is the total concentration of free radicals, $N_{M,j}$ is the number of moles of monomer j, and ϕ_i is the mole fraction of radicals ending in repeat unit i. Defined as $k_{p,ij}$, the propagation rate constant for radicals ending in repeat unit (monomer) i, adding monomer j, can be described by the following three relations.

$$k_{p,ij} = k_{p,0,ij} \cdot dcpFactor_j \tag{2.11}$$

$$k_{p,0,ij} = \frac{k_{p,0,ii}}{r_{ij}} \tag{2.12}$$

$$dcpFactor_j = \begin{cases} 1 & \left(V_F > V_{F,crit,p,j}\right) \\ \exp\left(-B_j\left(\dfrac{1}{V_F} - \dfrac{1}{V_{F,crit,p,j}}\right)\right) & \left(V_F \le V_{F,crit,p,j}\right) \end{cases} \tag{2.13}$$

where $k_{p,0,ij}$ is the chemically-controlled (before the occurrence of diffusion-controlled propagation effects) propagation rate constant for radicals ending in repeat unit i, adding monomer j. When $i = j$, $k_{p,0,ij}$ is a temperature-dependent parameter, which is a function of the terminal repeat unit i. When $i \neq j$, equation (2.12) is used, where r_{ij} is the reactivity ratio for radicals ending in repeat unit i, adding monomer j, which is also temperature dependent.

As with the initiation reaction, there is a critical free volume for the propagation of monomer j, $V_{F,crit,p,j}$, below which the propagation becomes diffusion-controlled. Equation (2.13) shows the diffusion-controlled propagation factor, $dcpFactor_j$, which

reduces $k_{p,0,ij}$ once $V_F \leq V_{F,crit,p,j}$. The variable B_j is the free volume theory exponential parameter for diffusion-controlled propagation. B_j is a constant, while $V_{F,crit,p,j}$ is a function of temperature, both of which are dependent on the type of monomer being added to the polymer radical but independent of the radical itself.

In some cases, an overall pseudo-kinetic propagation rate constant is required. A weighted average can be performed on the individual propagation rate constants to obtain an overall estimation.

$$k_{p,overall} = \sum_{i=1}^{n_M} \sum_{j=1}^{n_M} k_{p,ij} \phi_i f_{M,j} \tag{2.14}$$

The total concentration of free radicals, introduced in equation (2.10), can be evaluated using

$$Y_o = \frac{1}{2k_t} \left[\left(\sum_{j=1}^{n_{MSI}} \left(k_{MSI,j} \frac{N_{MSI,j}}{V_T} \right)^2 + 4k_t R_I \right)^{1/2} - \sum_{j=1}^{n_{MSI}} \left(k_{MSI,j} \frac{N_{MSI,j}}{V_T} \right) \right] \tag{2.15}$$

where k_t is the overall termination rate constant, $N_{MSI,j}$ is the number of moles of monomer soluble impurity j, and $k_{MSI,j}$ is the rate constant for reaction between radicals and MSI j (details in section 2.1.6). Equation (2.15) is only valid if the steady-state assumption is adopted (details in section 2.1.9).

Also introduced in equation (2.10), is the mole fraction of radicals ending in repeat unit i

$$\phi_i = \frac{\psi_i}{\sum_{i=1}^{n_M} \psi_i} \tag{2.16}$$

where ψ_i is simply an intermediate variable used to calculate ϕ_i. Following are expressions for ψ_i for a two-component system, i.e. where two different monomers contribute to the chain growth

$$\begin{aligned} \psi_1 &= k_{p,21} f_{M,1} \\ \psi_2 &= k_{p,12} f_{M,2} \end{aligned} \tag{2.17}$$

For a three-component system, the expressions are as follows

$$\begin{aligned}\psi_1 &= k_{p,21}k_{p,31}f_{M,1}f_{M,1} + k_{p,21}k_{p,32}f_{M,1}f_{M,2} + k_{p,23}k_{p,31}f_{M,1}f_{M,3}\\ \psi_2 &= k_{p,32}k_{p,12}f_{M,2}f_{M,2} + k_{p,32}k_{p,13}f_{M,2}f_{M,3} + k_{p,31}k_{p,12}f_{M,2}f_{M,1}\\ \psi_3 &= k_{p,13}k_{p,23}f_{M,3}f_{M,3} + k_{p,13}k_{p,21}f_{M,3}f_{M,1} + k_{p,12}k_{p,23}f_{M,3}f_{M,2}\end{aligned} \tag{2.18}$$

Other variables are also used as weighting factors to obtain overall properties from individual parameters. The *mole fraction of monomer j*, introduced in equation (2.8) as f_{Mj}, is used when monomer is involved in the property.

$$f_{M,j} = \frac{N_{M,j}}{\sum_{j=1}^{n_M} N_{M,j}} \tag{2.19}$$

Next, the *cumulative copolymer composition* (mole fraction of monomer j bound in the copolymer) is used when properties relating to the non-propagating polymer need to be weighted, and is calculated using

$$F_{cumul,j} = \frac{N_{P,j}}{\sum_{j=1}^{n_P} N_{P,j}} \tag{2.20}$$

where n_P is the number of polymers present in the system and N_{Pj} is the number of moles of polymer j. And finally, there is the *instantaneous copolymer composition* (mole fraction of monomer j bound in the polymer), which is used when properties relating to the growing polymer chain need to be weighted, and is calculated using

$$F_{inst,j} = \frac{R_{p,j}}{\sum_{j=1}^{n_P} R_{p,j}} \tag{2.21}$$

where R_{Pj} is calculated using equation (2.10).

2.1.5 Termination

The propagation would continue until the monomer source was exhausted if it were not for the polymer's natural tendency to terminate. At any point during the rapid

propagation, radicals may mutually terminate to produce *dead polymer*, i.e. saturated polymer that has ceased growing, via one of two termination reactions:

$$R_r^\bullet + R_s^\bullet \longrightarrow P_{r+s} \tag{2.22}$$

$$R_r^\bullet + R_s^\bullet \longrightarrow P_r + P_s \tag{2.23}$$

where P_r is a dead polymer of chain length r. Reactions (2.22) and (2.23) represent termination by combination and disproportionation, respectively.

In *termination by combination*, two growing radical chains of lengths r and s join together to form one large dead polymer of length $(r + s)$. *Termination by disproportionation* is somewhat more complex: two different polymer chains are produced. One chain becomes a dead polymer, while the other is unsaturated. The unsaturated polymer forms a terminal double bond, after relinquishing a hydrogen radical to another radical centre, to become more stable, and in doing so becomes susceptible to further propagation through the double bond. Terminal double bond reactions result in branching in free-radical polymerizations, as discussed in section 2.1.6. The rate constants for termination by disproportionation and combination are represented by equations (2.24) and (2.25), respectively.

$$k_{t,disp} = \gamma k_t \tag{2.24}$$

$$k_{t,comb} = (1-\gamma)k_t \tag{2.25}$$

Both are related by the overall termination rate constant, k_t, and the fraction of termination by disproportionation, γ. For multiple monomers, individual γ's, which are temperature-dependent parameters, are weighted using their respective $F_{inst,i}$.

Important to note is the notion that, unlike initiation and propagation, which use a critical value to activate the diffusion control, termination diffusion control can always be active. The overall termination rate constant is the amalgamation of three constants, each representing a different diffusion-controlled termination regime. Each regime corresponds to a different stage in the termination process. First, two propagating radicals approach each other. This stage is defined as *translational diffusion*, where the entire radical molecules move. The second stage is referred to as *segmental diffusion*. Once the radicals are in close proximity to each other, the end segments shift toward each other

until contact is made. Finally, the third stage, the *reaction*, consists of the actual termination reaction between the two radicals.

In the initial stages of the reaction, k_t is governed by segmental diffusion. At this point, growing polymer chains can move with ease toward each other to induce termination, and the reaction itself is very quick. The movement of the segments is the slowest stage, therefore segmental diffusion is the rate-limiting step. The segmental diffusion-controlled termination rate constant is determined by

$$k_{t,seg} = k_{t,0,overall}(1 + \delta c) \tag{2.26}$$

where $k_{t,0,overall}$ is the overall pseudo-kinetic termination rate constant at zero polymer concentration, δ is the segmental diffusion parameter, and c is the mass concentration of accumulated polymer in the reaction mixture. Following is an expression to obtain $k_{t,0,overall}$ from individual values

$$k_{t,0,overall} = \sum_{i=1}^{n_P}\sum_{j=1}^{n_P} k_{t,0,ij}\phi_i\phi_j \tag{2.27}$$

where $k_{t,0,ij}$ is the rate constant for termination between radicals ending in components i and j, at zero polymer concentration. When $i = j$, $k_{t,0,ij}$ is a temperature-dependent parameter which depends on the types of monomers (repeat units i and j) in the system. When $i \neq j$, $k_{t,0,ij}$ can be calculated using Walling's "phi-factor" method:[13]

$$k_{t,0,ij} = \Phi_{ij}\left(k_{t,0,ii}k_{t,0,jj}\right)^{\frac{1}{2}} \tag{2.28}$$

where Φ_{ij} is the cross-termination factor for termination between radicals ending in components i and j. The cross-termination factor is usually represented by the symbol ϕ_{ij} in the literature[1,14,15], but it was renamed here to distinguish it from the mole fraction of radicals. In equation (2.26), δ is a constant that is a function of the monomers in the system. For multiple monomers, individual δ's are weighted using their respective $F_{inst,i}$. The overall mass concentration is simply obtained from individual monomer physical properties

$$c = \frac{\sum_{i=1}^{n_P} \left(N_{P,i} MW_{M,i} \right)}{V_T} \tag{2.29}$$

Later in the reaction, the presence of polymer chains becomes more considerable and the reaction medium is more viscous. The movement of the large radical chains is hindered, and the translational diffusion becomes the dominant factor in the termination process, and thus the rate-limiting step. The gel effect, introduced in section 2.1.2, becomes apparent at this point. After translational diffusion dominates the termination, but before the onset of propagation diffusion control, the auto-acceleration effect gradually takes place. Although the radical chains' movement is hindered, the much smaller monomers can still move freely and find radicals to continue the propagation. Since propagation is not unaffected, but the termination is diminished, the net effect is an increase in the overall rate of polymerization. Once propagation diffusion control is attained, the overall rate of polymerization decreases considerably. The translational diffusion-controlled termination rate constant is calculated using

$$k_{t,tr} = k_{t,crit} \left(\frac{\overline{M}_{w,crit}}{\overline{M}_w} \right)^n \exp\left(-A \left(\frac{1}{V_F} - \frac{1}{V_{F,crit,t}} \right) \right) \tag{2.30}$$

where $k_{t,crit}$ is the critical termination rate constant, $\overline{M}_w$ is the accumulated weight-average molecular weight (its calculation is shown in section 2.1.8), $\overline{M}_{w,crit}$ is the critical weight-average molecular weight, and $V_{F,crit,t}$ is the critical free volume of translational diffusion-control. A and n are constants that are a function of the monomers in the system. For multiple monomers, individual values are weighted using their respective $F_{inst,i}$. The determination of the critical values in equation (2.30) is demonstrated later in this section.

Finally, at higher conversions, the polymer mixture becomes so viscous that the radical chains can not move toward each other, nor can the end segments sway to make contact. Still capable of moving due to their lesser size, monomers add themselves to the trapped radicals, lengthening the chains further. With each added monomer, some chain ends grow closer to one another until two radicals are close enough to react. In this case,

there is relatively no translational or segmental diffusion, and the rate-determining step is reaction diffusion. In this model, two methods were implemented to address reaction diffusion. The first method was developed by Stickler *et al.*[16]. The reaction diffusion-controlled termination rate constant, using the Stickler method, can be obtained with

$$k_{t,rd} = \frac{8\pi N_{Av}\delta_{rr}D}{1000} \tag{2.31}$$

where

$$\delta_{rr} = \left(\frac{6V_m}{\pi N_{Av}}\right)^{\frac{1}{3}} \tag{2.32}$$

$$D = \frac{n_{M\,in\,P}\cdot l_0^2}{6} k_{p,overall} \frac{\sum_{i=1}^{n_M} N_{M,i}}{V_T} \tag{2.33}$$

$$V_m = \sum_{i=1}^{n_M}\left(\frac{MW_{M,i}}{\rho_{M,i}}\right) \tag{2.34}$$

δ_{rr} is the reaction radius, D is an intermediate parameter, V_m is the molar volume, $n_{M\,in\,P}$ is the number of monomer units per polymer chain segment, and l_0 is the length of a monomer unit. The parameters $n_{M\ in\ P}$ and l_0 are constants that are a function of the monomers in the system. For multiple monomers, weighted averages for each of these can be obtained using their respective $F_{inst,i}$. The variable N_{Av} represents Avogadro's number.

The second method, named after its authors, is the RNG method, which was developed by Russell, *et al.*[17]. The RNG method introduces the concept of *residual termination*, and provides upper and lower limits for $k_{t,rd}$. The reaction diffusion-controlled termination rate constant, using the RNG method, is calculated using

$$k_{t,rd} = k_{t,residual,\min}\,x + k_{t,residual,\max}\,(1-x) \tag{2.35}$$

where x is the overall mass conversion of monomer, calculated in section 2.1.8, which is used to determine an intermediate value for $k_{t,rd}$ within the calculated boundaries. The

minimum and maximum "residual" reaction diffusion-controlled termination constants, which correspond to the lower and upper limits, are, respectively,

$$k_{t,residual,\min} = \frac{4}{3}\pi k_{p,overall}\frac{N_M}{V_T}a^2\sigma N_{Av} \tag{2.36}$$

$$k_{t,residual,\max} = \frac{8}{3}\pi k_{p,overall}\frac{N_M}{V_T}a^3 j_c^{1/2} N_{Av} \tag{2.37}$$

In equations (2.36) and (2.37), a is the root-mean-square end-to-end distance per square root of the number of monomer units, σ is the Lennard-Jones diameter, and j_c is the entanglement spacing of pure polymer. All three constants are a function of the monomers in the system. For multiple monomers, weighted averages for each of these can be obtained using their respective $F_{inst,i}$. It should be noted that the lower bound of the RNG method coincides approximately with the Stickler method.

The effect of the transition from one termination regime to another on k_t will now be discussed. Unlike initiation and propagation, termination is more complex and does not simply use V_F to determine the onset of diffusion control. A free volume theory parameter, K_3, is first calculated,

$$K_3 = \overline{M}_w^m \exp\left(\frac{A}{V_F}\right) \tag{2.38}$$

The variables are the same as those used in the calculation of $k_{t,tr}$, equation (2.30).

When the polymerization begins, $k_t = k_{t,seg}$. However, when K_3 becomes greater than a certain critical value, K_3^*, the transition occurs. At the point where $K_3 = K_3^*$, the critical values from equation (2.30) are set, i.e. $k_{t,crit} = k_t$, $\overline{M}_{w,crit} = \overline{M}_w$, and $V_{F,crit} = V_F$. Beyond the critical point, i.e. $K_3 > K_3^*$, the termination rate constant becomes $k_t = k_{t,tr} + k_{t,rd}$. Since critical values are established from the transition, a simple linear interpolation routine was incorporated to obtain a sufficiently precise estimate of the critical point. K_3^* is a temperature-dependent parameter that is a function of the monomers in the system. For multiple monomers, individual K_3^* values are weighted using their respective $F_{inst,i}$.

2.1.6 Other Possible Reactions

Chain transfer occurs when hydrogen (or some atom or molecule), *H*, is transferred from a species, *HX*, in the reaction mixture to the propagating radical $R_r^\bullet$, which renders the polymer dead. The expression "chain transfer to *HX*" can be misleading: physically, the transfer is made to the radical, but conceptually, the chain (i.e. the propagating ability) is transferred to *HX*. The chain-transfer reaction can be depicted as

$$R_r^\bullet + HX \longrightarrow R_r H + X^\bullet \tag{2.39}$$

or equivalently

$$R_r^\bullet + HX \longrightarrow P_r + X^\bullet \tag{2.40}$$

where R_rH and P_r both represent dead polymer. The result of this premature termination is to lower the size of the polymer chain, hence decreasing the average molecular weight of the produced polymer. The number of radicals in the system remains the same, but the propagating chain starts anew. The species *X* involved in the transfer reaction described by reaction (2.40) may be monomer, initiator, solvent, chain transfer agent and/or polymer. The rate constants for each species will be presented next.

The overall pseudo-kinetic rate constant for *chain transfer to monomer* can be determined using (2.41)

$$k_{f,M} = \sum_{i=1}^{n_M} \sum_{j=1}^{n_M} \left(k_{f,M,ij} f_{M,j} \phi_i \, dcpFactor_i \right) \tag{2.41}$$

where $k_{f,M,ij}$ is the rate constant for transfer from a radical ending in repeat unit *i* to a monomer *j*. When all other transfer reactions are negligible, chain transfer to monomer places an upper limit on the achievable polymer molecular weight[12]. It may also lead to terminal double bonds, depending on the monomer being used.

Chain transfer to initiator was introduced earlier as "induced decomposition of initiator" in section 2.1.3. Its overall pseudo-kinetic rate constant is weighted as follows

$$k_{f,I} = \sum_{i=1}^{n_M} \sum_{j=1}^{n_I} \left(k_{f,I,ij} f_{I,j} \phi_i \, dcpFactor_i \right) \tag{2.42}$$

where $k_{f,I,ij}$ is the rate constant for transfer from a radical ending in repeat unit i to initiator j, and $f_{I,j}$ is the mole fraction of initiator j.

$$f_{I,j} = \frac{N_{I,j}}{\sum_{j=1}^{n_I} N_{I,j}} \tag{2.43}$$

The following relation allows the computation of the overall pseudo-kinetic rate constant for *chain transfer to solvent*:

$$k_{f,S} = \sum_{i=1}^{n_M} \sum_{j=1}^{n_S} \left(k_{f,S,ij} f_{S,j} \phi_i \, dcpFactor_i \right) \tag{2.44}$$

where $k_{f,S,ij}$ is the rate constant for transfer from a radical ending in repeat unit i to a solvent j, and $f_{S,j}$ is the mole fraction of solvent j, calculated similarly to equation (2.43).

A chain-transfer agent (CTA) is sometimes added when chain transfer is desirable, e.g. to control the molecular weight of the resulting polymer. The overall pseudo-kinetic rate constant for *chain transfer to CTA* can be calculated with

$$k_{f,CTA} = \sum_{i=1}^{n_M} \sum_{j=1}^{n_{CTA}} \left(k_{f,CTA,ij} f_{CTA,j} \phi_i \, dcpFactor_i \right) \tag{2.45}$$

where $k_{f,CTA,ij}$ is the rate constant for transfer from a radical ending in repeat unit i to a CTA j, and $f_{CTA,j}$ is the mole fraction of CTA j, calculated similarly to equation (2.43).

Chain transfer to polymer refers to both the propagating radical chains and the dead polymers. However, throughout the reaction, the concentration of polymer is much greater than the concentration of radicals. Chain transfer to polymer is significantly different from the other types mentioned above, because the polymer possesses many *H*'s along the chain that can be abstracted. When the radical site is transferred to any point along the chain other than the terminal unit of the polymer, subsequent propagation at this site leads to branching on the polymer chain. The effect of chain transfer to polymer can drastically affect the physical properties of the polymer and its applications. For

example, branching considerably decreases the crystallinity of a polymer. The effects of branching can be quantified, but it is beyond the scope of this thesis; the reader is referred to [15] for further details. The following equation allows the calculation of the overall pseudo-kinetic rate constant for chain transfer to polymer:

$$k_{f,P} = \sum_{i=1}^{n_M} \sum_{j=1}^{n_P} \left(k_{f,P,ij} F_{cumul,j} \phi_i dcpFactor_i \right) \tag{2.46}$$

where $k_{f,P,ij}$ is the rate constant for transfer from a radical ending in repeat unit i to a site on a polymer located at repeat unit j.

Another form of reaction, which resembles chain transfer, involves monomer soluble impurity (MSI). The MSI scavenges initiating and propagating radicals, acting as either a propagation retarder or inhibitor, depicted in reactions (2.47) and (2.48), respectively.

$$R_r^\bullet + MSI \longrightarrow P_r + MSI^\bullet \tag{2.47}$$

$$R_r^\bullet + MSI \longrightarrow P_r MSI \tag{2.48}$$

Propagation retardation is very similar to a transfer reaction, except that the resulting radical, $MSI^\bullet$, has a very low reactivity, slowing down the propagation dramatically. *Propagation inhibition*, on the other hand, attacks all of the radicals, halting the propagation completely, until all of the MSI's are consumed. The overall pseudo-kinetic rate constant for reaction between radical and MSI, which includes both retardation and inhibition, can be calculated using

$$k_{MSI} = \sum_{i=1}^{n_M} \sum_{j=1}^{n_{MSI}} \left(k_{MSI,ij} f_{MSI,j} \phi_i \, dcpFactor_i \right) \tag{2.49}$$

where $k_{MSI,ij}$ is the rate constant for reaction between a radical ending in repeat unit i and monomer soluble impurity j, and $f_{MSI,j}$ is the mole fraction of MSI j, calculated similarly to equation (2.43).

The last form of reaction that will be addressed is via double bonds. In this instance, the radical targets the double bond located on the dead polymer chain, combining to form a larger propagating chain.

$$R_r^{\bullet} + P_s \longrightarrow R_{r+s}^{\bullet} \tag{2.50}$$

Double-bonds can either be located at the end of the polymer or radical chain, i.e. terminal double bonds, or within the chain, i.e. internal double bonds. *Terminal double bonds* can lead to trifunctional branching points, and can occur when two radicals terminate via disproportionation or chain transfer to monomer reactions. The overall pseudo-kinetic rate constant for propagation with terminal double bonds is calculated using

$$k_{ptdb} = \sum_{i=1}^{n_M} \sum_{j=1}^{n_M} \left(k_{ptdb,ij} F_{cumul,j} \phi_i dcpFactor_i \right) \tag{2.51}$$

where $k_{ptdb,ij}$ is the rate constant for reaction with terminal double bonds (transfer from radical ending in repeat unit i to repeat unit j). *Internal double bonds* can yield tetrafunctional branching points, and arise when certain monomers are used, for example dienes, but cannot be generated during the polymerization. The overall pseudo-kinetic rate constant for propagation with internal double bonds can be obtained using

$$k_{pidb} = \sum_{i=1}^{n_M} \sum_{j=1}^{n_M} \left(k_{pidb,ij} F_{cumul,j} \phi_i dcpFactor_i \right) \tag{2.52}$$

where $k_{pidb,ij}$ is the rate constant for reaction with internal double bonds (transfer from radical ending in repeat unit i to repeat unit j). The rate constants k_{ptdb} and k_{pidb} are often referred to in the literature as k_p^* and k_p^{**}, respectively.

All of the individual rate constants considered in this section are temperature-dependent parameters which depend on both species, i and j, involved.

2.1.7 Material and Energy Balances

The basis for the free-radical polymerization model is a set of ordinary differential equations (ODE), which make use of all the algebraic equations introduced up to this point. Each ODE represents a balance on some element in the system, and adopts the following format

$$change\ in\ element = inflow - outflow + (generation - production) \tag{2.53}$$

A balance on the number of moles of monomer *i* yields

$$\frac{dN_{M,i}}{dt} = F_{M,i,in} - \frac{N_{M,i}}{V_T}\dot{V}_{out} - R_{p,i}V_T \tag{2.54}$$

where $dN_{M,i}/dt$ is the rate of change of $N_{M,i}$ with respect to time, $F_{M,in}$ is the inlet molar flow rate of monomer *i*, and $\dot{V}_{out}$ is the outlet volumetric flow rate.

A balance on the number of moles of monomer *i* bound in the polymer yields

$$\frac{dN_{P,i}}{dt} = F_{P,i,in} - \frac{N_{P,i}}{V_T}\dot{V}_{out} + R_{p,i}V_T \tag{2.55}$$

A balance on the number of moles of initiator *i* yields

$$\frac{dN_{I,i}}{dt} = F_{I,i,in} - \frac{N_{I,i}}{V_T}\dot{V}_{out} - k_{d,i}N_{I,i} \tag{2.56}$$

A balance on the number of moles of solvent *i* yields

$$\frac{dN_{S,i}}{dt} = F_{S,i,in} - \frac{N_{S,i}}{V_T}\dot{V}_{out} - k_{f,S,i}N_{S,i}Y_o \tag{2.57}$$

A balance on the number of moles of CTA *i* yields

$$\frac{dN_{CTA,i}}{dt} = F_{CTA,i,in} - \frac{N_{CTA,in}}{V_T}\dot{V}_{out} - k_{f,CTA,i}N_{CTA,i}Y_o \tag{2.58}$$

A balance on the number of moles of MSI *i* yields

$$\frac{dN_{MSI,i}}{dt} = F_{MSI,i,in} - \frac{N_{MSI,i}}{V_T}\dot{V}_{out} - k_{MSI,i}N_{MSI,i}Y_o \tag{2.59}$$

A balance on the total volume of the reaction mixture yields

$$\frac{dV_T}{dt} = \dot{V}_{in} - \dot{V}_{out} - V_T\sum_{i=1}^{n_M} R_{p,i}MW_{M,i}\left(\frac{1}{\rho_{M,i}} - \frac{1}{\rho_{P,i}}\right) \tag{2.60}$$

where $\dot{V}_{in}$ is the inlet volumetric flow rate.

An energy balance surrounding the reactor yields

$$\frac{d\left(\sum_{i=1}^{n_{TOT}} N_i MW_i C_{p,i}\left(T - T_{ref}\right)\right)}{dt} = \left[\begin{array}{l} \sum_{i=1}^{n_{TOT}} F_{in,i} MW_i C_{p,i}\left(T_{in} - T_{ref}\right) - \\ \sum_{i=1}^{n_{TOT}} F_{out,i} MW_i C_{p,i}\left(T - T_{ref}\right) + \\ \sum_{i=1}^{n_{TOT}} R_{p,i}\left(-\Delta H_{p,i}\right) V_T - UA_{jacket}\left(T - T_{jacket}\right) - Q_R \end{array}\right] \tag{2.61}$$

which can be manipulated to obtain a more practical form to solve for the temperature of the reaction mixture, T,

$$\frac{dT}{dt} = \frac{1}{\sum_{i=1}^{n_{TOT}} N_i MW_i C_{p,i}} \left[\begin{array}{l} \sum_{i=1}^{n_{TOT}} F_{in,i} MW_i C_{p,i}\left(T_{in} - T_{ref}\right) - \\ \sum_{i=1}^{n_{TOT}} F_{out,i} MW_i C_{p,i}\left(T - T_{ref}\right) + \\ \sum_{i=1}^{n_{TOT}} R_{p,i}\left(-\Delta H_{p,i}\right) V_T - UA_{jacket}\left(T - T_{jacket}\right) - Q_R \end{array}\right] \tag{2.62}$$

where n_{TOT} is the total number of species present in the reaction mixture, $C_{p,i}$ is the specific heat capacity of component i, T_{in} is the temperature of the stream entering the reactor, T_{ref} is some arbitrarily chosen reference temperature, $\Delta H_{p,i}$ is the heat of polymerization of monomer i, U is the overall heat transfer coefficient for the interface between the reactor and the surrounding cooling jacket, A_{jacket} is the cooling jacket heat transfer area, and Q_R is the heat loss from the reactor.

Similarly, an energy balance surrounding the cooling jacket yields, after manipulation for T_{jacket},

$$\frac{dT_{jacket}}{dt} = \frac{1}{\sum_{i=1}^{n_{TOT}} N_i MW_i C_{p,i}} \left[\begin{array}{l} \sum_{i=1}^{n_{TOT}} F_{in,i} MW_i C_{p,i}\left(T_{jacket,in} - T_{ref}\right) - \\ \sum_{i=1}^{n_{TOT}} F_{out,i} MW_i C_{p,i}\left(T_{jacket} - T_{ref}\right) + \\ UA_{jacket}\left(T - T_{jacket}\right) - Q_{jacket} \end{array}\right] \tag{2.63}$$

where $T_{jacket,in}$ is the temperature of the stream entering the cooling jacket, T_{jacket} is the temperature within the jacket, and Q_{jacket} is the heat loss from the jacket.

2.1.8 Conversion and Molecular Weights

The progress of the polymerization can be monitored using several measurements. The most common is the overall conversion, which is defined as the ratio of reacted mass to the total mass:

$$x = \frac{\sum_{j=1}^{n_M} \left(N_{P,j} MW_{M,j} \right)}{\sum_{j=1}^{n_M} \left(\left(N_{M,j} + N_{P,j} \right) MW_{M,j} \right)} \tag{2.64}$$

Two other frequently used assessment parameters are the accumulated number- and weight-average molecular weights, $\overline{M}_n$ and $\overline{M}_w$, respectively. The *method of moments* was developed to account for the inadequacy of the "method of instantaneous molecular weight distribution" when long-chain branching reactions such as transfer to polymer, and reaction with internal and terminal double bonds are significant. The method of moments consists of a set of three ODEs that, once solved, can be used to calculate $\overline{M}_n$ and $\overline{M}_w$. Their lengthy derivation requires the application of the steady-state hypothesis for radicals[18,19,20,21,22]. Following are the resulting equations, which, although somewhat reduced from those presented in the literature, are mathematically equivalent.

$$\frac{dV_T Q_0}{dt} = \left(\theta_{transfer} + \left(k_{t,disp} + \frac{k_{t,comb}}{2} \right) Y_o - k_{ptdb} Q_0 - k_{pidb} Q_1 \right) Y_o V_T \tag{2.65}$$

$$\frac{dV_T Q_1}{dt} = \left(\theta_{transfer} + k_p [M] \right) Y_o V_T \tag{2.66}$$

$$\frac{dV_T Q_2}{dt} = \left(\begin{array}{l} \left(\theta_{transfer} + k_p[M]\right) + k_{t,comb} Y_o \left(\frac{\theta_{numer}}{\theta_{denom}}\right)^2 \\ \quad + 2\left(\frac{\theta_{numer}}{\theta_{denom}}\right)\left(k_p[M] + k_{ptdb} Q_1 + k_{pidb} Q_2\right) \end{array} \right) Y_o V_T \tag{2.67}$$

where Q_0, Q_1, and Q_2 are the zeroeth, first, and second moments of the molecular weight distribution, and [ ] represents the molar concentration of the enclosed component. The θ terms are intermediate expressions created to simplify equations (2.65)-(2.67), and have no physical meaning. They are defined as follows:

$$\theta_{transfer} = k_{f,M}[M] + k_{f,I}[I] + k_{f,S}[S] + k_{f,CTA}[CTA] + k_{MSI}[MSI] \tag{2.68}$$

$$\theta_{numer} = k_p[M] + k_{ptdb} Q_1 + \left(k_{f,P} + k_{pidb}\right) Q_2 + \theta_{transfer} \tag{2.69}$$

$$\theta_{denom} = k_t Y_o + k_{f,P} Q_1 + \theta_{transfer} \tag{2.70}$$

Combined with the resulting V_T obtained from equation (2.60), solving equations (2.65)-(2.67) provides values for Q_0, Q_1, and Q_2, which can then be used to calculate the accumulated number- and weight-average molecular weights,

$$\overline{M}_n = \frac{Q_1}{Q_0} M_{w,eff} \tag{2.71}$$

$$\overline{M}_w = \frac{Q_2}{Q_1} M_{w,eff} \tag{2.72}$$

where $M_{w,eff}$ is the effective molecular weight of the copolymer, which is determined by

$$M_{w,eff} = \frac{\sum_{j=1}^{n_M} \left(N_{P,j} MW_{M,j}\right)}{\sum_{j=1}^{n_M} \left(N_{P,j}\right)} \tag{2.73}$$

2.1.9 Assumptions

Following are several widely-used assumptions that were formulated to simplify the development of the model. The validity and impact of each assumption is also discussed.

The *long chain assumption* states that the rate of propagation is independent of the radical chain length. Although theoretically, the propagation rate is a function of the radical size, experimental work has shown that the effect becomes negligible beyond radicals of length 2 or 3[23]. Since the chains grow rapidly, at any given time, the majority of the chains are greater than three units in length. The implication of this assumption is that the effect on propagation of short chain reactions and chain transfer reactions becomes negligible. For example, monomer is consumed not only through propagation, but also via initiation to form the primary radical. However, for every initiator radical, there is only one monomer molecule added during the initiation step (i.e. to form a primary radical) compared to hundreds, thousands or potentially millions of monomers added during the propagation step. Therefore, the consumption of monomer due to initiation is negligible compared to that of propagation in equation (2.54). The long chain assumption allows the derivation of a kinetic expression for the overall rate of polymerization. For linear polymers (i.e. no branching occurs), the long chain assumption directly implies the steady-state hypothesis[24].

The *steady-state hypothesis* for radicals is assumed to be valid, which states that the concentration of radicals increases initially, but almost instantly becomes constant. A rate of change in radical concentration equal to zero is equivalent to stating that $R_I = R_t$, where R_t is the rate of termination. This allows the derivation of a usable expression for R_p, shown in equation (2.10), and is also necessary in order to derive the ODEs used in the method of moments introduced in section 2.1.8. The theoretical validity of the steady-state assumption has been examined by Kondratiev[25], and its experimental validity has been demonstrated for many polymerizations[12].

Although the propagation rate theoretically depends on the composition and sequence distribution of the radical chain, only the end unit(s) near the radical is (are) considered in practice. Therefore, based on this assumption, combined with the long chain assumption, radical chains having different lengths and sequence distributions can be treated as kinetically equivalent, provided the end units are of the same type. For the terminal model, only the final radical unit is relevant, meaning there are only two types of radicals to be considered in a copolymerization. For the penultimate model, the final two radical units are applicable, which implies that there are four types of radicals present in

the copolymer reaction mixture, corresponding to the various combinations of terminal and penultimate units.

For the systems studied in this thesis, it was assumed that the presence of side reactions, such as depropagation, monomer partitioning, and various forms of complex formation, was negligible. If however, the polymerization system was suspected to exhibit a significant effect of a given side reaction, the appropriate equations should be added to account for this effect.

The size and steric arrangement of the initiator, solvent, CTA and MSI molecules is assumed to be comparable to that of the monomer(s). When the reaction medium exhibits propagation diffusion control, $dcpFactor_i$, which is a monomer-related property, should affect each of these species similarly, as applied in equations (2.42), (2.44), (2.45) and (2.49). Since it is known that the reactions involving polymer chains are also affected by diffusion control, and that the parameters k_{fP}, k_{ptdb}, and k_{pidb} can not be measured experimentally, it is reasonable to use $dcpFactor_i$ in equations (2.46), (2.51) and (2.52), despite polymers being much larger molecules.

Polymers, however, are much larger molecules and therefore, the use of $dcpFactor_i$ in equations (2.46), (2.51) and (2.52) would be invalid.

The reaction medium is assumed to be perfectly mixed within the reactor, which allows the use of the homogeneous relations discussed above; otherwise, a different approach is necessary. The size of the reactor and the manner in which the solution is mixed support this assumption.

The specific heat capacity of component i is assumed to be a weak function of temperature, which allows the manipulation from equation (2.61) to equation (2.62).

The densities of monomer and polymer are assumed to be additive. In reality, the densities are not additive; however, the effect on the polymerization outputs is negligible.

2.2 Glass transition temperature models

The glass transition temperature, T_g, is one of the most important characteristics of a polymer, which can affect certain physical properties, such as crystallinity and free

volume. The T_g of a polymer must be considered when selecting a polymer for a specific end-use.

Amorphous polymers (completely random molecules) always possess a T_g, but crystalline polymers (completely ordered molecules) do not exhibit such a transition due to their morphology. However, most polymers are semi-crystalline (mixture of amorphous and crystalline regions), albeit to varying degrees.

As a liquid polymer is cooled, the mixture reaches a point where its amorphous domains show signs of glassy properties such as brittleness, stiffness and rigidity. This phenomenon occurs due to a decrease in internal energy, which halts the segmental motion within the polymer chains.

2.2.1 *Modelling Copolymer T_g*

From a modelling point of view, the T_g has an important influence on the calculation of free volume. The free volume is used in the polymerization model to predict the onset of various diffusion control regimes. When a copolymer is formed, a simple weighting of the individual repeat unit T_g's is typically insufficient. Several models have been proposed over the years to combine these individual T_g values into a reasonably accurate estimate of the copolymer T_g; however, none of these models can be claimed as universal. Further work needs to be undertaken to remove the uncertainty in the constants and parameters used in the various models.

Gao and Penlidis[14] performed an extensive literature search in order to properly simulate the effects of copolymer T_g. An overview of their findings is presented here, followed by a description of the models selected for the simulations in this thesis.

2.2.2 *Overview of Copolymer T_g Models*

Although some copolymer T_g models are purely empirical, many models have been derived from theory, either via entropy or free volume approaches. It is important to note, however, that some of the models become equivalent when certain assumptions are made.

For models based on entropy theory, the configurational entropy of a polymer chain is zero at T_g. The Dimarzio-Gibbs[26], Barton[27] and Suzuki-Mathot[28] models are

examples of entropy-based models. In the Dimarzio-Gibbs model, the homopolymer T_g's are weighted with their respective mole fraction of rotatable bonds. The Barton model is an extension of the Dimarzio-Gibbs model, which takes into account the effects of microstructure on T_g. Suzuki-Mathot further extended this model to include the average number of both monomer sequences occurring in a copolymer per 100 monomer units.

Models based on free volume theory include the Gordon-Taylor[29] and the Wood[30] models. The Gordon-Taylor model includes a constant, which accounts for interactions of all diads in the copolymer. The Wood model makes use of adjustable parameters and weighting factors.

Other models include the Fox[31], Johnston[32], and Couchman[33] models. One of the first copolymer T_g models introduced, the Fox model uses a parallel approach by weighting individual T_g's with the monomer weight fractions.

$$\frac{1}{T_g} = \sum_{i=1}^{n_M} \left(\frac{W_i}{T_{g,i}} \right) \tag{2.74}$$

where W_i is the weight fraction of monomer i in the copolymer chain. Gao and Penlidis[14] reported that the Fox model is not valid for many copolymer systems.

Like the Fox model, the Johnston model is in parallel form; however, it accounts for the contribution from monomer sequence distribution. The equation, extended to n_M monomers, is shown below:

$$\frac{1}{T_g} = \sum_{i=1}^{n_M} \sum_{j=1}^{n_M} \frac{W_i P_{ij}}{T_{g,ij}} \tag{2.75}$$

where W_i is the weight fraction of monomer i in the copolymer chain, P_{ij} is the probability of sequence ij occurring. When $i = j$, $T_{g,ij}$ is the T_g of the homopolymer, whereas when $i \neq j$, $T_{g,ij}$ is the T_g of the alternating copolymer. According to Gao and Penlidis[14], the Johnston model appears to be the most general model amongst the ones studied. Their tests showed that their model predictions using this T_g model were satisfactory for most copolymer systems.

A thermodynamic approach was used to derive the Couchman model. Although the theory is more rigorous, additional parameters are required to predict the copolymer T_g in the Couchman model. The equation, for a two-monomer system, is as follows:

$$\ln(T_g) = \frac{r_{ij} f_{M,i}^2 \Delta C_{p,ii} \ln(T_{g,ii}) + r_{ji} f_{M,j}^2 \Delta C_{p,jj} \ln(T_{g,jj}) + 2 f_{M,i} f_{M,j} \Delta C_{p,ij} \ln(T_{g,ij})}{r_{ij} f_{M,i}^2 \Delta C_{p,ii} + r_{ji} f_{M,j}^2 \Delta C_{p,jj} + 2 f_{M,i} f_{M,j} \Delta C_{p,ij}} \quad (2.76)$$

where r_{ij} is the reactivity ratio describing the addition of monomer j to a growing radical chain ending in monomer i, $f_{M,i}$ is the mole fraction of monomer i in the reaction mixture, and $\Delta C_{p,ij}$ is the difference in heat capacity above and below the corresponding $T_{g,ij}$.

In some cases, a simplified form of the Couchman equation can be used, where all ΔC_p's are assumed to be equal, and therefore cancel out of equation (2.76). Under this assumption, no additional parameters need to be provided. Testing done by Gao and Penlidis[14] revealed that simulations using Couchman's equation agree well with experimental data and are very close to results using Johnston's model. In light of these findings, it was decided to implement both the Johnston and Couchman equations into the simulator, providing the user with the choice of equation. Although presently seldom used, the copolymer T_g weighted in parallel and in series (i.e. the Fox model) using monomer weight fractions were also implemented as options, for comparison purposes.

2.3 Other propagation models

For many years, it was believed that the terminal model, also known as the Mayo-Lewis[34] model, adequately described most copolymerizations. The reactivity ratios were measured directly using composition data, resulting in good predictions for many copolymer systems. The exceptional cases were assumed to be influenced by further factors inherent to the system; in these cases, additional or alternate models were proposed. Until relatively recent years, critical testing of the terminal model was rarely carried out due to experimental limitations. With improvements to experimental techniques, more accurate measurements of the reactivity ratios were obtained. Techniques such as pulsed laser propagation (PLP) were developed allowing the direct measurement of the propagation rate constants. Several studies, the first being by Fukuda

et al.[35], found that the reactivity ratios obtained traditionally and those obtained with PLP and equation (2.12) were significantly different for many copolymer systems when applying the terminal model.[36] In light of these findings, some researchers have looked more carefully at the alternate models previously reserved for exceptional cases, and have suggested their use in a more general manner.

Most model discrimination attempts based on model fitting between competing alternate models have proven to be unsuccessful since many of these models can be fitted equally well to the same experimental data. Other approaches to model discrimination are currently being investigated.[37,38] Work in this area is growing, and further rigorous studies will need to be conducted before the terminal model is abandoned for an alternate model.

Such alternatives include the *monomer-solvent complex model*[40], and the *bootstrap model*[39], which assumes that some form of monomer partitioning occurs. Two other examples, the implicit and explicit penultimate models, are discussed in more detail in the next section.

2.3.1 Penultimate models

As mentioned earlier, the penultimate model considers not only the final unit on the radical chains, as does the terminal model, but also the second last unit at the active chain end. Aside from the polymer propagation equations presented for the terminal model, the remaining equations presented in section 1.1 still hold for the penultimate model. As mentioned in section 2.1.4, the reactivity ratio for the terminal model can be defined as

$$r_{ij} = \frac{k_{p,0,ii}}{k_{p,0,ij}} \tag{2.77}$$

where r_{ij} is the reactivity ratio for monomer j adding to a radical ending in repeat unit i.

There are two forms of the penultimate model. First, the *explicit penultimate model* will be examined, as it is the broader of the two. In general terms, the equation for the monomer and radical reactivity ratios can be represented by the following

$$r_{wx,z} = \frac{k_{p,0,wx,y}}{k_{p,0,wx,z}} \tag{2.78}$$

where w represents the penultimate unit of the radical chain, x represents the terminal unit of the radical chain, and y and z represent either monomer being added to the radical chain. For a copolymerization, there are four *monomer reactivity ratios*

$$r_i = r_{ii,j} = \frac{k_{p,0,ii,i}}{k_{p,0,ii,j}} \tag{2.79}$$

$$r_i' = r_{ji,j} = \frac{k_{p,0,ji,i}}{k_{p,0,ji,j}} \tag{2.80}$$

and two *radical reactivity ratios*

$$s_i = s_{ji,i} = \frac{k_{p,0,ji,i}}{k_{p,0,ii,i}} \tag{2.81}$$

The first variable in equations (2.79)-(2.81) represents the notation adopted by Fuduka *et al.*[35] in their development of the penultimate model, while the second variable is a more explicit notation implemented in this work. The parameters $r_{ii,j}$, $r_{ji,j}$ and $s_{ji,i}$ are used to calculate

$$\bar{r}_{ij} = r_{ji,j}\left(\frac{f_i r_{ii,j} + f_j}{f_i r_{ji,j} + f_j}\right) \tag{2.82}$$

and

$$\bar{k}_{p,0,ii} = k_{p,0,ii,i}\left(\frac{f_i r_{ii,j} + f_j}{f_i r_{ii,j} + f_j / s_{ji,i}}\right) \tag{2.83}$$

The modified parameters $\bar{r}_{ij}$ and $\bar{k}_{p,0,ii}$ are then used in the terminal model equation (2.12), in place of r_{ij} and $k_{p,0,ii}$. In equations (2.79)-(2.83), i and j represent two different monomers. For systems having more than two monomers, the sequence of equations is repeated for each monomer pair combination.

The *implicit penultimate model*, which is a simplified form of the explicit penultimate model, was proposed by Fuduka *et al.*[35], before it was generalized to the explicit form. In this case, the penultimate unit effect is removed from the monomer reactivity ratios, but retained for the radical reactivity ratios. The following reduction is applied to the explicit penultimate model.

$$\bar{r}_{ij} = r_{ii,j} = r_{ji,j} = \frac{k_{p,0,ji}}{k_{p,0,ij}} \tag{2.84}$$

In other words, the magnitude of the penultimate unit effect on reactivity is not affected by the type of monomer with which it is reacting. The monomer reactivity ratios are thus replaced by their terminal model values, while maintaining the penultimate values for the radical reactivity ratios.

Coote and Davis[36] concluded that the explicit penultimate unit effect model should be considered as a more comprehensive basis for most copolymerizations. They emphasize that the terminal model reactivity ratios do not adequately represent the underlying copolymerization processes. The implication of this statement is that the terminal model reactivity ratios should only be considered as adjustable parameters. A number of studies reveal that many factors are jointly responsible for the penultimate unit effect, such as polar interactions[41], radical stabilization effects[42], entropic effects[43] and direct interactions.

It should be kept in mind that the penultimate model uses three reactivity ratio parameters, compared to one reactivity ratio found in the terminal model. As with any system, an increase in parameters typically improves the model fit to the experimental data. However, the penultimate unit effect theory appears to be sounder than the terminal counterpart.

2.4 Modelling in Java™

2.4.1 Evolution of programming languages

In the early to mid 1950s, programs were written directly in machine language. This required a complete understanding of the machine's architecture, and made even the

simplest of tasks time-consuming. Between the late 1950s and mid 1960s, higher level languages such as Fortran and Cobol were developed, which were more user-friendly. However, lengthy programs became difficult to interpret and debug. In the 1970s, languages such as Pascal and C allowed programs to be subdivided into logical tasks (functions), giving birth to procedural programming. In the 1980s and early 1990s, object-oriented programming built upon procedural programming and introduced a completely different method of designing programs. In the late 1990s and early 2000s, object-oriented programming was extended, with emphasis on building large programs out of components (sub-programs), which may be written in different languages. In component-based programming, components can be replaced without affecting the other components.

2.4.2 Procedural and object-oriented programming languages

Most of today's programming languages are typically grouped into two categories: *procedural* and *object-oriented*. The design strategy behind each is conceptually quite different.

Programs written procedurally are task-oriented. The code is divided into procedures, each one designed for certain operations. To perform a task, data are passed to the procedure, and the procedure returns the result.

As the name implies, object-oriented programs are designed with objects in mind. They offer a more intuitive, real-world representation of the system being modelled. The components in the system, tangible (e.g. a reactor) or otherwise (e.g. a numerical solver), are grouped into *classes*, which are templates for objects. A class defines an object's properties (data) and functionality (procedures). Each class is like a procedural program, and it can interact with other classes. Like a blueprint, a single class can be used to create many objects. Tasks are accomplished by communicating with the object, invoking one of its procedures, which may use data received from the caller and/or data encapsulated within the object itself.

Object-oriented programming allows the maintenance and enhancement of code with minimal effort. With the help of inheritance, code can be extended and reused among classes, which reduces the number of source lines of code.

It is the author's opinion that object-oriented programming is more intricate to design, yet more intuitive, whereas procedural programming is simpler to design and write, but not as clear to read. The choice between the two approaches is dependent on the system to be simulated, and can also be influenced by the programmer's preference.

2.4.3 Java™ programming language

Following is a brief overview of Java™, its advantages and disadvantages, and the motivation behind its selection. For a more detailed overview of Java™, the reader is referred to [46].

Java™ is an object-oriented programming language, which received a lot of attention in the early 1990s due to its platform independence. Unlike most other object-oriented languages, programs written in Java™ on one type of computer using a certain operating system can operate on any Java™-compatible operating system, because they are compiled differently.

Aside from its object-oriented construct and its platform independence, Java™ possesses other important advantages. It is simpler to use than some of its object-oriented counterparts, like C++. Also, Java™ provides *multithreading*, i.e. it can execute several widely different tasks seemingly simultaneously, in a stable sequence. Another useful feature is Java™'s *javadoc* utility, which allows for an easy way of documenting the code. It extracts specially formatted comments in the code, and produces documentation in HTML format with links between associated classes.

Despite these compelling aspects, Java™ has one major drawback: its performance. Java™'s way of compiling and interpreting the code, which provides platform independence, is more costly in terms of performance. For many engineering applications, this can be problematic due to intensive numerical computations. In some cases, simulations can take up to ten times longer to run than other platform-dependent languages.

The intuitive object-oriented nature of the Java™ programming language, as well as its simpler structure compared to other object-oriented languages, were the main factors in the selection of Java™ to develop the simulation. Also, these features will allow the simulator to be easily extended to include further options and other models.

The inherent disadvantages associated with using Java™ were not found to be prohibitive during most polymerization simulations. Some systems were very stiff, which slowed down the simulation considerably, and in severe cases, halted the simulation. However, it is believed that the ODE solver is large part the culprit. Simulation times and further discussion can be found in section 7.5.1. For the purposes of this thesis, and keeping in mind that future work will be conducted to extend the simulator's capabilities, Java™ was an appropriate choice to develop a free-radical polymerization simulator.

2.5 Simulator design

Making use of an existing mechanistic model for free-radical polymerizations, the simulator was created to model bulk and solution homo- and copolymerizations. The Java™ programming language was used to exploit design advantages of object-oriented languages. Keeping in mind that future work will be performed to further broaden its capabilities, the simulator was designed to ensure that it could be easily understood and extended by other designers. Numerous options were provided for user input, adjustable in TXT files. The database values for the ingredients used in the case studies in this thesis are presented in Appendix A. Currently, the user interacts with the simulator via a DOS interface.

In this section, the expression *working directory* refers to the full file pathname where the `polymerSim` folder was copied, e.g. `C:\Simulations\polymerSim\`.

2.5.1 Java™ program design

The object-oriented design of the code is depicted using simplified Booch diagrams. Only the main interactions are depicted; some are omitted for conciseness. Figure 2.1 shows the three most common types of relationships between two objects. An arrow indicates an

inheritance, i.e. object **X** *is* of type **Y**, where object **Y** is the more general of the two. A full circle signifies *ownership*, i.e. object **Y** *has* one or more **X** objects as part of its properties. An empty circle represents *usage*, i.e. object **Y** *uses* one or more **X** objects.

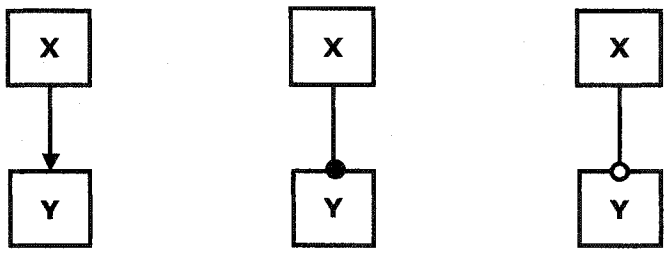

Figure 2.1: Types of relationships in Booch diagrams

In the subsequent diagrams, when (A) is found next to an object name, it means that the *class* (i.e. a template used to create an object) is *abstract*. An abstract class is a template that can not be used to create an object. A subclass of the abstract class must be defined to add further specifications. For example, it would not be practical to create a `Shape` object; not enough information is available. A subclass of `Shape`, for instance a `Square` class, could be defined, which could then be used to create a `Square` object. Creating abstract classes is useful for categorizing, and allows the designer to take advantage of the *inheritance* in object-oriented programming.

An interface is used in Java™ to allow *multiple inheritance* and exploit *polymorphism*. An object can therefore assume multiple identities, and its reference can be managed by various types of variables. In the following diagrams, interfaces are denoted by (I) next to their name.

The `Manager` object controls and begins the simulation, but the `PolymerSim` object performs the majority of the operations including the creation of all other objects, once requested by the `Manager`.

As seen in Figure 2.2, the `Reactor` object contains one or more `Stream` objects, which in turn own one or more `Component` objects. To describe the flow of elements (components, volume, energy), the `Reactor` object requires `ODEBalance` objects. It solves the system of equations using a `Stifbs` object, i.e. an ODE solver, as depicted in Figure 2.3. The `Reactor` object possesses database and ODE functionality through its

inheritance from the `Database` and `ODESolvable` interfaces. The `ReactorType` object, owned by the `Reactor`, allows the setting and change from batch to semi-batch to continuous configurations.

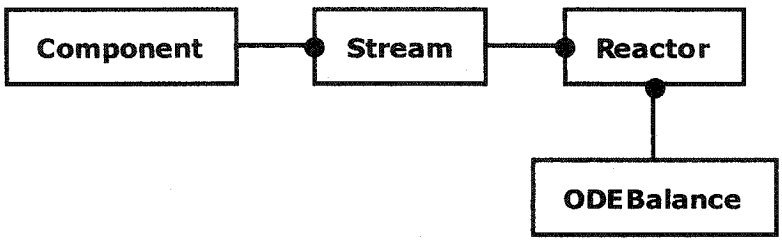

Figure 2.2: Overview of the major program components

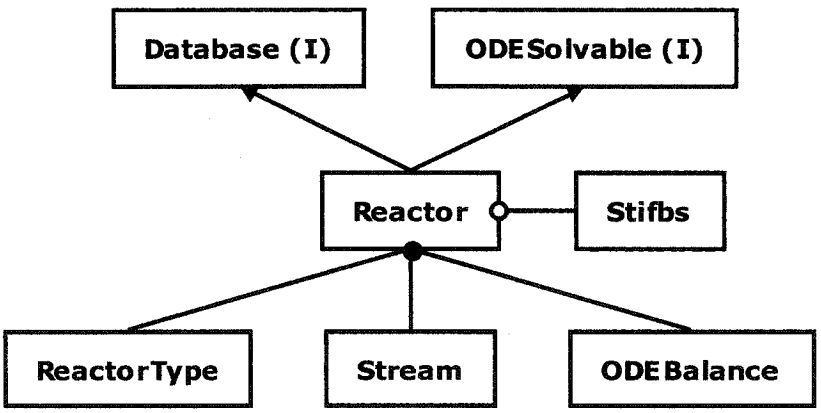

Figure 2.3: Program components related to the reactor

Shown in Figure 2.4, the `Balance` object owns the same `ReactorType` object, in addition to `MultivariateEquation` objects to describe the inflow, outflow and generation terms for the various components. The `ODEBalance` object inherits its properties and functionality from its parent class, `Balance`, as well as the `ODE` interface.

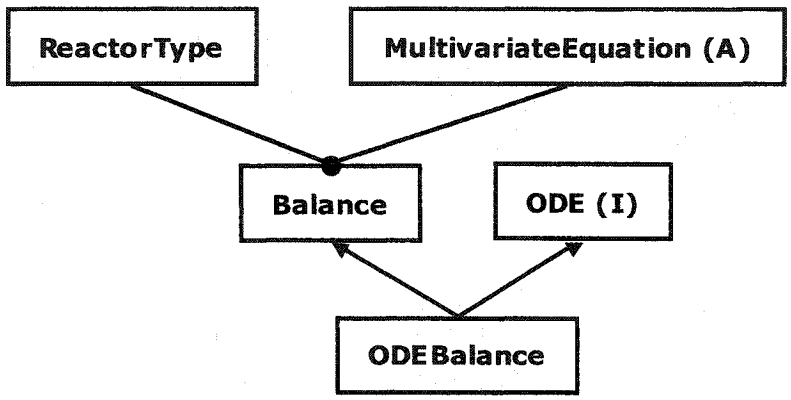

Figure 2.4: Program components related to the balances

The `Equation` object is a generic template to group all equations. A subclass of `Equation`, `ReactorEquation` is a more define d type of equation, which possesses more variables, including a `Stream` object. `ReactorEquation` is further specified, yielding four more types of equations, as seen in Figure 2.5. Although additional specifications were provided for these classes, they are all abstract. All of these are extended into additional subclasses, too numerous to list or show in Figure 2.5. Each equation is used to describe the entire polymerization system.

The `Stifbs` object is an implementation of Bulirsch-Stoer ODE solver for stiff systems, adapted from that found in [45]. As with all `ODESolver` objects (i.e. its parent class), the `Stifbs` object possesses `ODE` and `ODESolvable` objects, which is illustrated in Figure 2.6. In addition, the `Stifbs` object is capable of calculating derivatives (via the corresponding interface), and makes use of the semi-implicit midpoint rule as well as polynomial extrapolation.

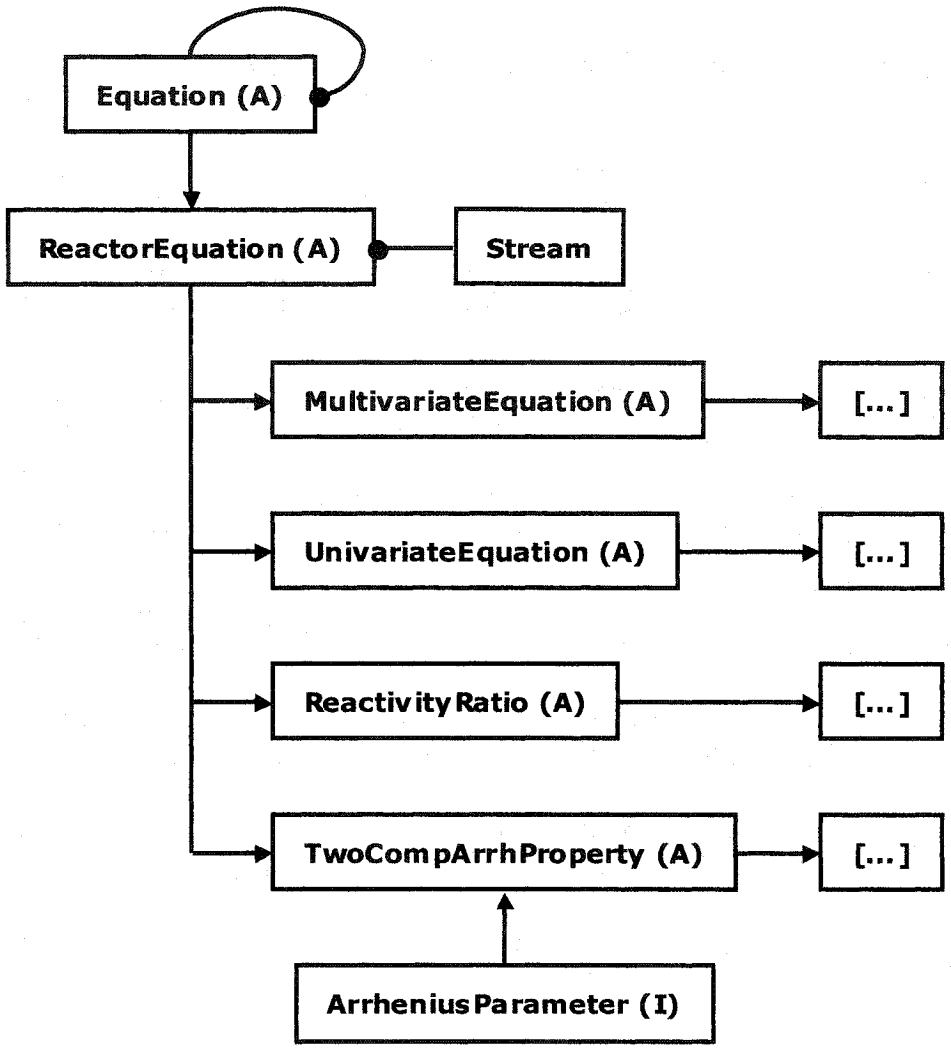

Figure 2.5: Program components related to the equations

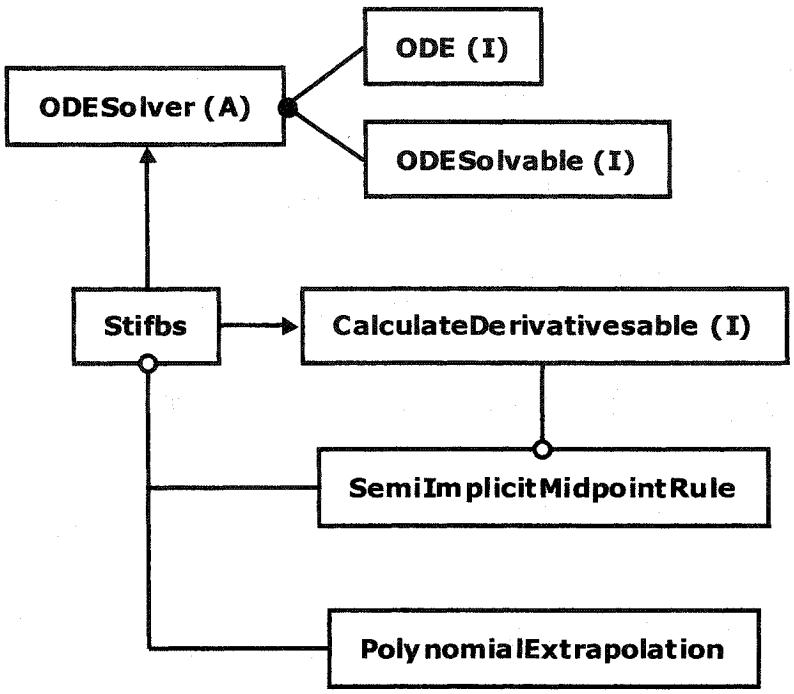

Figure 2.6: Program components related to the ODE solver

2.5.2 User input and output

Using a similar logic to the code design, inputs were grouped into appropriate TXT files. These files are located in the `C:\...\polymerSim\inputs\` folder. Following are the input files, followed by a brief description of their contents.

- `SimSettings.txt`
  - contains all the settings required to start a simulation
  - e.g. number and name of each component entering the reactor, selection of various polymerization models and simulation constraints
- `Reactor.txt`
  - contains the reactor specifications
  - e.g. reactor physical properties, initial quantities of each component
- `Monomer.txt`
  - contains the properties relevant to monomers
  - properties for multiple monomers are built-in; more monomers may be added to the database in the future by adding a column

- similarly for `Polymer.txt`, `Initiator.txt`, `Solvent.txt`, `CTA.txt`, `MSI.txt`, `Coolant.txt`

- Arrhenius parameters that depend on two components
  - the activation energy and the pre-exponential factor are in separate files for each Arrhenius parameter
  - each file is a two-dimensional table, with rows corresponding to component #1 and the columns corresponding to component #2
  - e.g. `k_fM_actEn.txt` and `k_fM_preExp.txt`
- constants that depend on two components
  - each file is a two-dimensional table, with rows corresponding to component #1 and the columns corresponding to component #2
  - e.g. `C_exponential.txt`
- streams
  - contains the properties relevant to streams
  - files exist for the inlet stream(s) for the reactor and the cooling jacket surrounding the reactor
  - blank files are created for the outlet stream(s), since the reactor outputs determine the outlet stream properties
  - e.g. `inletStreamReactor.txt`

For each simulation that is run, two output files are created:

- `SimOutputs#.txt` (where `#` is the simulation number)
  - contains all the outputs of the simulation
  - each row contains the various polymerization properties at the corresponding time
  - located in folder `C:\...\polymerSim\outputs\`
- `SimAndReactorSettings#.txt` (where `#` is the simulation number)
  - contains the simulator reactor inputs for the corresponding simulation, for reference purposes
  - located in folder `C:\...\polymerSim\storeSettings\`

An Excel file corresponding to the `SimOutputs.txt` format was created, allowing instant import and formatting of the outputs, as well as displaying the important results in graph form.

2.5.3 *Running a simulation*

Before any simulation can be run, a Java™ compiler must be installed. One can be obtained from the SunSystems website[46]. Once the compiler is installed, the `jdk.bat` file, located in the `polymerSim` working directory, must be opened and updated to reflect the location of the Java™ commands. The path must changed to the location of the compiler for the line `set path=...\jdk___\bin;`, where "..." is the path, and "___" is the version of the compiler installed.

The first time a simulation is run on a computer, the `Manager.java` file (located in the working directory) must be opened, and the `operatingFolder` variable must be updated to the working directory. The changes must be saved, and the file can then be closed.

To run a simulation in DOS, the file path must first be changed to the working directory. The user must type `jdk` at the command prompt to be able to access the Java™ commands. Once the desired reaction and simulation settings have been input into the appropriate TXT files (section 2.5.2), the user must enter the command `javac *.java` to compile all the `.java` files. Finally, `java Manager` must be typed to run the simulation.

Some outputs will displayed in the DOS window, signalling critical points throughout the reaction, and indicating the end of the simulation. The simulation number and its duration will appear on the screen. The results can then be viewed in the corresponding TXT file, or using the Excel file described in section 2.5.2.

2.6 Ordinary differential equation solver

2.6.1 *Stiffness of an ordinary differential equation system*

The system of ordinary differential equations (ODEs) describing free-radical polymerizations is known to be *stiff*. A rough definition of a stiff ODE system is that it

contains both very rapidly and very slowly decaying terms. More specifically, the Jacobian matrix **J**, with elements J_{ij} defined as

$$J_{ij} = \frac{\partial f_i(x, \underline{y})}{y_j} \tag{2.85}$$

of a stiff system possesses eigenvalues λ_i with real parts $\mathrm{Re}(\lambda_i)$ that vary largely in magnitude and are also predominantly negative. The solution varies locally as a linear combination of the exponentials $e^{x\mathrm{Re}(\lambda_i)}$, which all decay if all $\mathrm{Re}(\lambda_i)$ are negative. For sufficiently large x, the terms with the largest $|\mathrm{Re}(\lambda_i)|$ decay to insignificant levels while others are still active. In this case, the ODE system is said to be stiff. However, if the integration is not carried through to a sufficiently large x, the problem is not considered stiff[47].

A problem can still be labelled as stiff, even though it has some $\mathrm{Re}(\lambda_i)$ that are positive. For this to hold true, no positive $\mathrm{Re}(\lambda_i)$ can be large, and there must be at least one negative $\mathrm{Re}(\lambda_i)$ that is large in magnitude[48]. Stiffness is both local and relative. Because the λ_i generally vary with x, stiffness can be present in one interval, but not in another. Also, one problem may be considered more stiff than another. There are some measures of stiffness available, but they are beyond the scope of this study.

Solving stiff problems with standard ODE solvers, such as the popular explicit Runge-Kutta, becomes computationally prohibitive due to the excessively small step sizes that the method must take in order to maintain *stability*. Because solutions provided by ODE solvers are only approximations to the true solution, errors are introduced at each step. For a method to be stable, the error must not grow unbounded from step to step. To satisfy stability requirements, traditional ODE solvers must take small steps, even after the rapidly decaying components have become negligible. For stiff problems, the number of steps used by these methods becomes very large[47].

The *accuracy* of a numerical method, or more precisely its local truncation error, is usually measured by its order. A method is of order q if the local truncation error varies proportionally to h^{q+1}, where h is the step size at a given step. To make the distinction, accuracy refers to the magnitude of the error introduced in a given step, while stability refers to whether this error grows in subsequent steps.

2.6.2 *Stiff ordinary differential equation solvers*

To address the issue of stiffness, an appropriate ODE solver must be selected. Two general families of solvers can be used: predictor-corrector routines, or methods using Richardson extrapolation. The predictor-corrector methods are multi-step methods, which means they use information from previous steps in performing the numerical integration. Starting with user-defined initial conditions, ODEs are replaced with difference equations, and solved step by step. First a predictor step is used to obtain an estimate of the solution. Then, steps are taken to correct the initial guess iteratively until convergence is achieved, providing a reasonable approximation to the true solution. The superior predictor-corrector methods exhibit stiff stability, meaning that their step size is not constrained to small values once the rapid components are negligible[49]. The step size is only restricted by the accuracy imposed by the numerical solution.

Methods using Richardson extrapolation are based on the concept of obtaining a solution by extrapolating to a zero step size. A solution is obtained using a relatively large step size. A second solution is obtained with a smaller step size. This procedure is repeated, and an algorithm is used to extrapolate the "true" solution for an infinite number of steps, i.e. a zero step size. The Bulirsch-Stoer method was the first practical application of this concept to solve ODEs, and as a result, extrapolation methods are often referred to as Bulirsch-Stoer methods.

In many applications, Bulirsch-Stoer methods have replaced the more traditional predictor-corrector algorithms. Only the more sophisticated forms of the latter appear to be competitive with the Bulirsch-Stoer methods[45]. However, each routine has its limitations and advantages; therefore, the method selection is problem-specific.

References

2. Gao, J.; Penlidis, A. *Prog. Polym. Sci.*, **27**, 403 (2002).
3. Barclay, B.R.; Penlidis, A.; Gao, J. *Polymer Reaction Engineering*, **11**(4), 737 (2003).
4. Tobita, H.; Hamielec, A. *Polymer*, **32**, 2641 (1991).
5. Xie, T.Y.; Hamielec, A. *Macromol. Chem. Theory Simul.*, **6**, 421 (1993).
6. Xie, T.Y.; Hamielec, A. *Macromol. Chem. Theory Simul.*, **6**, 455 (1993).

7. Trommsdorff, E.; Köhle, H.; Lagally, P. *Macromol. Chem.*, **1**, 169 (1948).
8. O'Neil, G.A.; Torkelson, J.M. *Trends in Polym. Sci.*, **5**, 349 (1997).
9. Coote, M.L.; Davis, T.P.; Klumperman, B.; Monteiro, M.J. *J. Macromol. Sci. – Rev. Macromol. Chem. Phys.*, **C38**(4), 199 (1998).
10. Eastmond, G.C. *Comprehensive Chemical Kinetics*, vol. 14A, C.H. Bamford and C.F.H. Tipper, Eds., American Elsevier, New York, 1976.
11. Bamford, C.H. *Radical Polymerization*, pp. 708-867 in *Encyclopedia of Polymer Science and Engineering*, vol. 13, H.F. Mark, N.M. Bikales, C.G. Overberger and G. Menges, Eds., Wiley-Interscience, New York, 1988.
12. Odian, G. *Principles of Polymerization*, Third Edition, John Wiley & Sons, New York, 1991.
13. Walling, C. *J. Am. Chem. Soc.*, **71**, 1930 (1949).
14. Gao, J.; Penlidis, A. *J. Macromol. Sci. – Rev. Macromol. Chem. Phys.*, **C38**(4), 651 (1998).
15. Dubé, M.A.; Soares, J.B.P.; Penlidis, A.; Hamielec, A.E. *Ind. Eng. Chem. Res.*, **36**(4), 966 (1997).
16. Stickler, M.; Panke, D.; Hamielec, A.E. *J. Polym. Sci., Polym. Chem. Ed.*, **22**, 2243 (1984).
17. Russell, G.T.; Napper, D.H.; Gilbert, R.G. *Macromolecules*, **21**(7), 2133 (1988).
18. Ray, W.H. *J. Macromol. Sci., Rev. Macromol. Chem.*, **C8**, 1 (1972).
19. Broadhead, T. O.; Hamielec, A. E.; MacGregor, J. F. *Makromol. Chem., Suppl.*, **10/11**, 105 (1985).
20. Hamielec, A.E.; MacGregor, J.F.; Penlidis, A. *Makromol. Chem., Macromol. Symp.*, **10/11**, 521 (1987).
21. Xie, T.; Hamielec, A.E. *Makromol. Chem., Theory Simul.*, **2**, 421 (1993).
22. Xie, T.; Hamielec, A.E. *Makromol. Chem., Theory Simul.*, **2**, 455 (1993).
23. Kerr, J.A. *Rate Processes in the Gas Phase*, Chap. 1 in *Free Radicals*, vol. 1, J. K. Kochi, Ed., Wiley, New York, 1973.
24. Farina, M. *Makromol. Chem.*, **191**, 2795 (1990).
25. Kondratiev, V.N., *Chain Reactions*, Chap. 2 in Comprehensive Chemical Kinetics, vol. 2, C.H. Bamford and C.F.H. Tipper, Eds., American Elsevier, New York, 1969.
26. Dimarzio, E.A.; Gibbs, J.H. *J. Polym. Sci.*, **XL**, 121 (1959).
27. Barton, J.M. *J. Polym. Sci. Part C*, **30**, 573 (1970).
28. Suzuki, M.; Mathot, V.B.F. *Macromolecules*, 22, 1380 (1989).
29. Gordon, M.; Taylor, J.S. *J. Appl. Chem.*, **2**, 493 (1952).

30. Wood, L.A. *J. Polym. Sci.*, **XXVIII**, 319 (1958).

31. Fox, T.G. *Bull. Am. Phys. Soc.*, **1**, 123 (1956).

32. Johnston, N.W. *Polymer Prep.*, **10**, 608 (1969).

33. Couchman, P.R. *Macromolecules*, **15**, 770 (1982).

34. Mayo, F.R.; Lewis, F.M.J. *J. Am. Chem. Soc.*, **66**, 1954 (1944).

35. Fukuda, M.; Ma, Y.-D.; Inagaki, H. *Macromolecules*, **18**, 17 (1985).

36. Coote, M.L.; Davis, T.P. *Prog. Polym. Sci.*, **24**, 1217 (1999).

37. Burke, A.L.; Duever, T.A.; Penlidis, A. *Ind. Eng. Chem. Res.*, **36**, 1016 (1997).

38. Landry, R.; Duever, T.A.; Penlidis, A. *Polymer Reaction Engineering Journal*, **7**(3), 401 (1999).

39. Harwood, H.J. *Makromol. Chem., Macromol. Symp.*, **10/11**, 311 (1987).

40. Barton, J.; Borsig, E. *Complexes in Free Radical Chemistry*, Elsevier, Amsterdam, 1988.

41. Giese, B.; Engelbrecht, R. *Polym. Bull.*, **12**, 55 (1984).

42. Fukuda, T.; Ma, Y.D.; Inagaki, H. *Makromol. Chem., Rapid Commun.*, **8**, 495 (1987).

43. Heuts, J.P.A.; Gilbert, R.G.; Maxwell, I.A. *Macromolecules*, **30**(4), 726 (1997).

44. Badeen, C. *Modeling Free-Radical Polymerizations with Depropagation using Java™: Methyl Methacrylate/α-methylstyrene at Elevated Temperatures*, M.A.Sc. thesis, Department of Chemical Engineering, University of Ottawa, 2000.

45. Press, W.H.; Teukolsky, S.A.; Vetterling, W.T.; Flannery, B.P. *Numerical Recipes in C: The Art of Scientific Computing*, Second Edition, Cambridge University Press, New York, 1992.

46. http://java.sun.com

47. Radhakrishnan, K.; Hindmarsh, A.C. *Description and Use of LSODE, the Livermore Solver for Ordinary Differential Equations*, Lawrence Livermore National Laboratory, Report UCRL-ID-113855, 1993.

48. Shampine, L.F.; Gear, C.W. *SIAM Rev.*, **21**, 1 (1979).

49. Gear, C.W. *Numerical Initial Value Problems in Ordinary Differential Equations*, Prentice Hall, Englewood Cliffs (NJ), 1971.

Chapter 3: Simulator Validation

Before a program can be used with confidence, it must be validated against experimental data and/or another similar, well-established program. Object-oriented programming allows the use and testing of individual components independently of the others; whenever possible these classes were validated. The `Stifbs` (Bulirsch-Stoer for stiff systems) ODE solver was previously validated by Badeen[50]. Sample equations were tested for proper functioning, as well as the larger components, such as the `Reactor` class. The interaction of the simulator with the various databases was also verified.

Due to the complexity of the polymerization model, an analytical solution cannot be derived for the overall system. Initially, as a guideline, the outputs of the simulator were compared with the outputs from WatPoly, a Fortran-based polymerization simulator developed by Gao and Penlidis[51,52]. They used a similar model to generate their simulation data, and their simulator has been tested against a broad range of experimental data. Trends for both simulators were in excellent agreement: the resulting curves were overlapping, which is expected since the same database values were used.

The simulator was tested extensively against a variety of homopolymers. Two of these, which are well-known and have different characteristics, are shown here as an example: methyl methacrylate (MMA) and styrene (Sty). Table 3.1 lists the reaction conditions used for the 3 MMA runs[53] and the 2 styrene runs[54,55], where AIBN was used as the initiator and toluene was the solvent, when applicable.

Table 3.1: Experimental conditions for the MMA and Sty homopolymer validation.

Monomer	AIBN	Toluene	Temperature
MMA	0.3 wt.%	—	323 K
MMA	0.3 wt.%	—	343 K
MMA	0.3 wt.%	—	363 K
Sty	0.05 mol/L	—	343 K
Sty	0.04 mol/L	1.8 mol/L	343 K

In Figure 3.1, the MMA data is well predicted up to a conversion of approximately 80 wt.%, where the model levels off prematurely, more so at higher temperatures. Non-isothermal operation is likely the cause of this discrepancy. The model for Sty provides excellent agreement with the experimental data, as shown in Figure 3.2.

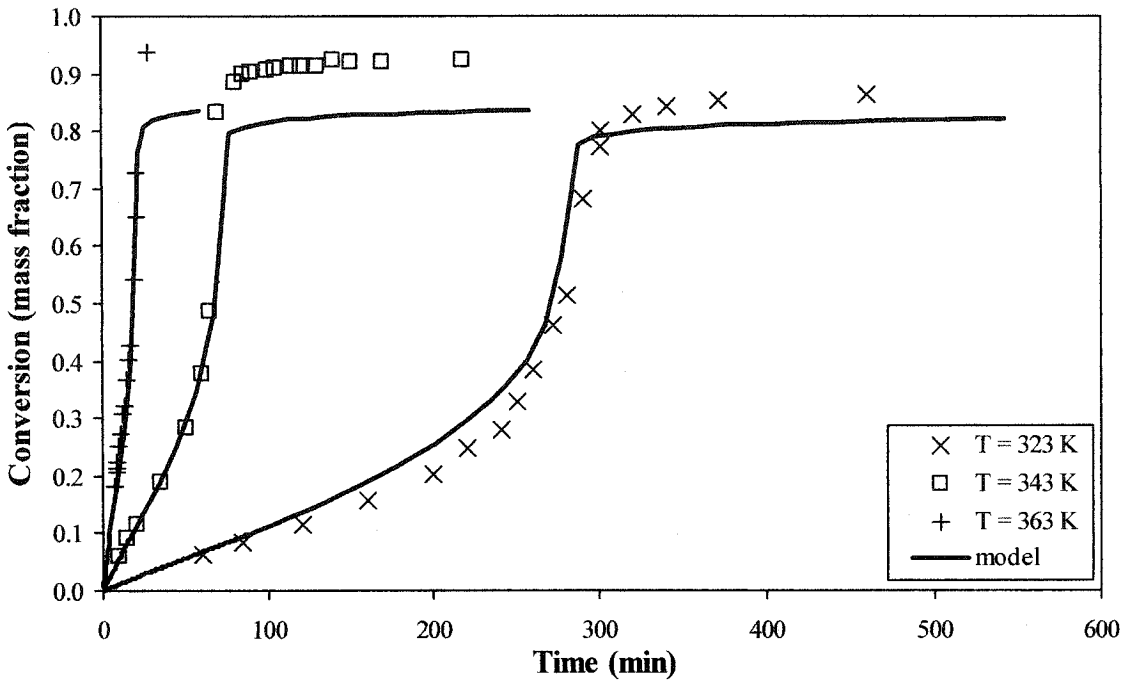

Figure 3.1: Validating the simulator using conversion data for bulk MMA homopolymer initiated with 0.3 wt.% AIBN.

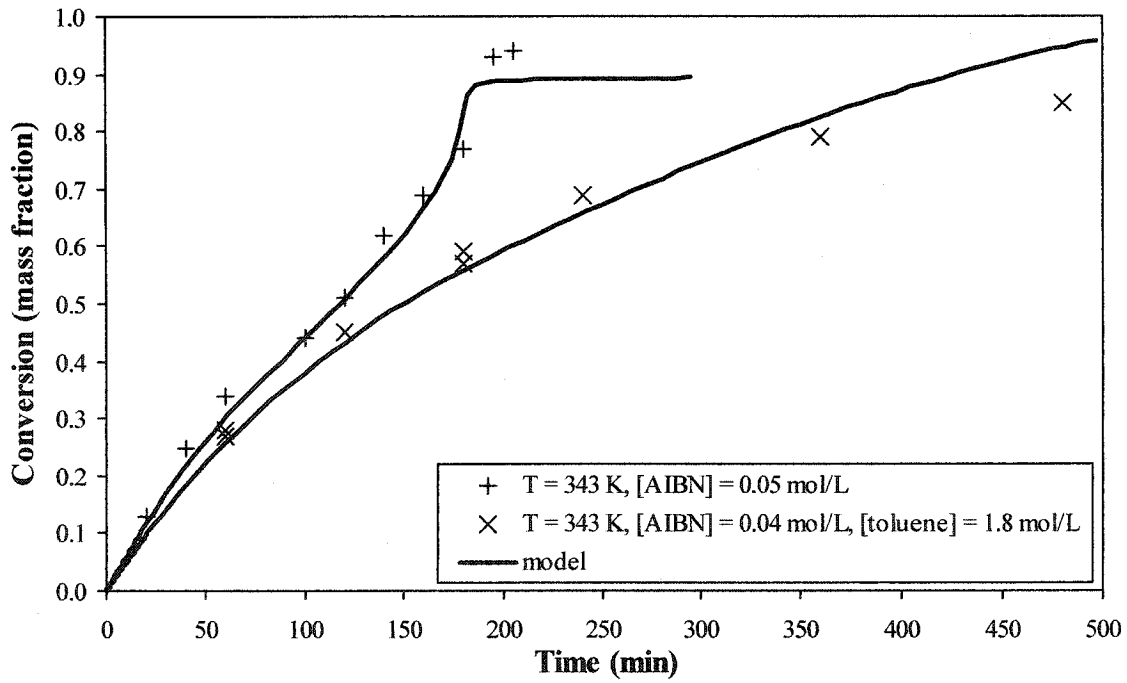

Figure 3.2: Validating the simulator using conversion data for bulk and solution Sty homopolymer.

References

50. Badeen, C. *Modeling Free-Radical Polymerizations with Depropagation using Java™: Methyl Methacrylate/α-methylstyrene at Elevated Temperatures*, M.A.Sc. thesis, Department of Chemical Engineering, University of Ottawa, 2000.
51. Gao, J.; Penlidis, A. *J. Macromol. Sci. – Rev. Macromol. Chem. Phys.*, **36**(2), 199 (1996).
52. Gao, J.; Penlidis, A. *J. Macromol. Sci. – Rev. Macromol. Chem. Phys.*, **38**(4), 651 (1998).
53. Balke, T.; Hamielec, A.E. *J. Appl. Polym. Sci.*, **17**, 905 (1973).
54. Marten, F.L.; Hamielec, A.E. *J. Appl. Polym. Sci.*, **27**, 489 (1982).
55. Nishimura, N. *J. Macromol. Sci.*, **1**, 257 (1966).

Chapter 4: Paper 1

The Solvent Effect on the Solution Copolymerization of Butyl Acrylate and Vinyl Acetate in Toluene

Marc Laplante and Marc A. Dubé*
Department of Chemical Engineering, University of Ottawa,
161 Louis Pasteur St., Ottawa ON, K1N 6N5 Canada
** dube@eng.uottawa.ca*

Abstract

The solvent effect of toluene on the butyl acrylate (BA) and vinyl acetate (VAc) homopolymerizations and copolymerization was investigated. Data were collected at different solvent concentrations, as well as a variety of BA:VAc ratios in the case of the BA/VAc copolymer. Conversion, cumulative copolymer composition, as well as cumulative weight-average molecular weight data are presented for all cases. Corresponding model predictions are also given. The lumped kinetic rate constant, $k_p/k_t^{0.5}$, decreased with an increase in toluene concentration, resulting in significant improvements in predicting conversion data, which confirms the presence of a solvent effect on the termination reaction. Preliminary results indicate the possible presence of solvent effects on monomer reactivity ratios. The BA reactivity ratio was varied with the solvent concentration, which improved cumulative copolymer composition and conversion predictions. There appears to be a solvent effect on both the propagation and termination reactions, but more accurate measurements of the individual BA and VAc rate constants are required to elucidate the solvent effect.

Introduction

Vinyl acetate (VAc) monomer is used as raw material for polymers having a wide variety of applications, including adhesives, paints, coatings and sealants. In many cases, the VAc properties are enhanced through its copolymerization with other monomers. One such case is the copolymer of vinyl acetate and butyl acrylate (BA), which is commonly used in the paint industry. The final properties of the polymer are dependent on the copolymer composition, molecular weight and the molecular weight distribution. The

individual monomer reactivities have an important impact on these polymer characteristics.

The BA and VAc monomers have significantly different reactivities, resulting in composition drift. The monomer having the highest reactivity, i.e. BA, is preferentially consumed in the early stages of the reaction, producing polymer chains rich in BA. Once the BA is depleted, what remains of the VAc monomer is polymerized, resulting in chains rich in VAc. Consequently, the final product has a distribution of compositions and microstructures. The tendency of monomer *j* to add itself to the polymer chain ending in monomer *i* is evaluated through the reactivity ratio, r_{ij}, which is a parameter in the Mayo-Lewis[56] equation (the terminal model). The reactivity ratios for BA and VAc are $r_{BA,VAc}$ = 5.94 and $r_{VAc,BA}$ = 0.0262, respectively[57]. One approach to control this composition drift is to operate the reactor in semi-batch mode, feeding the more reactive monomer gradually, to ensure a more uniform polymer composition. Coupled with on-line monitoring of the monomer concentrations, semi-batch policies are often used to accomplish this.[58] On the other hand, when batch reactions are conducted, it is necessary to have a model to predict composition drift.

A number of models have been developed to simulate free-radical homo- and copolymerizations, some of which are competing while others are simply extensions to some of these models.[59,60,61] Developed by Laplante,[59] the simulator used for this study is Java™-based, designed for multi-component free-radical polymerizations in bulk and solution. The free volume theory[62] was used to describe the kinetic behaviour of homo- and copolymerizations at high conversion, and the pseudo-kinetic rate constant approach was implemented.[58]

Few investigations have been conducted into the solution homo- and copolymerization of BA and VAc in toluene. Recent studies, including efforts by McKenna *et al.*,[63] McKenna and Villanueva,[64] Othman[65] and Jovanovic and Dubé,[66] have described the significance of radical-solvent effects for these ingredients. The importance of understanding radical-solvent interactions becomes apparent when attempting to model the solution copolymerization of BA and VAc in aromatic solvents, such as toluene. The addition of solvent introduces another level of complexity into the model.

The propagation and termination rate constants (k_p and k_t, respectively) may both be affected by the presence of the solvent.

A solvent can affect the propagation kinetics in free-radical polymerization reactions via several different means. Coote *et al.*[67] enumerated the following possible mechanisms: the polarity effect, radical-solvent complexes, monomer-solvent complexes, and the bootstrap model. In the case of vinyl monomers, it is generally believed that the predominant factor is the formation of complexes between the propagating radicals and the solvent.[67,68] When polar interactions in the transition structure of the propagation reaction are significant, a polar solvent can stabilize an unstable radical intermediate, such as VAc. The result would be a reduction in the reaction barrier, or in other words, a decrease in the propagation rate constant.[69]

In the case of termination kinetics, it is now widely accepted that the diffusion-controlled rate constant is chain-length dependent.[70,71,72,73] Shorter chains can move more freely, and can therefore terminate more easily. As the solvent concentration increases, so does the termination rate constant when transfer to solvent is severe.[63,64]

Determining propagation and termination rate constants for BA and VAc exactly is not yet possible with today's technology, even when using pulsed laser polymerization techniques.[74] Due to these obstacles in understanding the solvent effect on the propagation and termination reactions, it is useful to combine both effects and estimate the *lumped kinetic constant*, i.e. the ratio of the propagation rate constant to the square root of the termination rate constant, $k_p/k_t^{0.5}$. The term $k_p/k_t^{0.5}$ appears in the rate of polymerization expression, R_p, which is known to be affected by the presence of solvent. McKenna *et al.*[63] and McKenna and Villanueva[64] used this approach for the solution homopolymerizations of BA and VAc in toluene and ethyl acetate, and the copolymerization of BA/VAc in ethyl acetate.

Experimental

The procedures employed to obtain experimental data were identical to that of Jovanovic and Dubé,[66] and are summarized here.

Reagents

The BA and VAc monomers were received inhibited by hydroquinone, and were subsequently purified appropriately. Toluene was used as solvent, 2,2'-azobisisobutyronitrile (AIBN) was the initiator, and n-dodecyl mercaptan was the chain transfer agent (CTA).

Procedures

The polymerization reactions were carried out in 5-mL glass ampoules, at a temperature of 60°C. Ampoules were removed and analyzed at predetermined sampling times. Gravimetric analysis of the consumption of monomer was used to estimate the conversion on a mass basis. In the case of copolymers, the sample was subsequently analyzed for cumulative copolymer composition using proton nuclear magnetic resonance (^{1}H-NMR) spectroscopy. The cumulative weight- and number-average molecular weights were determined using gel permeation chromatography (GPC).

Instrumentation

Cumulative copolymer compositions were obtained through spectra taken by a Bruker AMX-500 Fourier-transform ^{1}H-NMR spectrometer. The cumulative number- and weight-average molecular weights were determined with a Waters Associates GPC system equipped with three Waters Styragel-HR columns (10^3, 10^4, and 10^6 Å pore size) installed in series, thermostated to 30°C, and a Waters 410 differential refractometer thermostated to 38°C. Tetrahydrofuran (THF) was used as the eluent at a flow rate of 0.3 ml/min.

The cumulative number- and weight-average molecular weights were determined using a universal calibration curve. The Mark-Houwink K and α parameters determined in THF are given in Table 4.1. For the copolymers, the weighted averages of these parameters were calculated using the cumulative copolymer composition data obtained through ^{1}H-NMR spectroscopy.

Table 4.1: Mark-Houwink K and α parameters

Polymer	K (mL/g)	α	Reference
poly(butyl acrylate)	0.0110	0.708	63
poly(vinyl acetate)	0.0156	0.708	75
polystyrene	0.0160	0.700	76

Results and Discussion

BA and VAc homopolymers: Experimental data

Two sets of homopolymerization runs were carried out to assess the effect of solvent on the monomer conversion for BA and VAc. The reaction conditions for these runs are listed in Table 4.2.

Table 4.2: Experimental conditions for homopolymer solvent effect study

BA (wt.%)	VAc (wt.%)	Toluene (wt.%)	Initiator (mol/L)	CTA (mol/L)
100	0	0	0.001	0
70	0	30	0.002	0
50	0	50	0.002	0
20	0	80	0.002	0
0	70	30	0.002	0.02
0	50	50	0.002	0.02
0	20	80	0.002	0.02

The BA conversion data, shown in Figure 4.1, show a decrease in conversion with time as the toluene concentration is increased. A similar trend can be seen for VAc in Figure 4.2. These observations are in agreement with Coote *et al.*'s[67] statement that the rate constants are affected by the presence of a solvent within the reaction mixture. Comparing both figures, the conversion for the BA homopolymer is greater than that of its VAc counterpart. Furthermore, the solvent effect is more pronounced for VAc than for BA, which was also reported by McKenna *et al.*[63] and McKenna and Villanueva.[64]

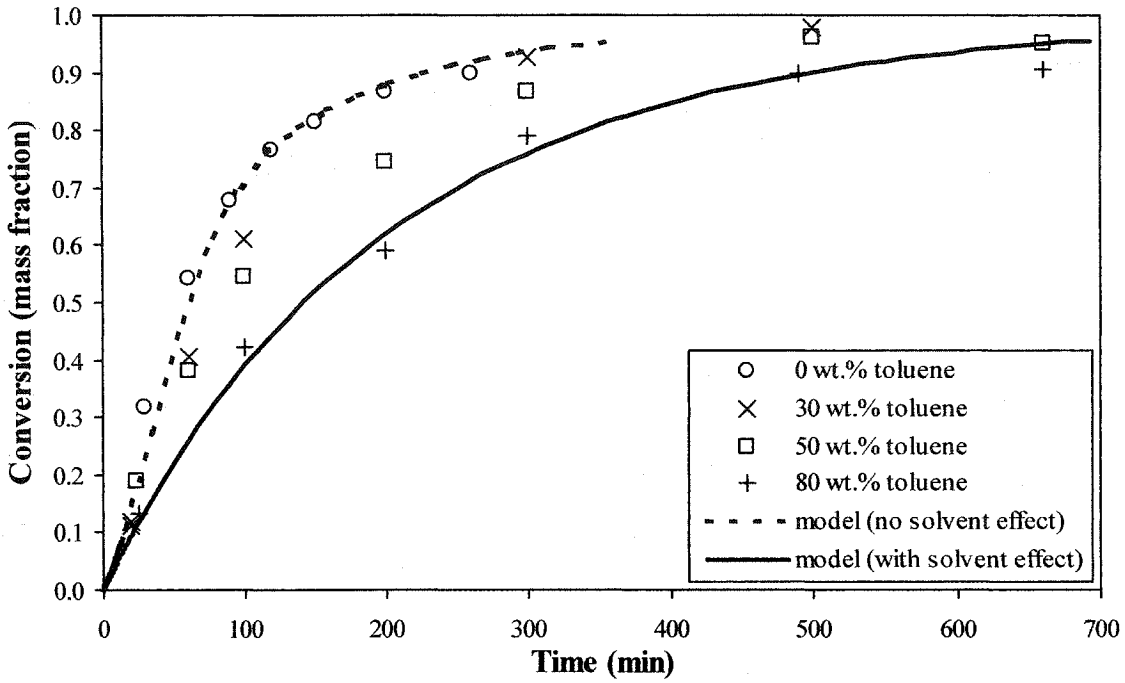

Figure 4.1: Solvent effect on conversion versus time at various solvent concentrations for BA in toluene.

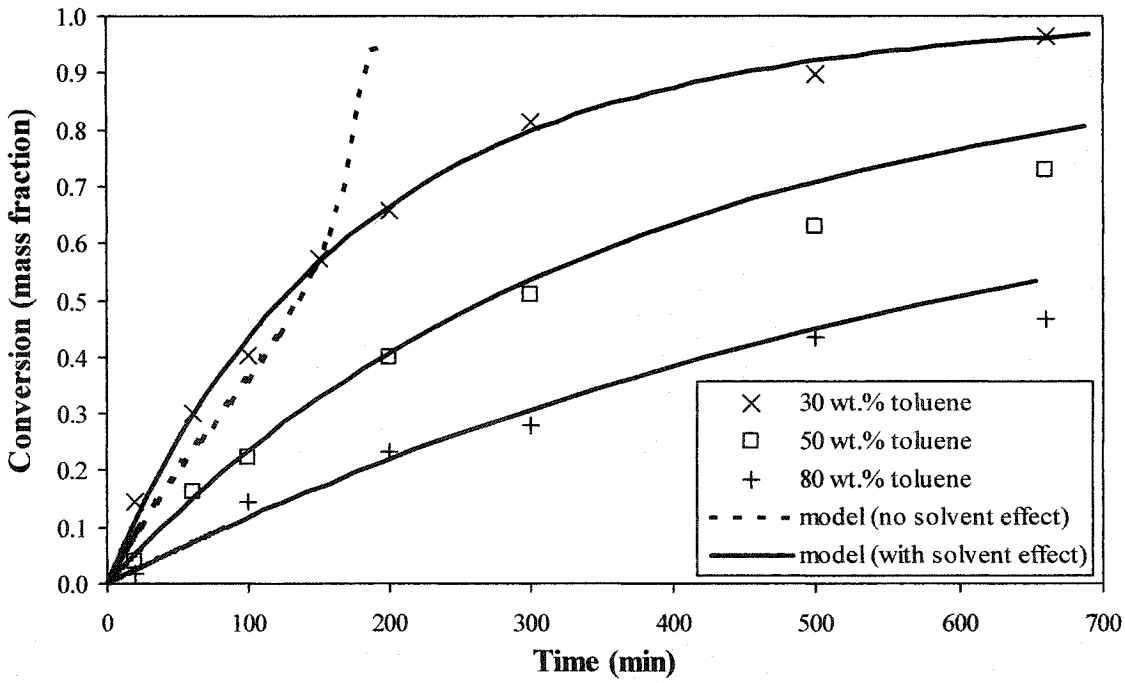

Figure 4.2: Solvent effect on conversion versus time at various solvent concentrations for VAc in toluene.

In Figure 4.3, the cumulative-weight average molecular weight for BA decreased with an increase in the solvent concentration. VAc exhibits a similar tendency, albeit slightly larger, as shown in Figure 4.4. Under similar conditions, the BA homopolymerizations produced a polymer mixture with greater molecular weight (roughly one order of magnitude) when compared to VAc. These observations are consistent with an increase in transfer to solvent. In Figure 4.3, a positive slope indicates that k_t dominates the molecular weight equations calculated in section 2.1.8, while a negative slope implies that chain transfer becomes the dominant factor.

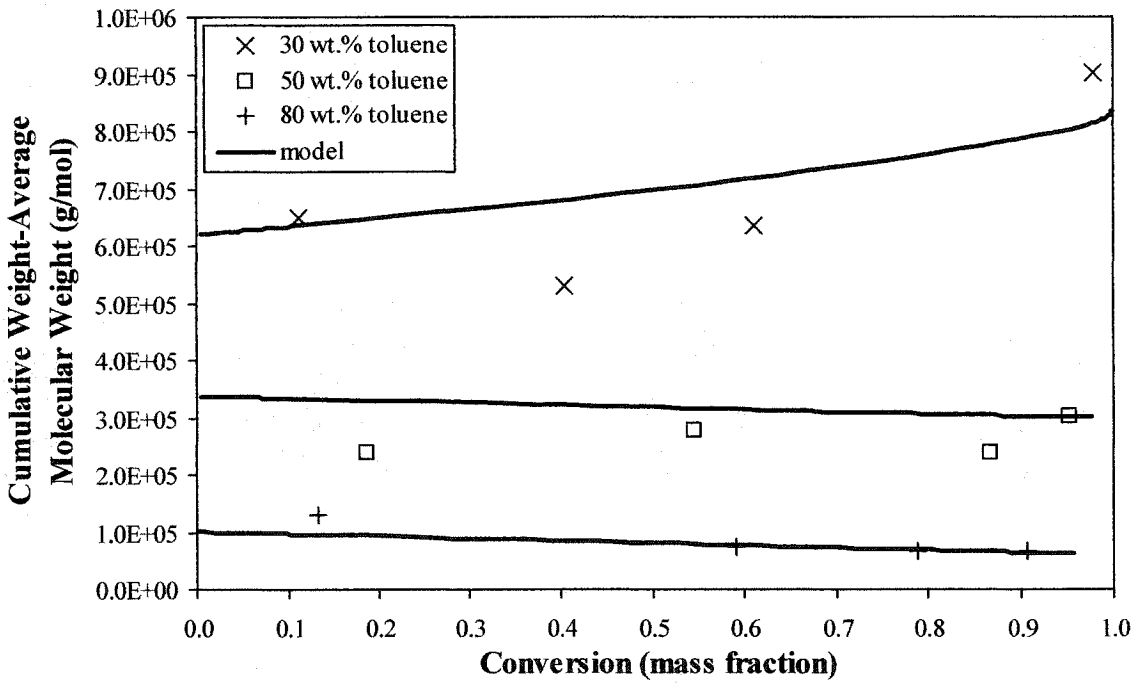

Figure 4.3: Solvent effect on the cumulative weight-average molecular weight versus conversion at various solvent concentrations for BA in toluene.

The effect of chain transfer agent (CTA) on the BA and VAc homopolymers was also examined. Each monomer was polymerized in 30, 50 and 80 wt.% toluene, and each of these was run using three CTA concentrations. Two of these sets were selected for demonstration; the reaction conditions used appear in Table 4.3. As Figure 4.5 illustrates, a changing concentration of CTA has no significant impact on both the BA and VAc monomer conversions. Similarly, no noticeable trends are observed with the other four sets of data. The effect of CTA on the cumulative weight-average molecular weight of

BA in 30 wt.% toluene is demonstrated in Figure 4.6. A CTA is used to increase the transfer of propagating radicals from the growing chains to the CTA itself, thereby terminating the growing chains prematurely. The result is a decrease in the molecular weight of the mixture due to these shorter chains. Figure 4.6 clearly demonstrates this, with a substantial decrease in the cumulative weight-average molecular weight corresponding to an increase in the CTA concentration.

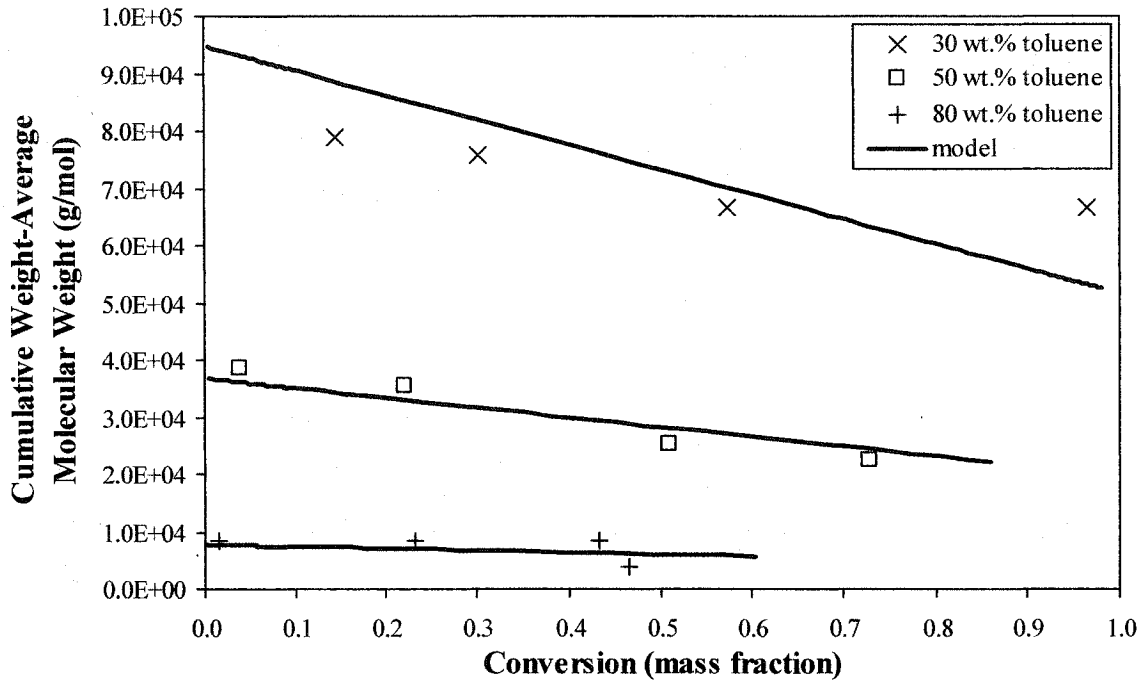

Figure 4.4: Solvent effect on the cumulative weight-average molecular weight versus conversion at various solvent concentrations for VAc in toluene.

Table 4.3: Experimental conditions for CTA effect study

BA (wt.%)	VAc (wt.%)	Toluene (wt.%)	Initiator (mol/L)	CTA (mol/L)
70	0	30	0.002	0
70	0	30	0.002	0.02
70	0	30	0.002	0.06
0	50	50	0.002	0
0	50	50	0.002	0.02
0	50	50	0.002	0.06

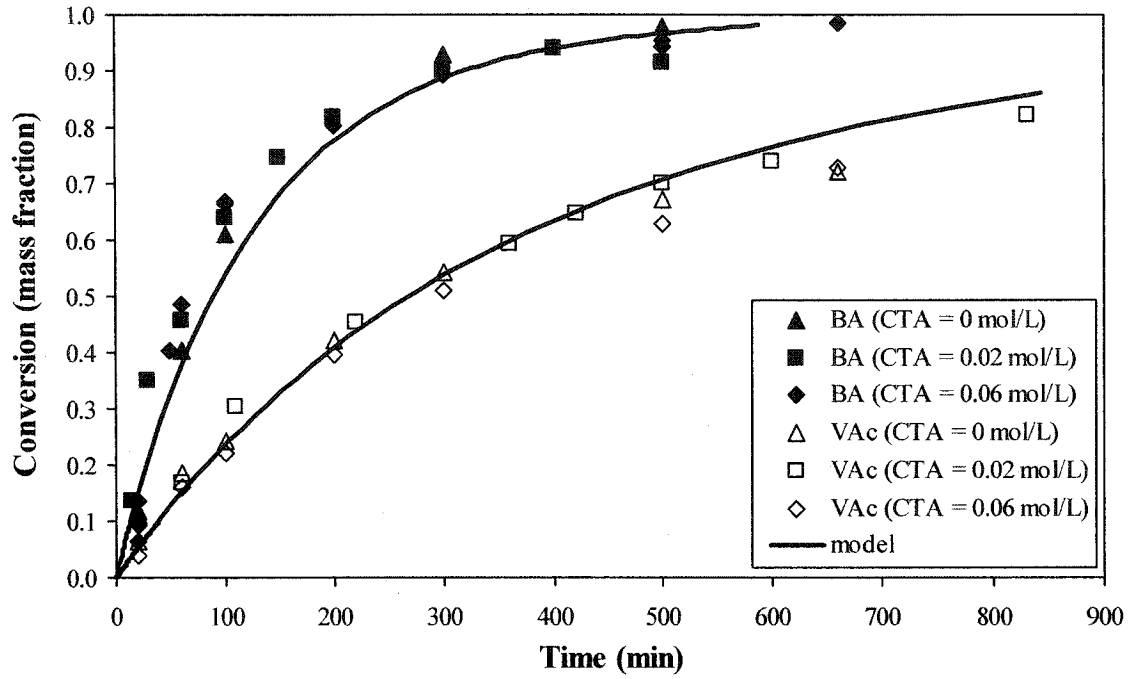

Figure 4.5: Effect of CTA on conversion for BA and VAc homopolymers in toluene. BA:toluene = 70:30 wt.%, VAc:toluene = 50:50 wt.%. Model lines for the three CTA concentrations overlap.

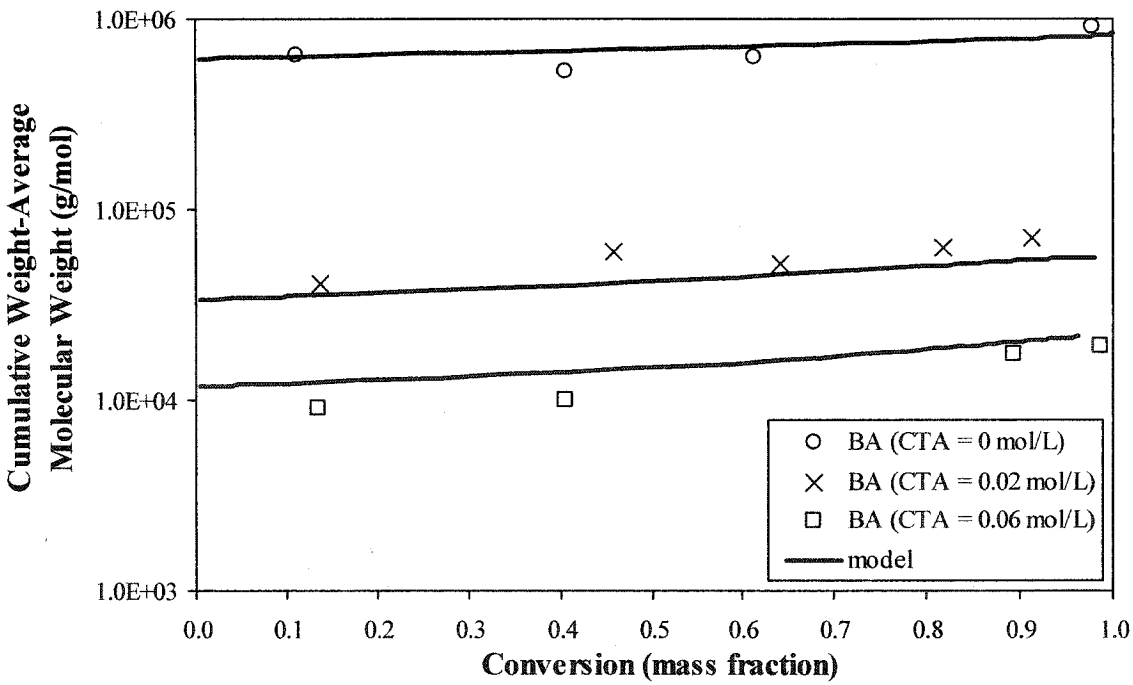

Figure 4.6: Effect of CTA on the cumulative weight-average molecular weight for BA homopolymers in toluene. BA:toluene = 70:30 wt.%.

BA and VAc homopolymers: Modelling

First, simulations were run without accounting for the effect of the solvent. Figure 4.1 and Figure 4.2 show the conversion curves (dashed line) for bulk BA and VAc homopolymers, respectively. Examining Figure 4.1, it can be seen that the model predicts the 0 wt.% toluene concentration data well.

Subsequently, the solvent effect was incorporated into the model. The procedure, recently used by McKenna *et al.*[63] and McKenna and Villanueva,[64] consists of modifying the initial termination rate constant, k_t, to achieve the best conversion-time fit to the data. In this case, the pre-exponential factor in the Arrhenius expression for k_t was modified, leaving the activation energy unchanged. This approach was performed for multiple runs, finding overall optimal k_t values at a given solvent concentration. The procedure was then repeated for the other solvent concentrations. Previously published data at 50 wt.% toluene[66] were included in the analysis. Modelling was performed for each solvent concentration conducted experimentally, i.e. [toluene] = 30, 50 and 80 wt.%. As previously mentioned, because solvent effects on the termination and propagation reactions are possibly occurring simultaneously, the propagation rate constant, k_p, is combined with k_t to form the lumped kinetic constant, $k_p/k_t^{0.5}$.

The values resulting from the k_t fitting are presented using the lumped kinetic constant, and appear in Figure 4.7. It can be seen that the presence of toluene significantly decreases the calculated lumped kinetic constant, and greater solvent concentrations further decrease its value. This phenomenon can be explained by the chain-length dependence of k_t.[70] Chain transfer to solvent reactions are responsible for a significant number of short chain radicals. Shorter radical chains can move more freely, and therefore can terminate more easily, which results in higher k_t values, and thus lower lumped kinetic constant values as the solvent concentration increases. Furthermore, the effect is more pronounced with VAc. It is recognized that VAc polymerizations are impeded by aromatic solvents such as toluene.[67] The solvent effect on the lumped kinetic constant as well as the greater retardant effect of toluene on VAc polymerizations were reported by McKenna *et al.*[63] and McKenna and Villanueva,[64] who observed the effect on BA and VAc homopolymerizations in both toluene and benzene.

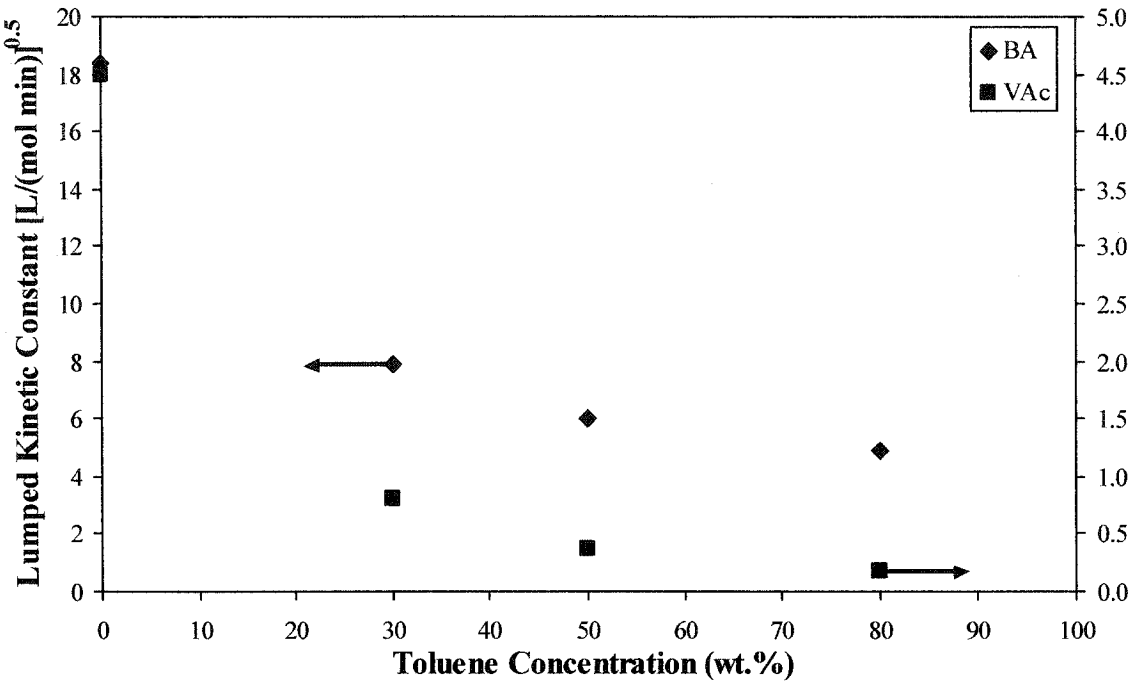

Figure 4.7: Solvent effect on the lumped kinetic constant for BA and VAc at 60°C.

Because of the closeness of the data points in Figure 4.1, only the 80 wt.% toluene model for BA is shown for clarity. Figure 4.2 contains all three toluene concentrations for VAc. In all cases, adjusting the k_t values resulted in an excellent fit to the data, accounting for the solvent effect.

In Figure 4.3 and Figure 4.4, the cumulative-weight average molecular weights for BA and VAc, respectively, are well predicted. The transfer constants used to obtain these results are the same for all three solvent concentrations for the solution polymerization runs, as well as for the bulk polymerization runs. All reported values for transfer constants are taken at 60°C.

In the case of BA, the transfer to monomer constant, $C_{f,M}$ (ratio of k_p over the transfer to monomer rate constant, $k_{f,M}$), was 1.46×10^{-4}. McKenna *et al.*[63] reported a $C_{f,M}$ of 1.0×10^{-4}, while a value of 6.6×10^{-5} was obtained through the use of Maeder and Gilbert's[77] results. The constant for the transfer of BA to the toluene solvent, $C_{f,S}$ (ratio of k_p over the transfer to solvent rate constant, $k_{f,S}$), was 4.1×10^{-4}, compared to a value of 1.8×10^{-4} reported by McKenna *et al.*[63] The BA transfer to CTA constant, $C_{f,CTA}$ (ratio of k_p over the transfer to CTA rate constant, $k_{f,CTA}$), was 1.7. De la Fuente and Madruga[78]

reported values of 0.455–1.056 for the copolymerization of BA with methyl methacrylate using n-dodecyl mercaptan as CTA.

The $C_{f,M}$ value for VAc homopolymerizations was 1.75×10^{-4}, which is at the lower boundary of the interval of $1.75–2.8 \times 10^{-4}$ listed in the Polymer Handbook.[75] The value used for $C_{f,S}$ was 2.1×10^{-3}, which is at the lower end of the range $(2.1–3.4) \times 10^{-3}$ reported by Ham.[79] A $C_{f,CTA}$ value of 3.5 was obtained for VAc.

In Figure 4.5, it is apparent that the model provides an adequate fit to the experimental data. It should be noted that the resulting model curves were virtually identical irrespective of the amount of CTA input into the simulation recipe, for a given monomer. The model fit was adequate for the cumulative weight-average molecular weight for the BA homopolymer, shown in Figure 4.6. Similar agreement was achieved for the case of VAc homopolymer.

BA/VAc copolymer: Experimental data and modelling

Table 4.4 lists the reaction conditions for the eight solution BA/VAc copolymerization runs that were conducted. One set was carried out in 80 wt.% toluene, while the other, which contained a replicate run, was carried out in 30 wt.% toluene. In both cases, varying BA:VAc ratios were investigated.

Table 4.4: Experimental conditions for the copolymer solvent effect study

BA (wt.%)	**VAc** (wt.%)	**Toluene** (wt.%)	**Initiator** (mol/L)	**CTA** (mol/L)
8	12	80	0.064	0.02
10	10	80	0.037	0.02
12	8	80	0.021	0.02
14	6	80	0.008	0.02
28	42	30	0.025	0.02
28 *	42	30	0.025	0.02
35	35	30	0.016	0.02
42	28	30	0.008	0.02

* replicate run

Aside from the work of McKenna and Heredia,[80] who used ethyl acetate as solvent, recent work on the solution copolymerization of BA with VAc is scarce. The method used to model the BA/VAc copolymerization data in this work was as follows. The BA and VAc homopolymerization rate constants were applied to the copolymerizations without adjustment. The pseudo-kinetic rate constant approach was employed to obtain overall weighted values for the various BA/VAc rate constants. Therefore, for each solvent concentration, corresponding copolymer termination rate constants were obtained.

In Figure 4.8, the BA cumulative copolymer composition, F_{cumul}, is presented as a function of conversion, for four different BA:VAc ratios, increasing from a) to d) for a solvent concentration of 80 wt.%. Figure 4.9 shows the corresponding plots for three different BA:VAc ratios in 30 wt.% toluene, increasing from a) to c), the fourth run being a replicate run. Obviously, the cumulative copolymer composition increases with an increasing BA:VAc ratio. With more BA available for polymerization, the produced chains are richer in BA. Also, at low conversions, the polymer chains are richer in BA due to its higher reactivity ratio compared to that of VAc. As the reaction progresses, BA monomer is consumed, reducing the BA:VAc ratio remaining in the reaction mixture, which reduces the BA cumulative copolymer composition. Also, an increase in solvent concentration results in a slight increase in F_{cumul}, which may be a sign of solvent effect on the propagation reaction.

It can be seen from Figure 4.8 that the inclusion of the solvent effect does not significantly affect F_{cumul}. The model without solvent effect ("no S.E.") is very close to that with solvent effect on k_t ("S.E. on k_t"), both of which underestimating F_{cumul}. Since significant radical-solvent effects are known to take place between the monomers and aromatic solvents,[67,68] an impact on the propagation reaction can be expected. With that in mind, it was decided to modify the BA reactivity ratio, $r_{BA,VAc}$, to improve the model fit. It should be noted that the following is merely a rough investigation performed to gain insight into the solvent effect on $r_{BA,VAc}$. No monomer reactivity ratio estimation was performed. Modelling was used as a tool to guide future work.

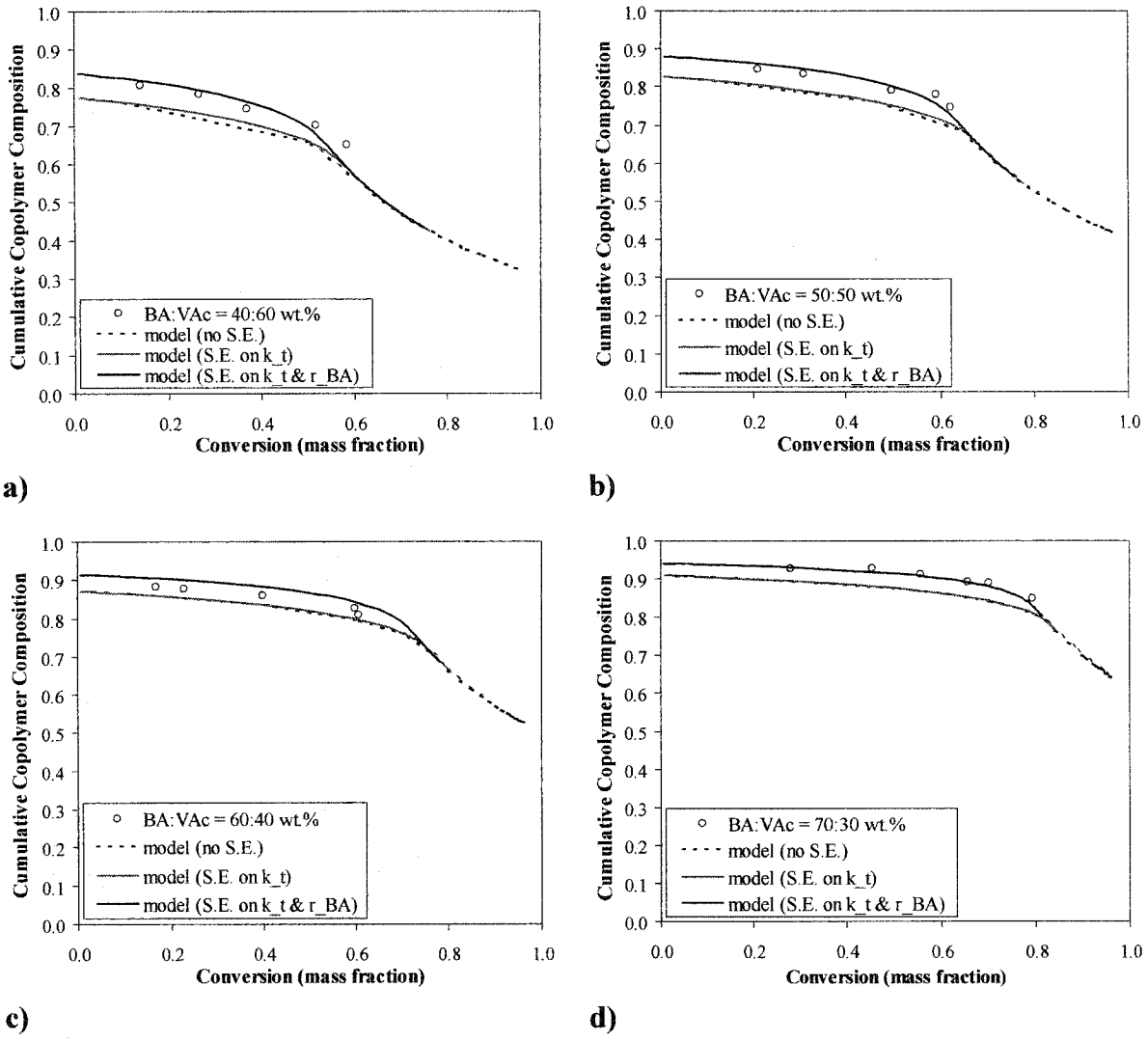

Figure 4.8: Solvent effect (S.E.) on the BA-VAc copolymers in 80 wt.% toluene at various BA:VAc ratios, evaluated using the cumulative copolymer composition of BA.

Compared to the bulk value of 5.94 for $r_{BA,VAc}$, values of 10.0 and 8.0 were found to provide better fits to the data for the F_{cumul} curves for toluene concentrations of 80 and 30 wt.%, respectively. As can be expected, the effect of solvent on F_{cumul} is greater for higher solvent concentrations, which can be seen by comparing Figure 4.8 and Figure 4.9. An increase in $r_{BA,VAc}$ results in a decrease in the overall copolymer k_p, as can be seen from equations (2.12) and (2.14). This is consistent with the findings of Kamachi *et al.*,[81] who reported that solvent effects on VAc homopolymerization caused a reduction of k_p.

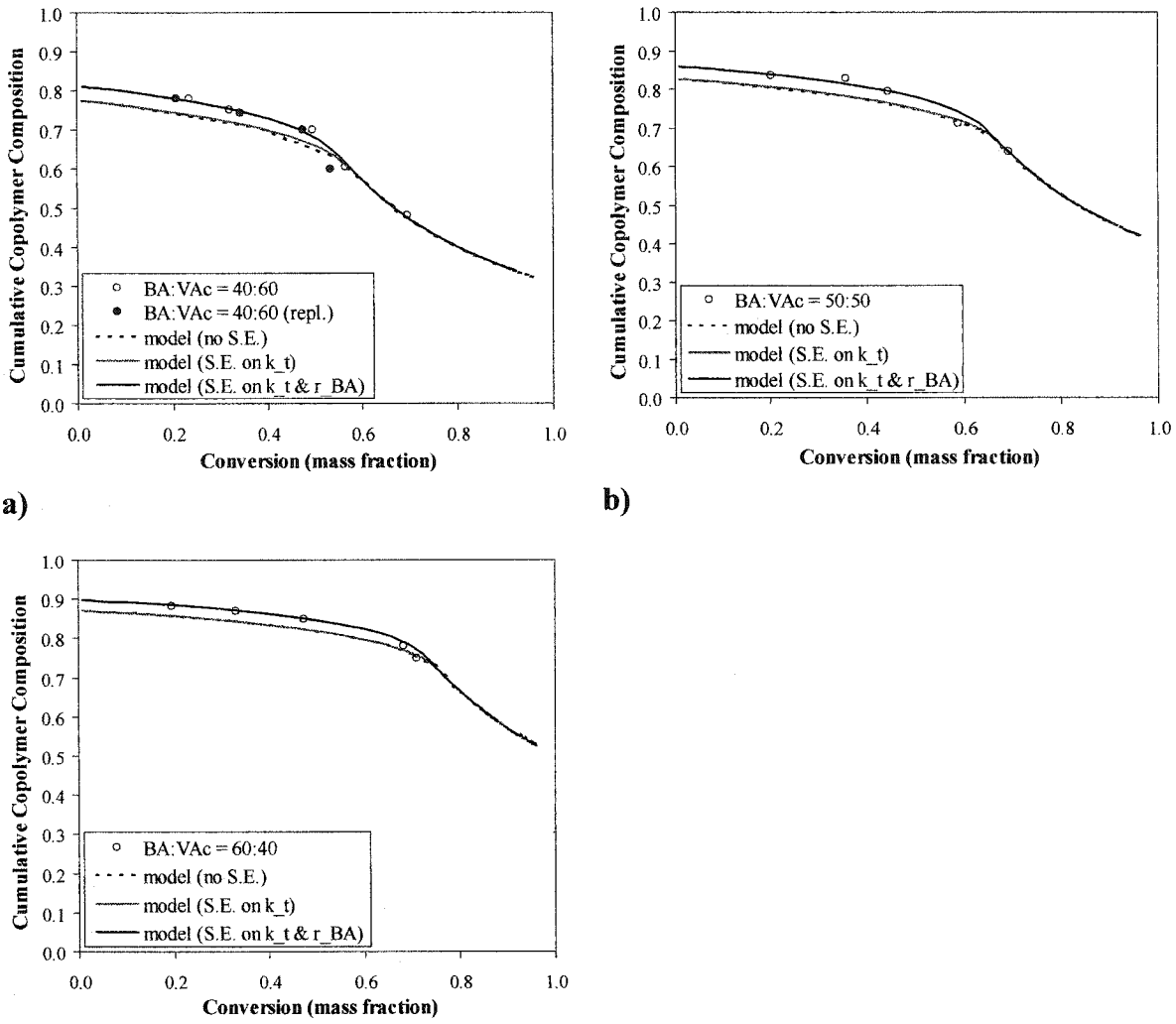

Figure 4.9: Solvent effect (S.E.) on the BA-VAc copolymers in 30 wt.% toluene at various BA:VAc ratios, evaluated using the cumulative copolymer composition of BA.

In Figure 4.10 and Figure 4.11, the overall conversion as a function of time for varying BA:VAc ratios is presented for toluene concentrations of 80 and 30 wt.%, respectively. Both figures confirmed that an increase in the BA:VAc ratio resulted in an increase in the conversion. This is consistent with the homopolymerization data, where the BA homopolymer resulted in higher conversions relative to its VAc counterpart under similar conditions. Both figures clearly show a vast improvement for the overall conversion when adding the solvent effect on k_t compared to no solvent effect. In the

former case, the fit is adequate, but the conversions are consistently overestimated. The change in $r_{BA,VAc}$ conducted to improve the F_{cumul} fit results in a further improvement in the conversion fit, although conversions remain slightly overestimated. The impact of the solvent effect on the reactivity ratio is slightly more pronounced at higher toluene concentrations.

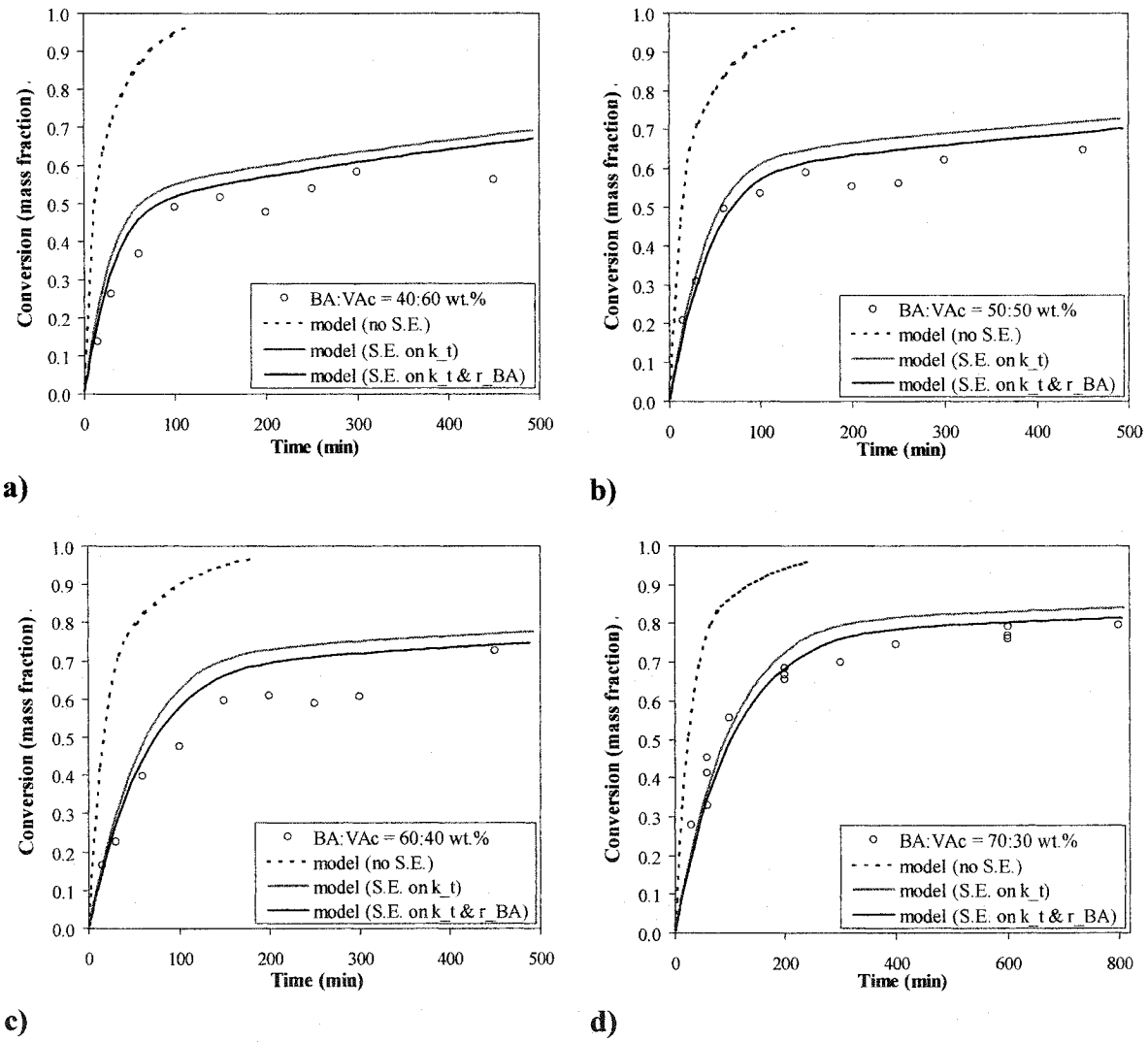

Figure 4.10: Solvent effect (S.E.) on the BA-VAc copolymers in 80 wt.% toluene at various BA:VAc ratios, evaluated using the overall conversion.

These findings appear to indicate that toluene has an effect on the BA/VAc reactivity ratios, which would subsequently modify the values of the cross-propagation rate constants, $k_{p,ij}$. This solvent effect on reactivity ratios was reported by de la Fuente

and Madruga[82] for BA and methyl methacrylate, where the monomer reactivity ratios varied according to the solvent present in the reaction medium. They compared their results using benzonitrile as solvent with other works using toluene, benzene and no solvent, and found that all fours cases provided considerably different reactivity ratios. Fernandez *et al.*[83] also reported a slight solvent effect on monomer reactivity ratios for the copolymerization of styrene with BA. Their results in benzene were observable, but not statistically significant.

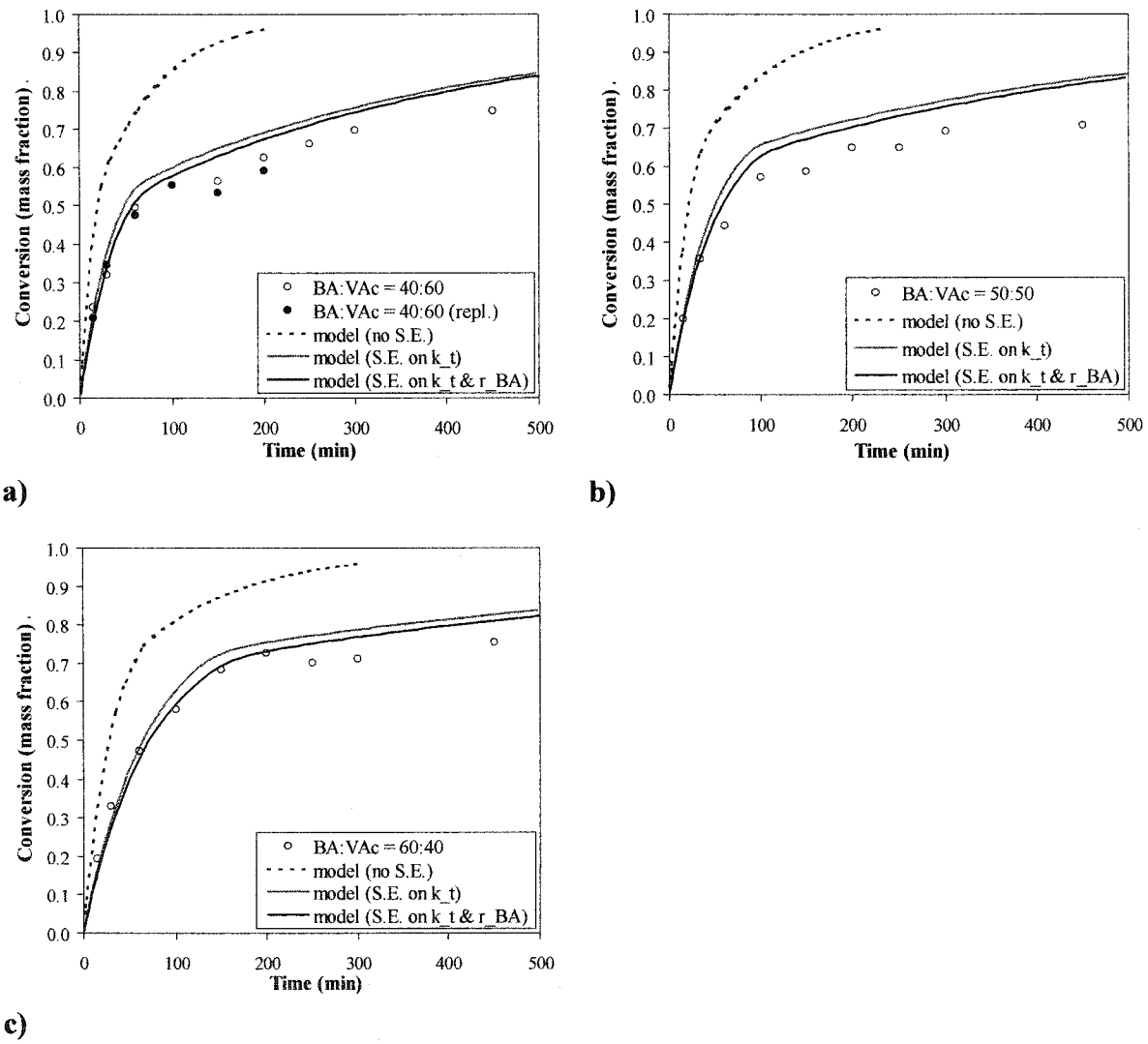

Figure 4.11: Solvent effect (S.E.) on the BA-VAc copolymers in 30 wt.% toluene at various BA:VAc ratios, evaluated using the overall conversion.

These rough simulations indicate that modified reactivity ratio values improve the model-to-data fit for F_{cumul} versus conversion plots, while also slightly improving the fit for conversion versus time plots. Although these results may not be significant, the power of modelling has allowed some preliminary work to be conducted, and direct further research. In order to draw definite conclusions that there is indeed such a solvent effect on the monomer reactivity ratios, experimental reactivity ratio estimation in solvent needs to be performed.

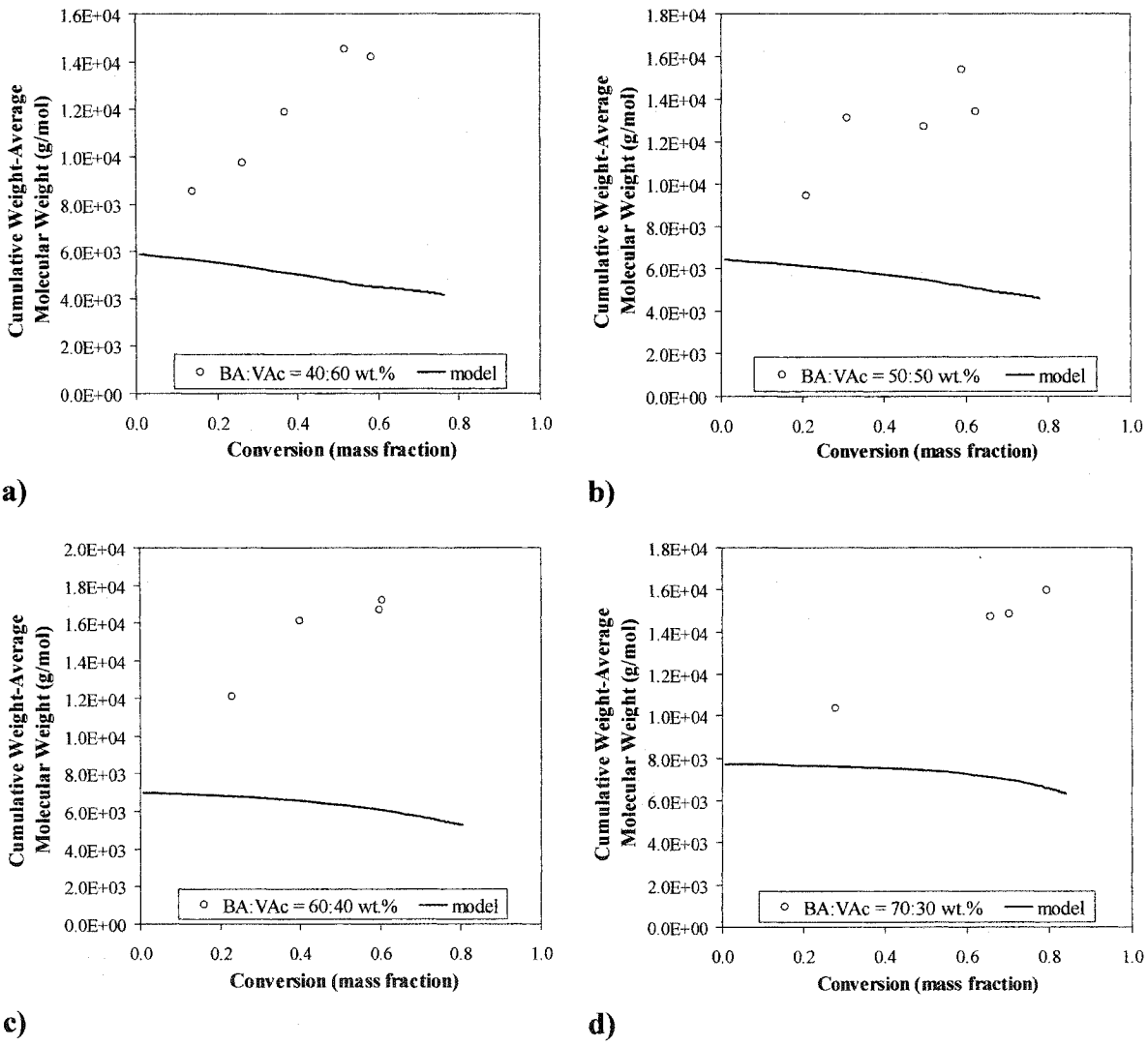

Figure 4.12: Solvent effect (S.E.) on the BA-VAc copolymers in 80 wt.% toluene at various BA:VAc ratios, evaluated using the cumulative weight-average molecular weight.

Figure 4.12 and Figure 4.13 show the cumulative weight-average molecular weight, $\overline{M}_w$, as a function of conversion for toluene concentrations of 80 and 30 wt.%, respectively. In both cases, no apparent trend is noticeable as the BA:VAc ratio increases. One possible explanation is that the molecular weights may be governed some mechanism other than termination. Transfer to polymer is suspected, but no measurements of branching are available. It is, however, clear that higher solvent concentrations result in lower $\overline{M}_w$ values. As with the homopolymers, this result is expected since the greater amounts of solvent result in more transfer to solvent reactions, which translate into more short chains. Furthermore, added solvent facilitates the termination reaction, which reduces the propagation. The $\overline{M}_w$ modelling did not provide an adequate fit to the experimental data, more so in the case of the copolymerization in 80 wt.% toluene. Experimental runs designed to obtain better estimates of the transfer constants would likely improve the $\overline{M}_w$ fit.

Finally, Figure 4.9, Figure 4.11 and Figure 4.13 indicate very good data reproducibility. The variability is within experimental error.

Conclusions

A series of solution polymerizations was conducted to investigate the solvent effect of toluene on BA and VAc homopolymerizations and copolymerizations, by varying the solvent concentrations, as well as the BA:VAc ratios in the case of the BA/VAc copolymer.

BA and VAc homopolymers show a decrease in conversion with a corresponding increase in solvent concentration, the effect being more pronounced with VAc because it acts as a retardant for polymerization in the presence of aromatic solvents such as toluene. The cumulative-weight average molecular weight for both monomers decreased with an increase in the solvent concentration. The BA and VAc monomer conversions were not significantly affected by a changing concentration of CTA.

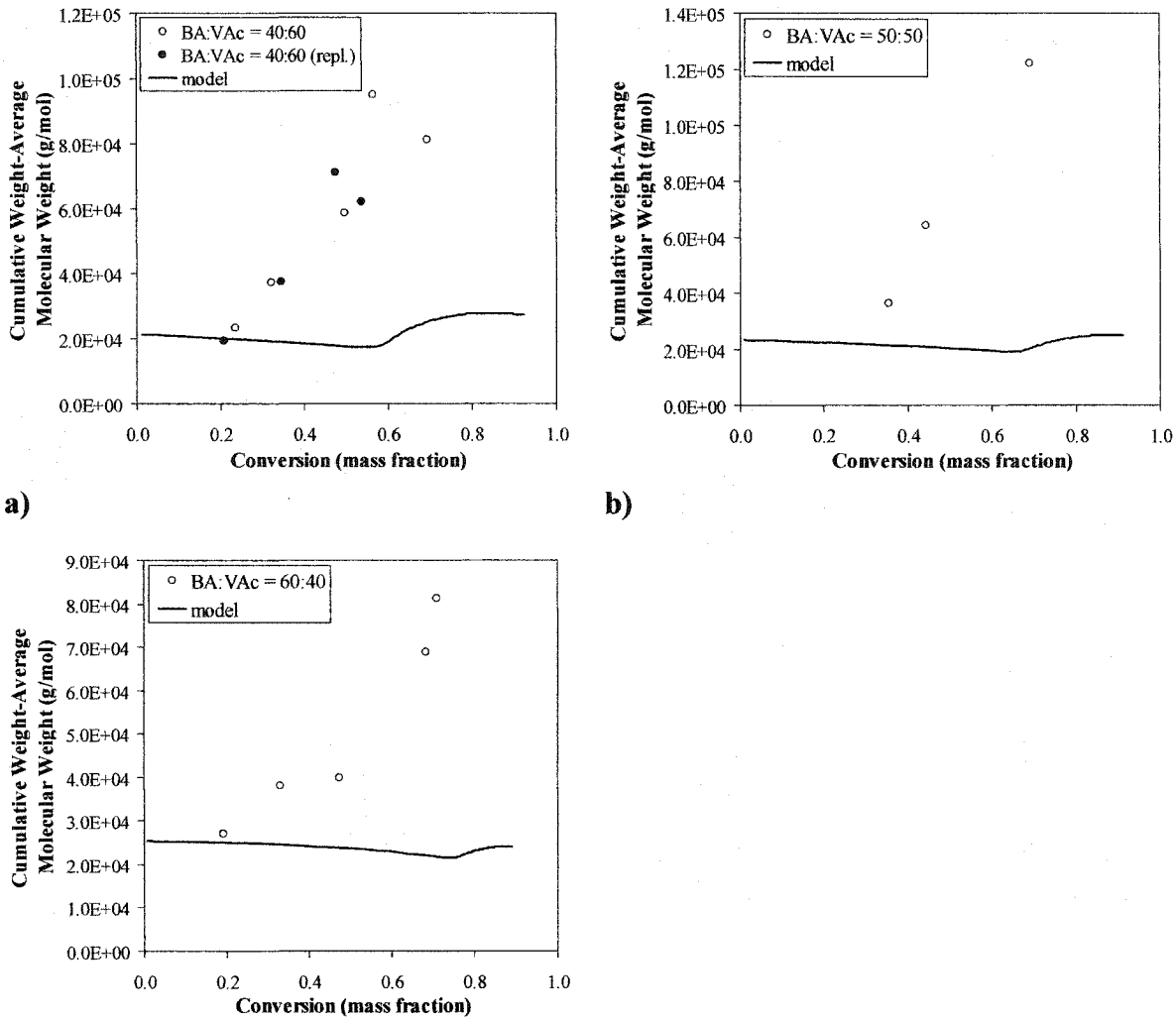

Figure 4.13: Solvent effect (S.E.) on the BA-VAc copolymers in 30 wt.% toluene at various BA:VAc ratios, evaluated using the cumulative weight-average molecular weight.

To account for the solvent effect, the lumped kinetic constant, $k_p/k_t^{0.5}$, was indirectly adjusted by manipulating the termination rate constant, k_t, for each solvent concentration. Values for $k_p/k_t^{0.5}$ decreased with increasing toluene concentration. Simulations using the modified lumped kinetic constants showed excellent agreement with experimental data for both BA and VAc hompolymerizations.

BA/VAc copolymerization data indicated that, for an increase in solvent concentration, the cumulative copolymer composition, F_{cumul}, increased slightly, the

overall conversion decreased and the cumulative weight-average molecular weight decreased. Also, an increase in the BA:VAc ratio corresponded to an increase in F_{cumul} and an increase in conversion.

Copolymerization simulations made use of homopolymer rate constants. The initial modelling efforts suggested the need for further adjustments. The BA reactivity ratios, $r_{BA,VAc}$, were adjusted to 10.0 and 8.0 for toluene concentrations of 80 and 30 wt.%, respectively, allowing improved model predictions for the F_{cumul} and conversion data.

Until accurate measurements of the reactivity ratios can be performed, one cannot ascertain whether the solvent effect is due to termination or propagation reactions, or a combination thereof.

Acknowledgements

The authors wish to gratefully acknowledge the contributions of Jean-Philippe St-Pierre, Renata Jovanovic, Melissa Dorval and Catherine Goubko to the experimental work, as well as financial support from the Natural Science and Engineering Research Council (NSERC) of Canada, the Ontario Graduate Scholarship in Science and Technology (OGSST) established by Mr. David McLimont.

References

56. Mayo, F.R.; Lewis, F.M.J. *J. Am. Chem. Soc.*, **66**, 1954 (1944).
57. Dubé, M.A.; Penlidis, A. *Polymer*, **36**, 587 (1995).
58. Dubé, M.A.; Soares, J.B.P.; Penlidis, A.; Hamielec, A.E. *Ind. Eng. Chem. Res.*, **36**(4), 966 (1997).
59. Laplante, M. M.A.Sc. thesis, Department of Chemical Engineering, University of Ottawa, 2004.
60. Gao, J.; Penlidis, A. *J. Macromol. Sci. – Rev. Macromol. Chem. Phys.*, **C36**(2), 199 (1996).
61. Gao, J.; Penlidis, A. *J. Macromol. Sci. – Rev. Macromol. Chem. Phys.*, **C38**(4), 651 (1998).
62. Marten, F.L.; Hamielec, A.E. In Henderson, H.N.; Bouton, T.C., Eds., ACS Symposium Series 104, Polymerization Reactors and Processes, American Chemical Society, Washington (DC), 1979, p.43.

63. McKenna, T.F.; Villanueva, A.; Santos, A.M. *J. Polym. Sci. Part A: Polym. Chem.*, **37**, 571 (1999).

64. McKenna, T.F.; Villanueva, A. *J. Polym. Sci. Part A: Polym. Chem.*, **37**, 589 (1999).

65. Othman, S.; Barudio, I.; Fevotte, G.; McKenna, T.F. *Polym. React. Eng.*, **7**, 1 (1999).

66. Jovanovic, R.; Dubé, M.A. *J. Appl. Polym. Sci.*, **82**, 2958 (2001).

67. Coote, M.L.; Davis, T.P.; Klumperman, B.; Monteiro, M.J. *J. Macromol. Sci. – Rev. Macromol. Chem. Phys.*, **C38**(4), 567 (1998).

68. Kamachi, M. *Adv. Polym. Sci.*, **38**, 55 (1981).

69. Coote, M.L.; Davis, T.P. *Prog. Polym. Sci.*, **24**, 1217 (1999).

70. Russell, G.T.; Gilbert, R.G.; Napper, D.H. *Macromolecules*, **25**, 2459 (1992).

71. Russell, G.T.; Gilbert, R.G.; Napper, D.H. *Macromolecules*, **26**, 3538 (1993).

72. Russell, G.T. *Macromol. Theory Simul.*, **4**, 497 (1995).

73. Fernandez-Garcia, M.; Fernandez-Sanz, M.; Madruga, E.L. *Macromol. Chem. Phys.*, **201**, 1840 (2000).

74. Hutchinson, R.A.; Richards, J.R.; Aronson, M.T. *Macromolecules*, **27**, 4530 (1994).

75. Brandrup, J.; Immergut, E.H.;Grulke, E.A., Eds., *Polymer Handbook*, 4th ed., Wiley, New York, 1999.

76. American Polymer Standards Corp. α and K values. http://www.ampolymer.com/mark-%20houwink%20parameters.htm.

77. Maeder, S.; Gilbert, R.G. *Macromolecules*, **31**, 4410 (1998).

78. de la Fuente, J.L.; Madruga, E.L. *J. Polym. Sci. Part A: Polym. Chem.*, **23**, 2913 (1998).

79. Ham, G.E. *Vinyl Polymerization*, vol.1, Marcel Dekker, New York, 1967.

80. McKenna, T.F.; Heredia, M.F. *Polym. J.*, **31**, 7 (1999).

81. Kamachi, M.; Liaw, D.J.; Nokazura, S. *Polym. J.*, **12**, 921 (1979).

82. De la Fuente, J.L.; Madruga, E.L. *Macromol. Chem. Phys.*, **200**, 1639 (1999).

83. Fernandez-Garcia, M.; Fernandez-Sanz, M.; Madruga, E.L.; Cuervo-Rodriguez, R.; Hernandez-Gordo, V.; Fernandez-Monreal, M.C. *J. Polym. Sci. Part A: Polym. Chem.*, **38**(1), 60 (2000).

Chapter 5: Paper 2

Styrene/Butyl Acrylate Copolymerizations Modelling

Marc Laplante and Marc A. Dubé*
Department of Chemical Engineering, University of Ottawa,
161 Louis Pasteur St., Ottawa ON, K1N 6N5 Canada
** dube@eng.uottawa.ca*

Abstract

Styrene (Sty) and butyl acrylate (BA) homopolymerizations and copolymerizations were carried out in toluene as solvent. Copolymer data were collected at two different solvent concentrations, and four Sty:BA ratios were run for each of those two sets. Conversion, cumulative copolymer composition, as well as cumulative weight-average molecular weight data are presented for all cases, along with the corresponding model predictions. The change in amount of solvent did not significantly affect the conversion or the cumulative copolymer composition data, but the cumulative weight-average molecular weight was noticeably greater at the lower toluene concentration. Diffusion control only took place in two of the runs, and occurred toward the end of the polymerization.

Introduction

Because of its practical significance, many researchers have been interested in the copolymerization of styrene (Sty) with butyl acrylate (BA). Sty/BA copolymers are commercially important binders in many paints, adhesives and coatings. Gao and Penlidis[84] have conducted extensive studies into the reaction kinetics of this copolymer system in bulk and solution polymerizations.

The copolymer composition, molecular weight and the molecular weight distribution each play a role in the final properties of the copolymer. In turn, the individual monomer reactivities have a significant impact on these polymer characteristics. The Sty and BA monomers have moderately different reactivities, resulting in polymer composition drift during a batch polymerization. The reactivity ratios for Sty and BA are $r_{Sty,BA} = 0.956$ and $r_{BA,Sty} = 0.183$, respectively.[85] When this drift cannot be avoided, e.g. by using semi-batch policies coupled with on-line monitoring of

the monomer concentrations,[86] it becomes necessary to have a model to predict the composition drift.

A number of models have been developed to simulate free-radical homo- and copolymerizations.[84,87,88] Developed by Laplante,[88] the Java™-based simulator used for this study was designed for multi-component free-radical polymerizations in bulk and solution. Diffusion-controlled rate constants were modeled using the free volume theory,[89] and the pseudo-kinetic rate constant approach[86] was implemented.

The glass transition temperature, T_g, is one of the most important characteristics of a polymer, which can affect certain physical properties, such as crystallinity and free volume. From a modelling point of view, the T_g has an important influence on the calculation of free volume. The free volume is used in the polymerization model to predict the onset of various diffusion control regimes. When a copolymer is formed, a simple weighting of the individual repeat unit T_g's is typically insufficient. Several models have been proposed over the years to combine these individual T_g values into a reasonably accurate estimate of the copolymer T_g; however, none of these models can be claimed as universal. Gao and Penlidis[84] performed an extensive literature search in order to properly simulate the effects of copolymer T_g. An overview of their findings is presented here, followed by a description of the models selected for the simulations in this study.

Although some copolymer T_g models are purely empirical, many models have been derived from theory, either via entropy or free volume approaches. It is important to note, however, that some of the models become equivalent when certain assumptions are made.

For models based on entropy theory, the configurational entropy of a polymer chain is zero at T_g. The Dimarzio-Gibbs,[90] Barton[91] and Suzuki-Mathot[92] models are examples of entropy-based models. In the Dimarzio-Gibbs model, the homopolymer T_g's are weighted with their respective mole fraction of rotatable bonds. The Barton model is an extension of the Dimarzio-Gibbs model, which takes into account the effects of microstructure on T_g. Suzuki-Mathot further extended this model to include the average number of both monomer sequences occurring in a copolymer per 100 monomer units.

Models based on free volume theory include the Gordon-Taylor[93] and the Wood[94] models. The Gordon-Taylor model includes a constant, which accounts for interactions of all diads in the copolymer. The Wood model makes use of adjustable parameters and weighting factors.

Other models include the Fox,[95] Johnston[96] and Couchman[97] models. One of the first copolymer T_g models introduced, the Fox model uses a parallel approach by weighting individual T_g's with the monomer weight fractions.

$$\frac{1}{T_g} = \sum_{i=1}^{n_M} \left(\frac{W_i}{T_{g,i}} \right) \tag{5.1}$$

where W_i is the weight fraction of monomer i in the copolymer chain.

Like the Fox model, the Johnston model is in parallel form; however, it accounts for the contribution from monomer sequence distribution. The equation, extended to n_M monomers, is shown below:

$$\frac{1}{T_g} = \sum_{i=1}^{n_M} \sum_{j=1}^{n_M} \frac{W_i P_{ij}}{T_{g,ij}} \tag{5.2}$$

where P_{ij} is the probability of sequence ij occurring. When $i = j$, $T_{g,ij}$ is the T_g of the homopolymer, whereas when $i \neq j$, $T_{g,ij}$ is the T_g of the alternating copolymer.

A thermodynamic approach was used to derive the Couchman model. Although the theory is more rigorous, additional parameters are required to predict the copolymer T_g in the Couchman model. The equation, for a two-monomer system, is as follows:

$$\ln(T_g) = \frac{r_{ij} f_{M,i}^2 \Delta C_{p,ii} \ln(T_{g,ii}) + r_{ji} f_{M,j}^2 \Delta C_{p,jj} \ln(T_{g,jj}) + 2 f_{M,i} f_{M,j} \Delta C_{p,ij} \ln(T_{g,ij})}{r_{ij} f_{M,i}^2 \Delta C_{p,ii} + r_{ji} f_{M,j}^2 \Delta C_{p,jj} + 2 f_{M,i} f_{M,j} \Delta C_{p,ij}} \tag{5.3}$$

where r_{ij} is the reactivity ratio describing the addition of monomer j to a growing radical chain ending in monomer i, $f_{M,i}$ is the mole fraction of monomer i in the reaction mixture, and $\Delta C_{p,ij}$ is the difference in heat capacity above and below the corresponding $T_{g,ij}$.

In some cases, a simplified form[97] of the Couchman equation can be used, where all ΔC_p's are assumed to be equal, and therefore cancel out of equation (5.3). Under this assumption, no additional parameters need to be provided.

Experimental

The procedures employed to obtain experimental data were identical to that of Hua *et al.*,[98] and are summarized here.

Reagents

The Sty and BA monomers were received inhibited by hydroquinone, and were subsequently purified appropriately. Toluene was used as solvent, 2,2'-azobisisobutyronitrile (AIBN) was the initiator, and n-dodecyl mercaptan was the chain transfer agent (CTA).

Procedures

The polymerization reactions were carried out in 5-mL glass ampoules, at a temperature of 60°C. Ampoules were removed and analyzed at predetermined sampling times. Gravimetric analysis of the consumption of monomer was used to estimate the conversion on a mass basis. In the case of copolymers, the sample was subsequently analyzed for cumulative copolymer composition using proton nuclear magnetic resonance (^{1}H-NMR) spectroscopy. The cumulative weight- and number-average molecular weights were determined using gel permeation chromatography (GPC).

Instrumentation

Cumulative copolymer compositions were obtained through spectra taken by a Bruker AMX-500 Fourier-transform ^{1}H-NMR spectrometer. The cumulative number- and weight-average molecular weights were determined with a Waters Associates GPC system equipped with three Waters Styragel-HR columns (10^3, 10^4, and 10^6 Å pore size) installed in series, thermostated to 30°C, and a Waters 410 differential refractometer thermostated to 38°C. Tetrahydrofuran (THF) was used as the eluent at a flow rate of 0.3 ml/min.

The cumulative number- and weight-average molecular weights were determined using a universal calibration curve, by means of the Mark-Houwink K and α parameters determined in THF. For the copolymers, the weighted averages of these parameters were calculated using the cumulative copolymer composition data obtained through ^{1}H-NMR spectroscopy.

Results and Discussion

Styrene homopolymer

Two styrene homopolymerization runs were carried out in toluene. The reaction conditions for these runs are listed in Table 5.1.

Table 5.1: Experimental conditions for the solution Sty homopolymer runs

Sty:Tol (wt.%)	Styrene (g)	Toluene (g)	AIBN (g)	CTA (g)
40:60	8.0106	12.0088	0.3727	0.1175
50:50	6.0032	6.0018	0.2255	0.0776

The Sty monomer conversion is shown in Figure 5.1 for both solvent concentrations. It can be seen that the increase in toluene does not significantly affect the conversion, where the difference is within experimental error. Showing excellent fit, the model corroborates this trend, which is apparent from the overlapping curves.

Figure 5.2 displays the cumulative weight-average molecular weight, $\overline{M}_w$, as a function of conversion for Sty in 50 and 60 wt.% toluene. The data show that higher solvent concentrations resulted in lower molecular weights. This result is expected since the greater amounts of solvent result in more transfer to solvent reactions, which translate into shorter chains. Furthermore, added solvent facilitates the termination reaction, which reduces the propagation. Although the model does not predict the curvature of $\overline{M}_w$ well, it exhibits the same behaviour as the data. Furthermore, the model values are of the same magnitude as the data points. The discrepancy in trends between the data and the model

predictions would likely be remedied by performing experimental runs designed to obtain better estimates of the transfer constants.

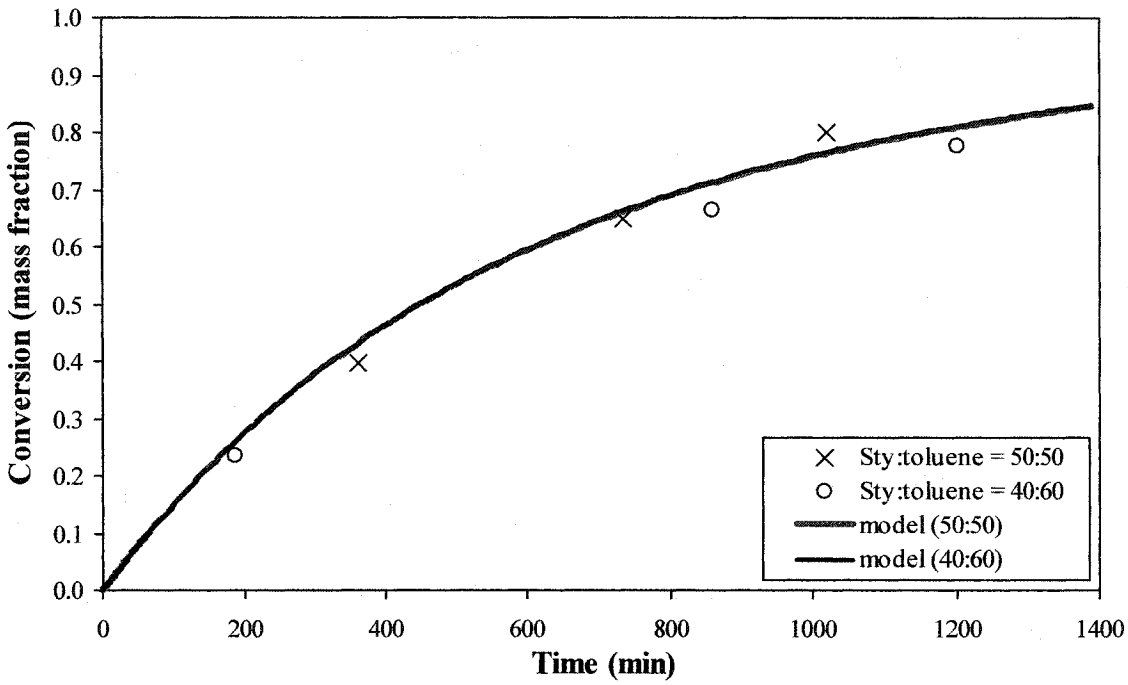

Figure 5.1: Conversion versus time for the Sty homopolymer in toluene.

BA homopolymer runs were also conducted and modelled.[88] The model provided excellent predictions of both the conversion and the $\overline{M}_w$ data. Although the reaction conditions were different, for the same solvent concentration (50 wt.%), the Sty and BA homopolymer trends indicate that Sty polymerizes at a much slower rate than BA. Also, the molecular weight of the Sty polymer is approximately half that of the BA polymer.

Sty/BA copolymer

In this work, the Sty/BA copolymerization data were modelled using the pseudo-kinetic rate constant approach, to obtain overall weighted values for the various Sty/BA rate constants.

Table 5.2 lists the reaction conditions for the eight solution Sty/BA copolymerization experiments that were performed. Two sets of four runs each were

carried out in 50 and 65 wt.% toluene. In both sets, varying Sty:BA ratios were investigated.

Table 5.2: Experimental conditions for the solution Sty/BA copolymer runs

Sty:BA (wt.%)	Sty:BA:Tol (wt.%)	Sty (g)	BA (g)	Toluene (g)	AIBN (g)	CTA (g)
20:80	10:40:50	10.01	40.04	50.11	1.8787	0.5802
40:60	20:30:50	20.01	30.02	50.08	1.8921	0.5787
60:40	30:20:50	30.00	20.00	50.04	1.8627	0.5868
80:20	40:10:50	40.02	10.04	50.11	1.8639	0.6438
20:80	7:28:65	3.02	12.39	28.14	0.8027	0.2608
40:60	15:23:62	6.72	10.10	27.86	0.8149	0.2586
60:40	21:14:65	7.59	5.01	23.22	0.5026	0.2235
80:20	28:7:65	16.04	4.03	37.17	1.0730	0.3453

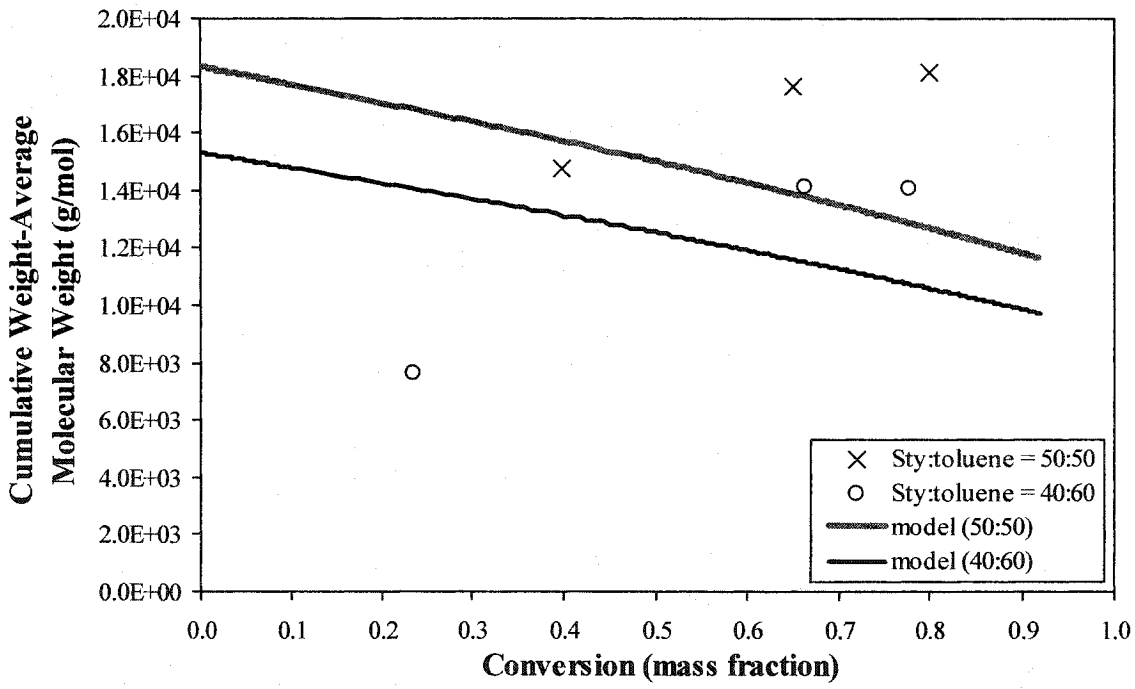

Figure 5.2: Cumulative weight-average molecular weight versus conversion for the Sty homopolymer in toluene.

In Figure 5.3 and Figure 5.4, the Sty cumulative copolymer composition, F_{cumul}, is presented as a function of conversion for four different Sty:BA ratios, in toluene concentrations of 50 and 65 wt.%, respectively. Obviously, the cumulative copolymer composition increases with an increasing Sty:BA ratio. With more Sty available for polymerization, the produced chains are richer in Sty. Also, at low conversions, the polymer chains are richer in Sty due to its higher reactivity ratio compared to that of BA. As the reaction progresses, Sty monomer is consumed, reducing the Sty:BA ratio remaining in the reaction mixture, which reduces the Sty cumulative copolymer composition. Varying the solvent concentration had a negligible impact on the F_{cumul} data, which indicates there is no solvent effect on the propagation reaction. In all cases, the model predictions follow the F_{cumul} data exceptionally well.

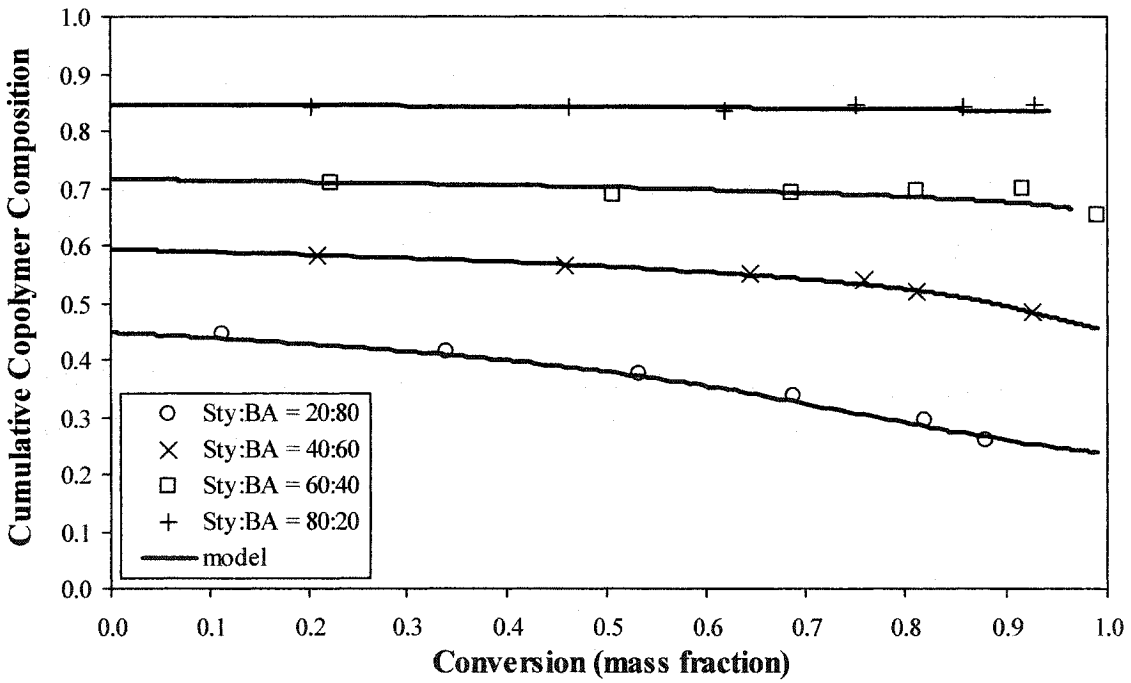

Figure 5.3: Cumulative copolymer composition versus conversion at various Sty:BA ratios in 50 wt.% toluene.

The conversion data as a function of time for the 50 and 65 wt.% toluene concentrations appear in Figure 5.5 and Figure 5.6, respectively. In both cases, an increase in the Sty:BA ratio results in a decrease in conversion. This trend was expected, based on the homopolymerization data, where higher conversions were observed for BA.

When comparing the two solvent concentrations, there is very little difference between the two sets of data. The two Sty:BA = 60:40 runs are the only exception, where the discrepancy may be due to experimental error, since it does not follow the trends of the other runs. Also, although the curve for both Sty:BA = 20:80 runs are similar, the 65 wt.% toluene run continues to a higher conversion than its 50 wt.% counterpart. In most cases, the model predicted the data adequately.

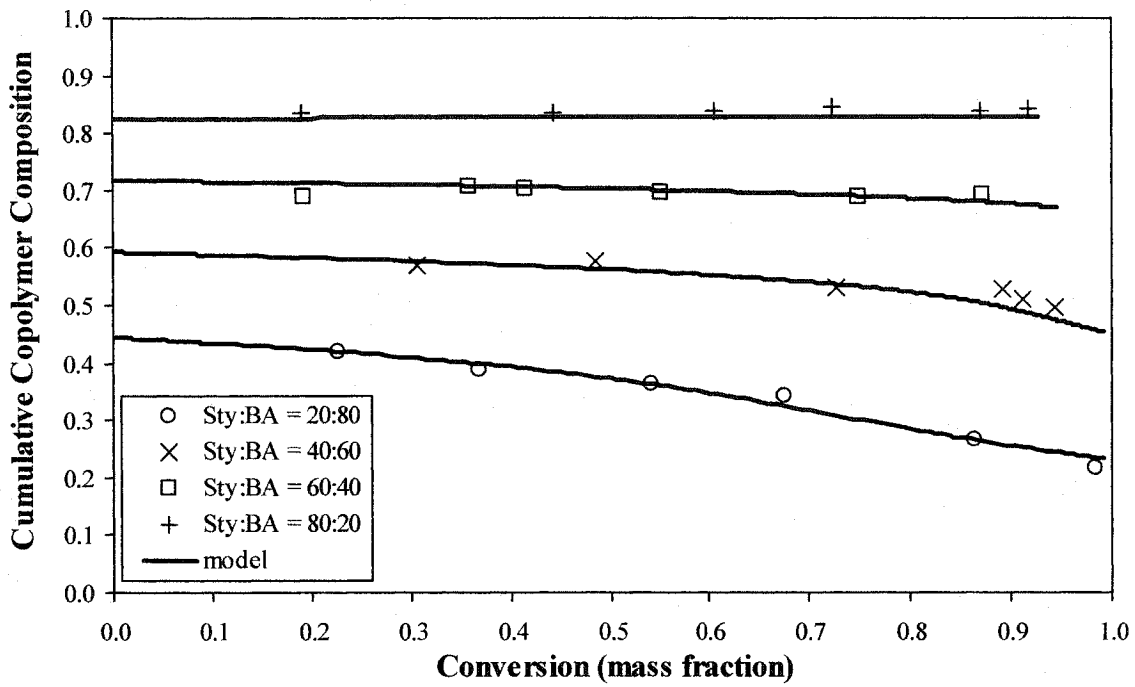

Figure 5.4: Cumulative copolymer composition versus conversion at various Sty:BA ratios in 65 wt.% toluene.

Figure 5.7 and Figure 5.8 show the cumulative weight-average molecular weight as a function of conversion for toluene concentrations of 50 and 65 wt.%, respectively. Although not consistent, an overall trend indicates a slight decrease in $\overline{M}_w$ values with a corresponding increase in the Sty:BA ratio. Also, a higher solvent concentration resulted in lower $\overline{M}_w$ values, as with the homopolymers. The $\overline{M}_w$ simulations indicate lack of fit. It is likely that parameters related to chain transfer reactions are not optimal. Targeted experiments coupled with parameter estimation may offer improved predictions in the future. It should be noted that diffusion-controlled regimes were not attained in most of the polymerizations due to the high solvent concentrations used. Thus, the molecular

weight would tend to have little influence on the prediction of conversion, unlike the case for bulk polymerization.

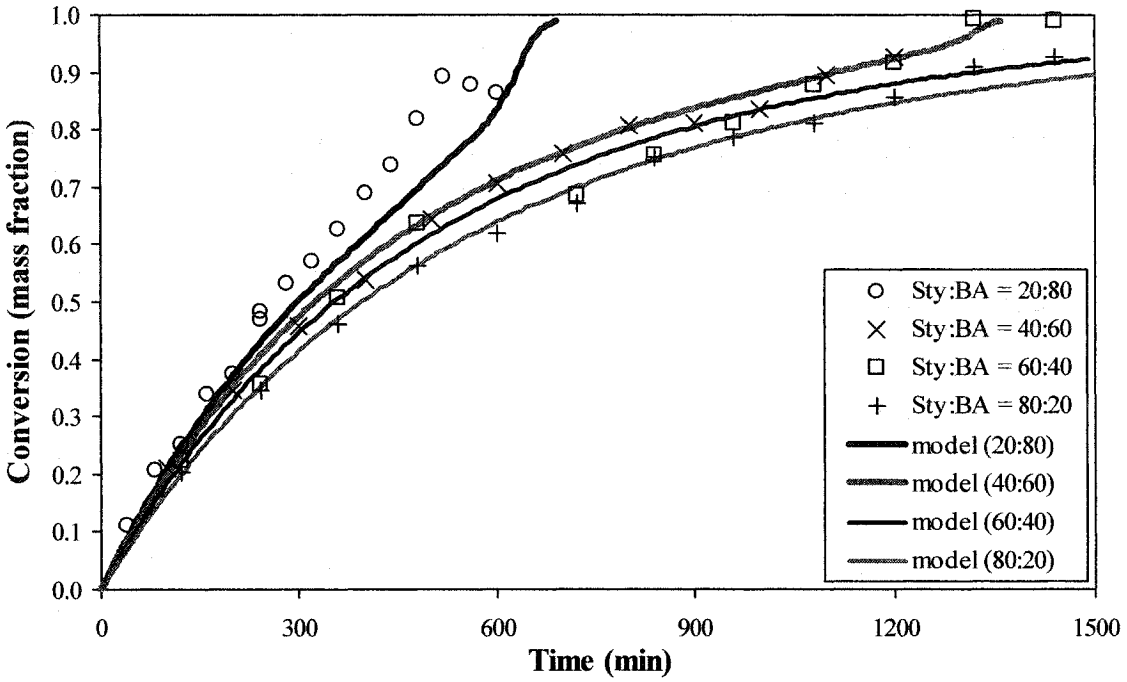

Figure 5.5: Conversion versus time at various Sty:BA ratios in 50 wt.% toluene.

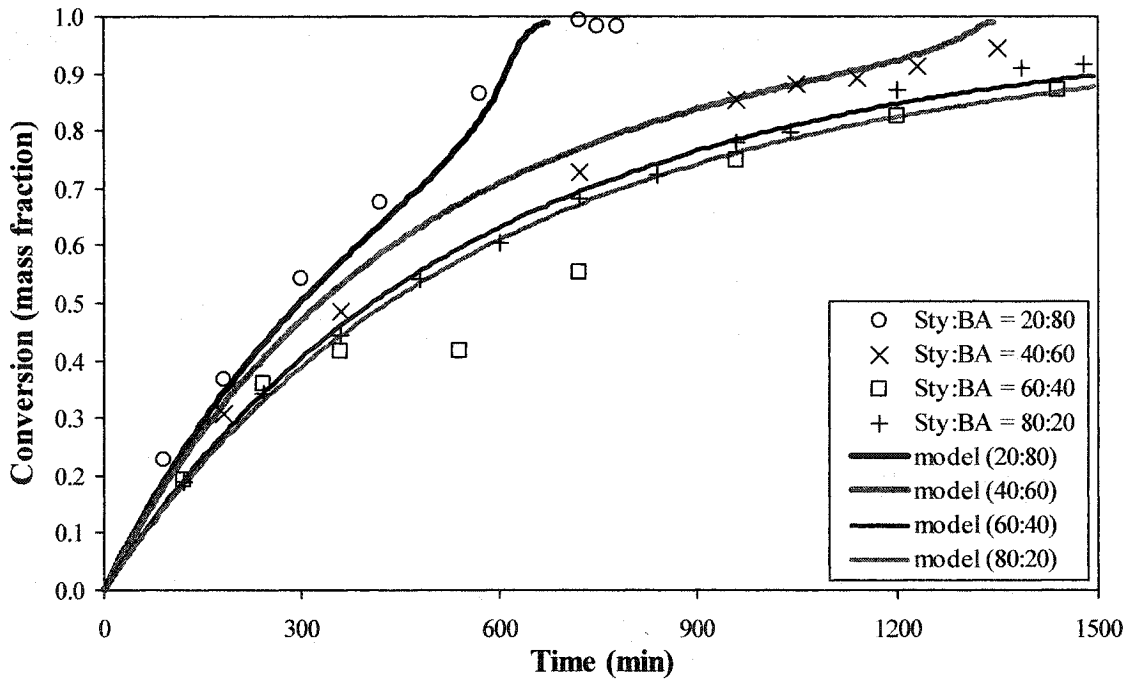

Figure 5.6: Conversion versus time at various Sty:BA ratios in 65 wt.% toluene.

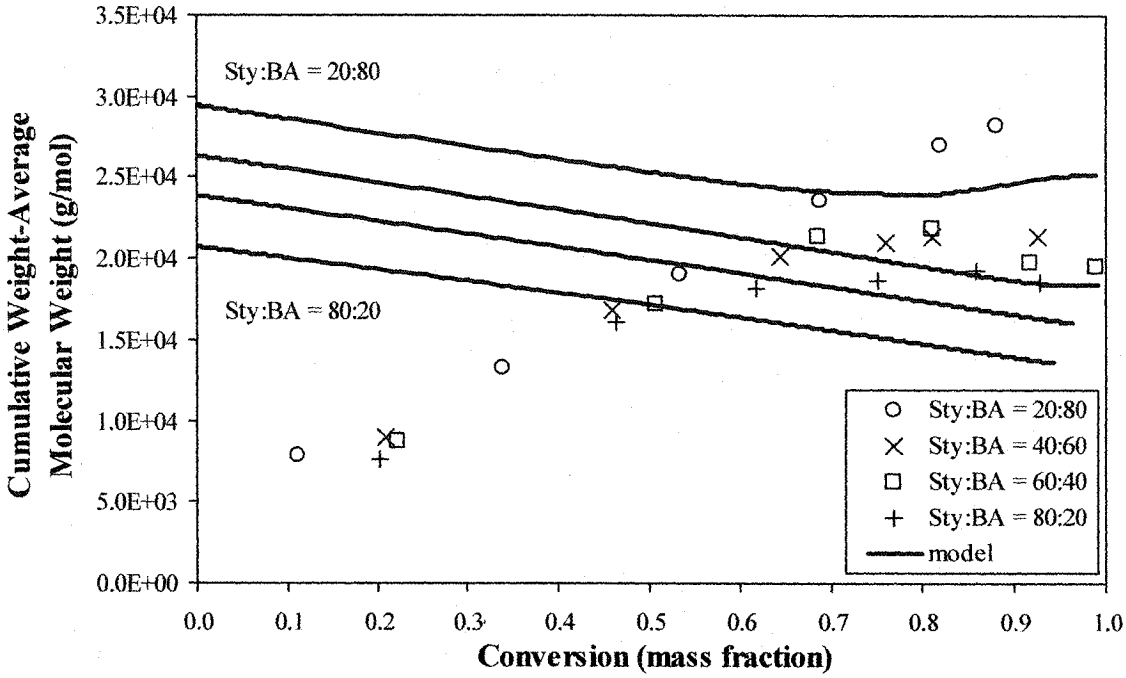

Figure 5.7: Cumulative weight-average molecular weight versus conversion at various Sty:BA ratios in 50 wt.% toluene.

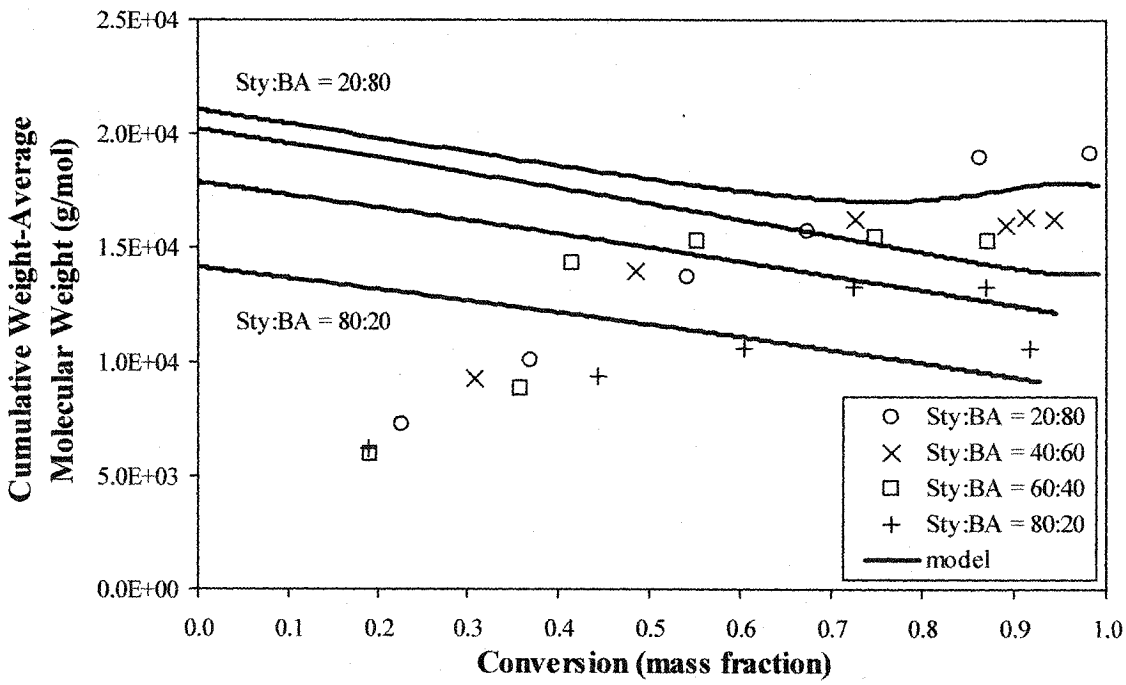

Figure 5.8: Cumulative weight-average molecular weight versus conversion at various Sty:BA ratios in 65 wt.% toluene.

Glass transition temperature models

Based on the findings of Gao and Penlidis,[84] it was decided to implement both the Johnston and Couchman equations into the simulator, providing the user with the choice of model. Although presently seldom used, the copolymer T_g weighted in series (i.e. the Fox model) using monomer weight fractions was also implemented as an option, for comparison purposes. Two of the eight copolymer runs were used to make the comparison. Initially, it was intended for the two runs to be at both extremes to provide a broader comparison. However, upon closer inspection of the simulation outputs, it was discovered that only two runs exhibited any diffusion control: Sty:BA = 20:80 and 40:60 in 50 wt.% toluene. Since the copolymer T_g is used indirectly to determine the onset of diffusion control, these two latter runs must be used.

Figure 5.9 shows the conversion versus time for the Sty:BA = 40:60 run, accompanied by model predictions using the three copolymer T_g models. It can be seen that the curves are virtually identical. Only towards the end of the reaction can a slight deviation be observed, once diffusion control dominates the reaction kinetics. Although the addition of solvent has practical applications and can improve the reaction conditions, it prevents the comparison of the copolymer T_g models. Larger amounts of solvent reduce the viscosity of the reaction medium, delaying and in some cases preventing the onset of diffusion-controlled kinetics.

Gao and Penlidis[84] stated that the Johnston model appears to be the most general model amongst the ones studied. Their tests showed that their model predictions using this T_g model were satisfactory for most copolymer systems. Further testing revealed that simulations using Couchman's equation agreed well with experimental data and were very close to results using Johnston's model. They also reported that the Fox model is not valid for many copolymer systems. Unfortunately, these statements cannot be confirmed with the present set of data due to the elevated quantities of solvent.

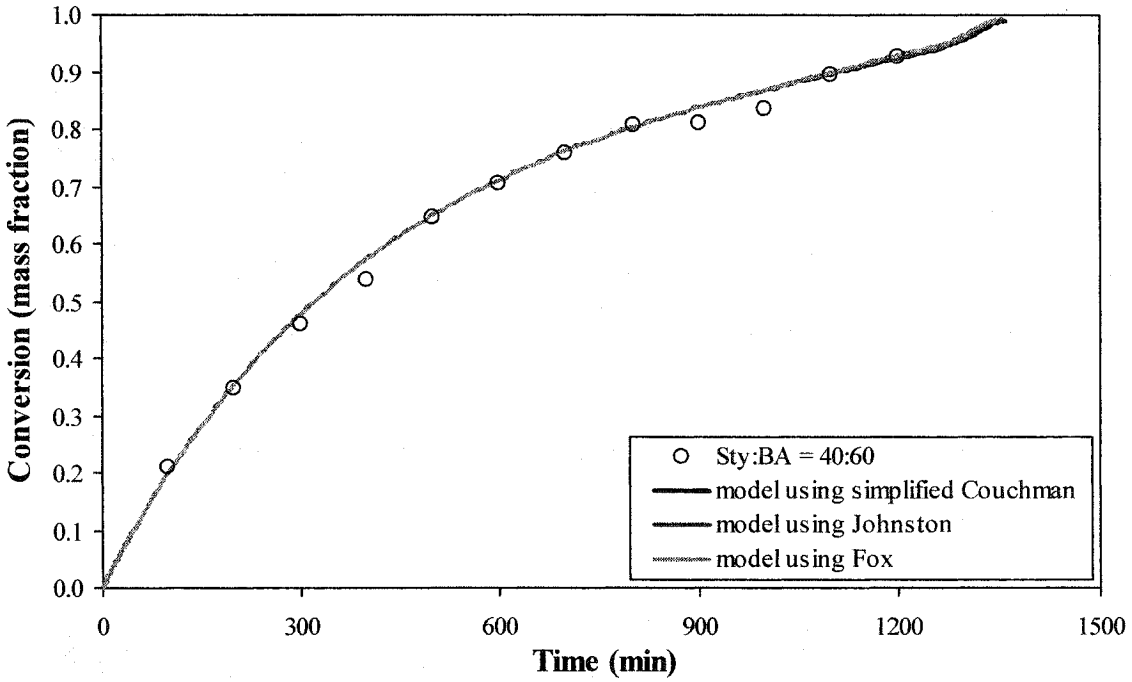

Figure 5.9: Conversion versus time for Sty:BA = 40:60 in 50 wt.% toluene, using various copolymer T_g models.

Conclusions

The multi-component free-radical polymerization simulator showed good agreement with all Sty and BA homopolymer runs, as well as the Sty/BA copolymer runs. In both cases, the changing solvent concentration had little effect on the conversion and cumulative copolymer composition data, but had a noticeable and expected impact on the cumulative weight-average molecular weights. An increase in the Sty:BA ratio resulted in a predictable cumulative copolymer composition increase. Based on the homopolymerization data, it was foreseeable that the conversion would decrease with an increasing Sty:BA ratio. Cumulative weight-average molecular weight data were somewhat inconsistent, but seemed to indicate a slight decrease in $\overline{M}_w$ values with a corresponding increase in the Sty:BA ratio.

The amount of solvent present in the reaction mixture proved to be too large to allow a proper study of the glass transition temperature model. Diffusion control occurred at the end of only two of the polymerization runs.

Acknowledgements

The authors wish to gratefully acknowledge the contribution of Hong Hua to the experimental work, as well as financial support from the Natural Science and Engineering Research Council (NSERC) of Canada, the Ontario Graduate Scholarship in Science and Technology (OGSST) established by Mr. David McLimont.

References

84. Gao, J.; Penlidis, A. *J. Macromol. Sci. – Rev. Macromol. Chem. Phys.*, **C38**(4), 651 (1998).

85. Dubé, M.A.; Penlidis, A.; O'Driscoll, K.F. *Can. J. Chem. Eng.*, **68**, 974 (1990).

86. Dubé, M.A.; Soares, J.B.P.; Penlidis, A.; Hamielec, A.E. *Ind. Eng. Chem. Res.*, **36**(4), 966 (1997).

87. Gao, J.; Penlidis, A. *J. Macromol. Sci. – Rev. Macromol. Chem. Phys.*, **C36**(2), 199 (1996).

88. Laplante, M. M.A.Sc. thesis, Department of Chemical Engineering, University of Ottawa, 2004.

89. Marten, F.L.; Hamielec, A.E. In Henderson, H.N.; Bouton, T.C., Eds., ACS Symposium Series 104, Polymerization Reactors and Processes, American Chemical Society, Washington (DC), 1979, p.43.

90. Dimarzio, E.A.; Gibbs, J.H. *J. Polym. Sci.*, **XL**, 121 (1959).

91. Barton, J.M. *J. Polym. Sci. Part C*, **30**, 573 (1970).

92. Suzuki, M.; Mathot, V.B.F. *Macromolecules*, 22, 1380 (1989).

93. Gordon, M.; Taylor, J.S. *J. Appl. Chem.*, **2**, 493 (1952).

94. Wood, L.A. *J. Polym. Sci.*, **XXVIII**, 319 (1958).

95. Fox, T.G. *Bull. Am. Phys. Soc.*, **1**, 123 (1956).

96. Johnston, N.W. *Polymer Prep.*, **10**, 608 (1969).

97. Couchman, P.R. *Macromolecules*, **15**, 770 (1982).

98. Hua, H.; Rivard, T.; Dubé, M.A. *Polymer*, **45**, 345 (2004).

Chapter 6: BA/MMA/VAc terpolymerization

The results presented in this chapter are incomplete. Due to limitations of the ordinary differential equation (ODE) solver, many of the simulations conducted were unable to get past a certain point, where diffusion control was too severe. The component balances, described by ODEs, became extremely stiff and difficult to solve. Although the simulator did not crash, the solver took prohibitively small steps in solving the system. Even allowing the simulation to run for a full day did not result in the solver converging to a solution.

6.1 Introduction

The copolymerization of methyl methacrylate (MMA) and vinyl acetate (VAc) has been extensively studied in bulk and solution.[99] due to its industrial applications. By using butyl acrylate (BA), another commercially important polymer can be produced. The BA/MMA/VAc terpolymer has applications as coatings, adhesives and resins depending on the formulation, i.e. monomer feed composition. Gao and Penlidis[100] were the first to publish successful simulations of a free-radical terpolymer. It was shown that the BA/MMA/VAc terpolymer is exceptionally challenging to model due to extreme composition drift and the "double-rate phenomenon".[100,101,102]

The copolymer composition, molecular weight and the molecular weight distribution each play a role in the final properties of the copolymer. In turn, the individual monomer reactivities have a significant impact on these polymer characteristics. Table 6.1 shows the wide-ranging reactivity ratios for each copolymer pair, which results in polymer composition drift during a batch polymerization.

Table 6.1: Monomer reactivity ratios for the copolymer pairs in the BA/MMA/VAc system.

Monomer pair [*i*/*j*]	$r_{i,j}$	$r_{j,i}$	Reference
BA/MMA	0.291	1.871	103
BA/VAc	5.939	0.0262	101
MMA/VAc	24.025	0.0261	104

As with homo- and copolymers, the diffusion-controlled rate constants were modeled using the free volume theory, and the pseudo-kinetic rate constant approach was implemented for the terpolymer system. The Johnston model, described in section 2.2.2, was used to estimate the terpolymer glass transition temperature.

To model the terpolymerizations, the database used to model homopolymerizations was left unchanged, and the copolymer reactivity ratios were applied. The simulator has general applications and is highly flexible, as it allows the simulation of multi-component polymerizations based on homopolymerization characteristics without the need for further parameters. Therefore, adequate simulations of the BA/MMA, BA/VAc and MMA/VAc copolymers should provide equally good predictions of the BA/MMA/VAc terpolymer.

6.2 Results and Discussion

The reaction conditions for the bulk MMA/VAc copolymerization, and bulk and solution BA/MMA/VAc terpolymerization runs that were carried out appear in Table 6.2.

Table 6.2: Experimental conditions for the MMA/VAc copolymer and BA/MMA/VAc terpolymer runs

BA (wt.%)	MMA (wt.%)	VAc (wt.%)	Toluene (wt.%)	AIBN (mol/L)	CTA (mol/L)	Temp. (°C)
—	54	46	—	0.100	0.0058	60
30	30	40	—	0.010	—	50
18	18	24	40	0.071	—	70

6.2.1 MMA/VAc copolymer

In Figure 6.1, the overall conversion as a function of time is presented for the MMA/VAc run, and the cumulative copolymer composition, F_{cumul}, is presented as a function of conversion in Figure 6.2. As mentioned at the beginning of the chapter, the MMA/VAc system exhibits above-average diffusion-controlled kinetics. Compared to the BA/MMA and BA/VAc copolymers, MMA/VAc has the largest difference between its two reactivity ratios, as shown in Table 6.1; therefore, it is expected that the MMA/VAc is the

stiffest of the three systems. Figure 6.2 shows that up to 60% conversion, the produced polymer contains over 90% MMA. An auto-acceleration is seen to occur at about 60% conversion due to the near depletion of the MMA. At this point, a sudden change in properties occurs, where the polymerization begins to behave more like VAc. The rate of polymerization increases rapidly, which is expected since VAc has a larger propagation rate constant compared to MMA.

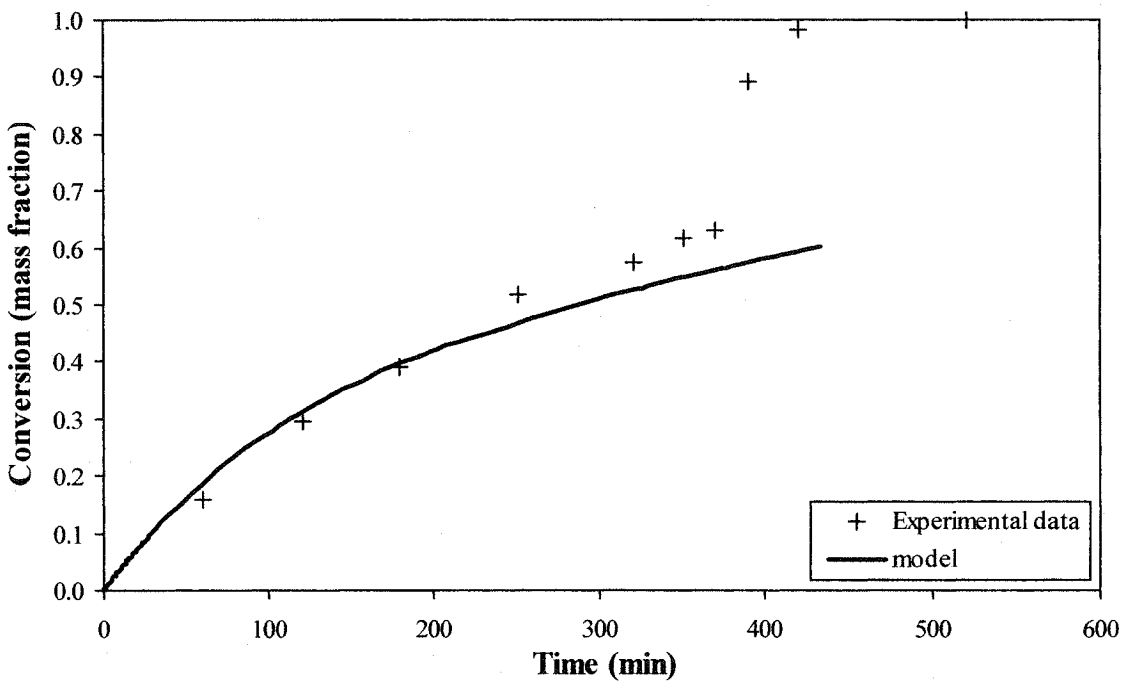

Figure 6.1: Conversion versus time for MMA/VAc at 60°C in bulk.

The ODE solver used by the simulator cannot cope with the extreme stiffness, which is reflected in the premature ending of the model curve. The model fit to the data up to that point is reasonably good. With a more robust solver, it is expected that the conversion curve would turn upward sharply, and both F_{cumul} curves would follow the data. Similarly, the cumulative weight-average molecular weight, $\overline{M}_w$, shown in Figure 6.3 as a function of conversion, would be expected to increase abruptly due to the system autoacceleration.

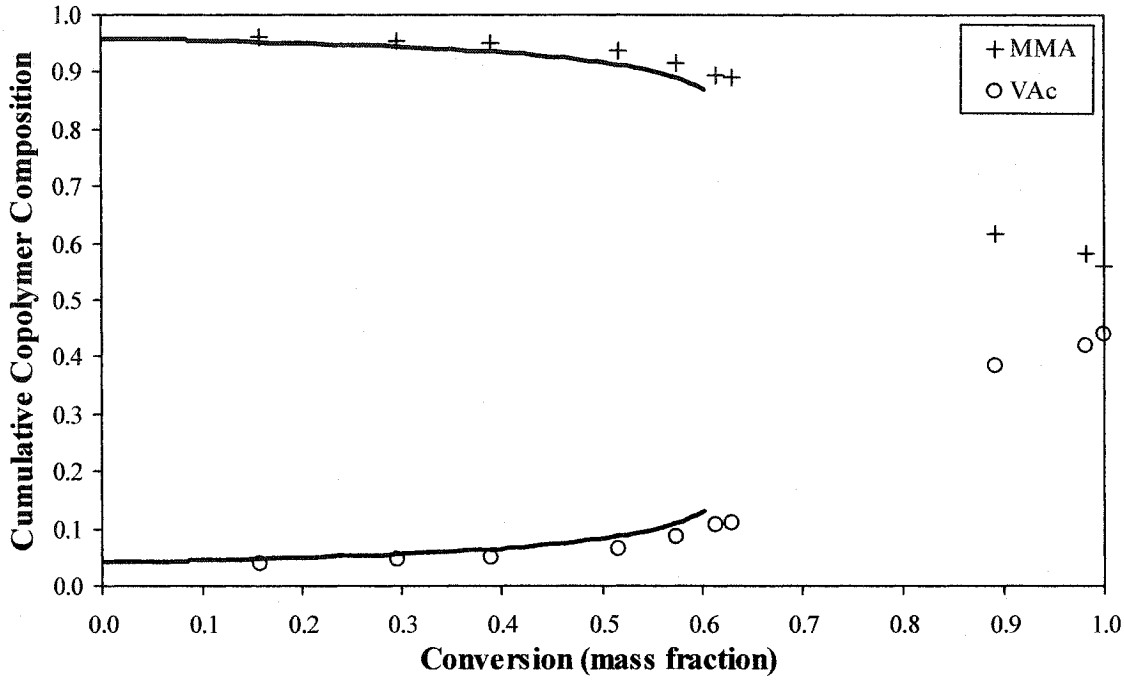

Figure 6.2: Cumulative copolymer composition versus conversion for MMA/VAc at 60°C in bulk.

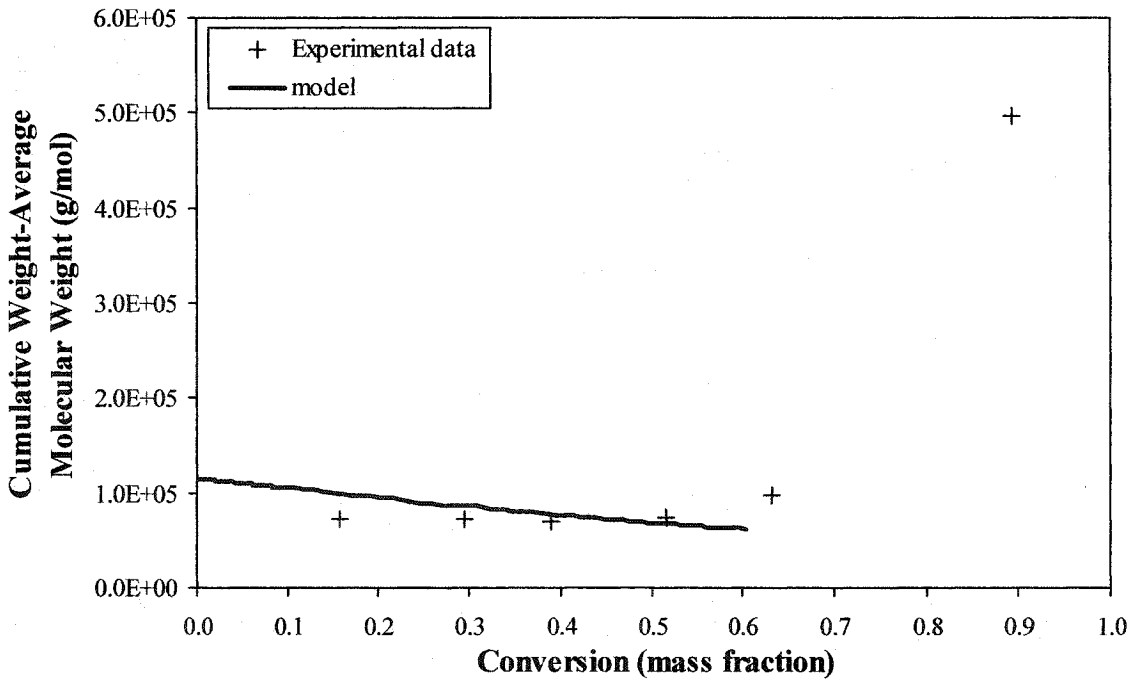

Figure 6.3: Cumulative weight-average molecular weight versus conversion for MMA/VAc at 60°C in bulk.

6.2.2 BA/MMA/VAc terpolymer

The conversion for the BA/MMA/VAc terpolymer run at 50°C appears in Figure 6.4. Although the model ends prematurely, there appears to be the beginning of an auto-acceleration effect at about 60% conversion. As with the MMA/VAc copolymer, VAc's greater k_p increased the polymerization rate. Also, there was a severe composition drift, as shown in Figure 6.5. At low conversions, there is little VAc monomer being added to the polymer chains. As described by Gao and Penlidis,[100] the terpolymerization at this stage behaved more like a copolymerization of BA and MMA, with VAc acting as a solvent. After approximately 60% conversion, most of the BA and MMA were depleted, and VAc began to dominate the reaction kinetics, which is confirmed by the cumulative terpolymer compositions in Figure 6.5. The $\overline{M}_w$, plotted in Figure 6.6, is somewhat well predicted, although slightly underestimated, by the model.

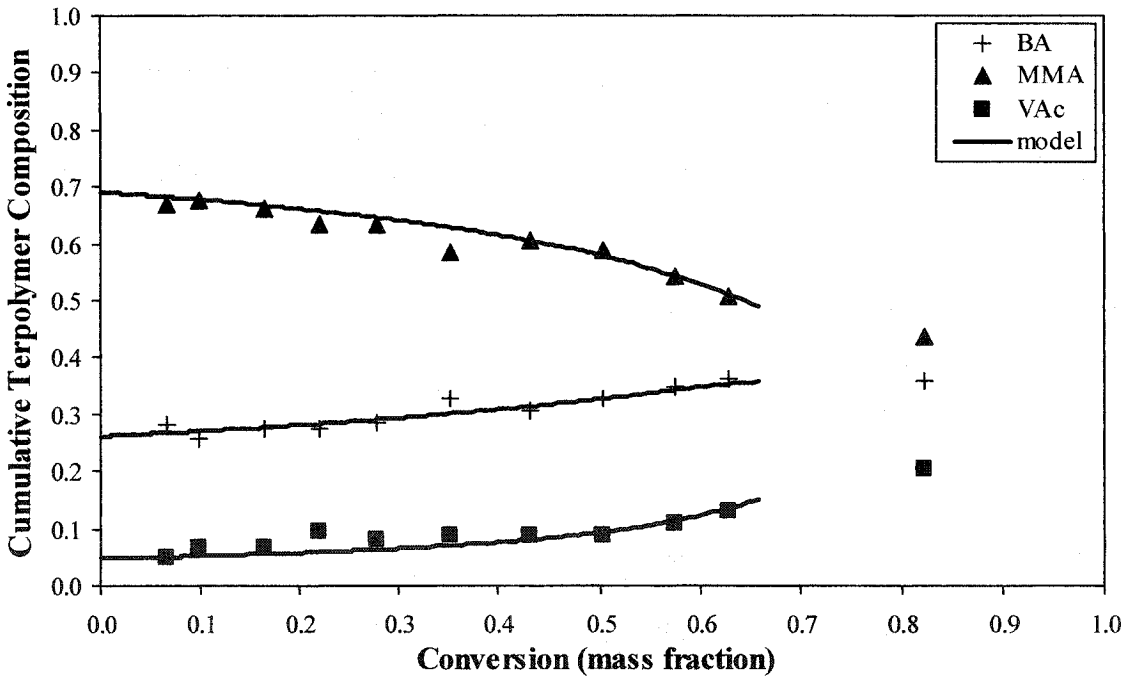

Figure 6.4: Conversion versus time for BA/MMA/VAc at 50°C in bulk.

Similar observations can be made for the other run, which started with the same monomer feed ratio, but was conducted in 40 wt.% toluene at 70°C. After the 60% conversion point, BA and MMA cumulative terpolymer compositions drastically

dropped, while an equally severe increase was observed for VAc. This trend was not as pronounced in the data for the previous bulk due to the lower temperature, nor was it observable in the incomplete model prediction.

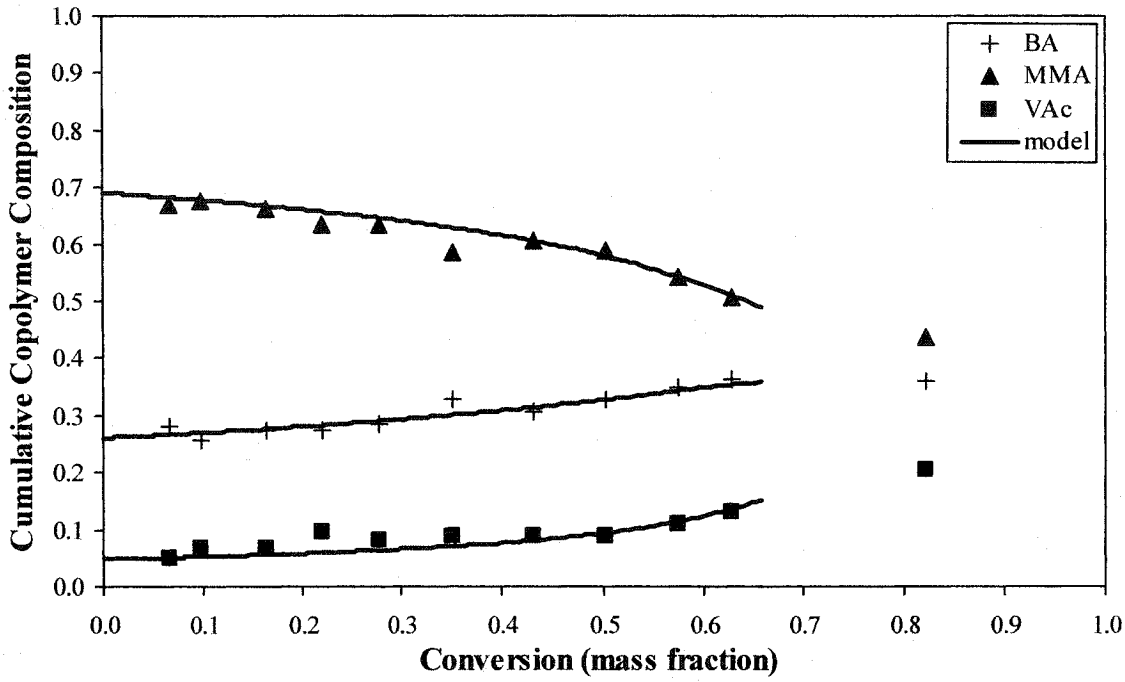

Figure 6.5: Cumulative terpolymer composition versus conversion for BA/MMA/VAc at 50°C in bulk.

Despite being incomplete, it can be seen from the "model (no solvent effect)" curve in Figure 6.7 that the conversion is not well predicted beyond a value of 65%. The slope becomes higher rather than lower to match the data. Because this run is conducted in 40 wt.% toluene, the same strategy as that described in Chapter 4 was employed for solvent effects. The lumped kinetic constants, $k_p/k_t^{0.5}$, for BA and VAc were indirectly adjusted by manipulating the corresponding termination rate constant, k_t. The value for each k_t was obtained by interpolating between the 30 and 50 wt.% concentrations obtained in Chapter 4. The resulting curve is displayed in Figure 6.7, as "model (with solvent effect)". The model incorporating the solvent effect shows a large improvement when compared to the model without solvent effects. Also, due to a decrease in the system stiffness, the simulator proceeded further along the reaction. The discontinuity in both curves corresponds to the transition where VAc becomes more dominant.

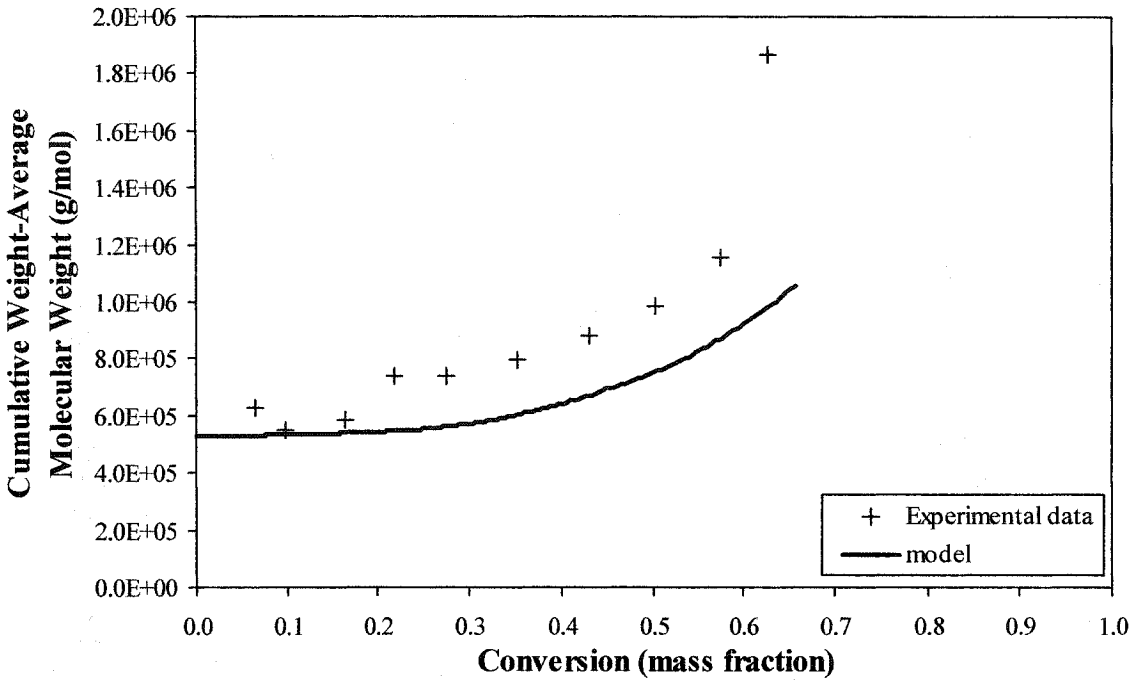

Figure 6.6: Cumulative weight-average molecular weight versus conversion for BA/MMA/VAc at 50°C in bulk.

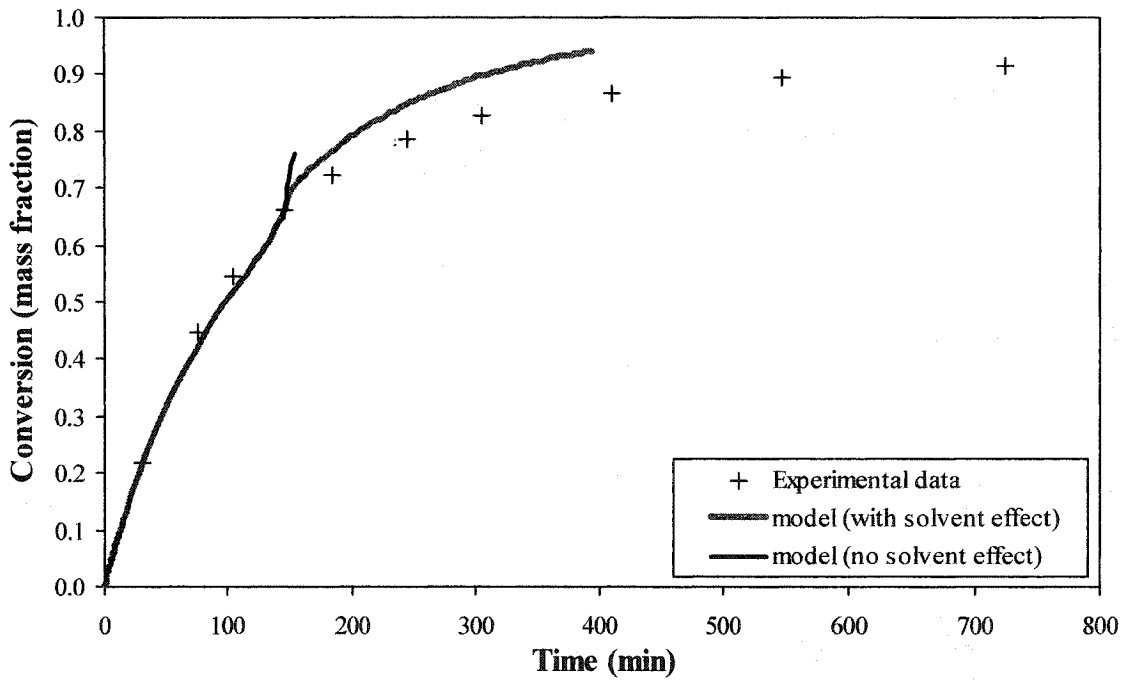

Figure 6.7: Conversion versus time for BA/MMA/VAc at 70°C in 40 wt.% toluene.

The model with solvent effect showed excellent agreement with the cumulative terpolymer compositions shown in Figure 6.8. However, there was no indication of a solvent effect on composition since both model predictions were overlapping.

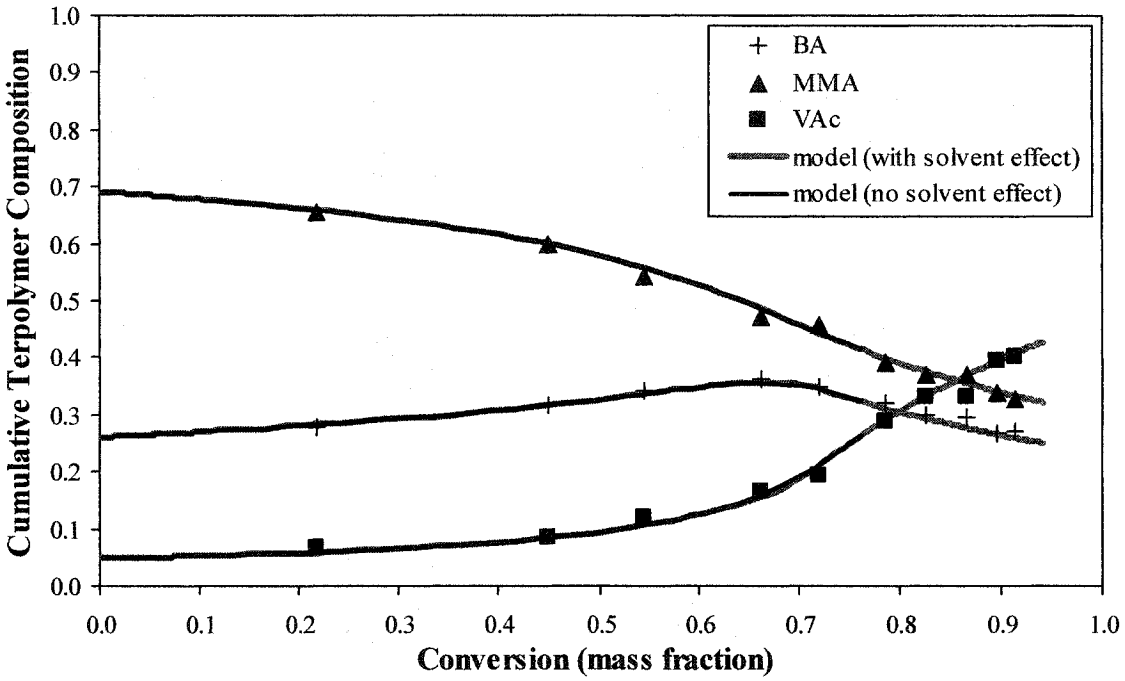

Figure 6.8: Cumulative terpolymer composition versus conversion for BA/MMA/VAc at 70°C in 40 wt.% toluene.

As shown in Figure 6.9, the two $\overline{M}_w$ model predictions were significantly different beyond the 65% conversion mark. The model accounting for the solvent effect shows better agreement. At the end of the reaction, the model remained low, which is typical of a solution polymerization.

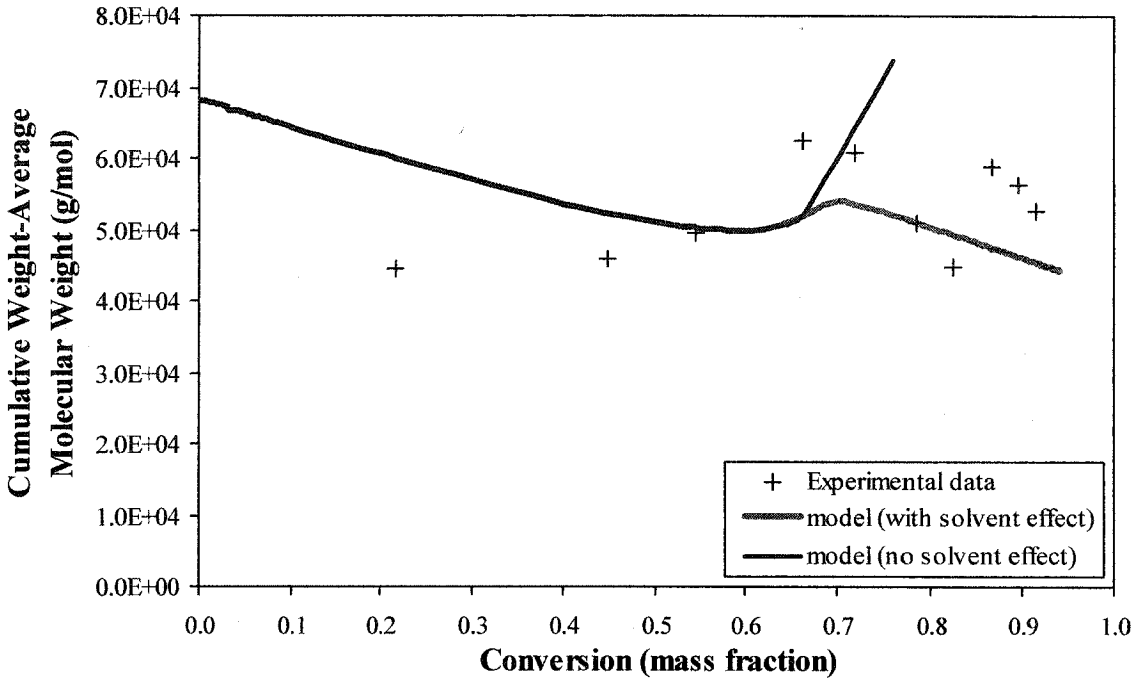

Figure 6.9: Cumulative weight-average molecular weight versus conversion for BA/MMA/VAc at 70°C in 40 wt.% toluene.

References

99. Gao, J.; Penlidis, A. *J. Macromol. Sci. – Rev. Macromol. Chem. Phys.*, **C38**(4), 651 (1998).

100. Gao, J.; Penlidis, A. *Macromol. Chem. Phys.*, **201**(11), 1176 (2000).

101. Dubé, M.A.; Penlidis, A. *Polymer*, **36**(3), 587 (1995).

102. Dubé, M.A.; Penlidis, A. *Macromol. Chem. Phys.*, **196**, 1101 (1995).

103. McManus, N.T.; Dubé, M. A.; Penlidis, A. *Polym. React. Eng.*, **7**(1), 131.

104. Scorah, M.J.; Hua, H.; Dubé, M.A. *J. Appl. Polym.*, **82**, 1238 (2001).

Chapter 7: Conclusions and Recommendations

A Java™-based simulator was programmed in order to model free-radical bulk and solution homopolymerizations, as well as multi-component polymerizations. The simulator was designed to provide the user with flexibility and many options, including the choice of several glass transition temperature models, and the use of the penultimate model. Once the simulator was proven to function properly, it was used to model three systems: butyl acrylate/vinyl acetate (BA/VAc), styrene/butyl acrylate (Sty/BA), and butyl acrylate/methyl methacrylate/vinyl acetate (BA/MMA/VAc).

7.1 Paper 1

The solvent effect on free-radical polymerizations has been the object of many studies, and there are still no universal models to account for the effect. In addition, few of these studies have focussed on BA and VAc. In this thesis, the solvent effect of toluene on the BA and VAc homopolymerizations and copolymerization was investigated. The simulator was run against data that were collected at different solvent concentrations, as well as at a variety of BA:VAc ratios in the case of the BA/VAc copolymer. The solvent effect was investigated by varying the lumped kinetic constant, $k_p/k_t^{0.5}$. The lumped kinetic constant showed a decrease with an increase in toluene concentration, resulting in significant improvements in predicting conversion data, confirming the presence of a solvent effect on the termination reaction. Preliminary results also indicate the possible presence of solvent effects on monomer reactivity ratios. There appears to be a solvent effect on both the propagation and termination reactions, but further runs should be conducted to elucidate the solvent effect.

More specifically, reactivity ratio estimation experiments should be conducted to investigate the solvent effect on the propagation reaction for the BA/VAc copolymer system. The preliminary study described in Chapter 4 suggests the presence of a small, yet perhaps significant, solvent effect on the reactivity ratios.

Improvements to the cumulative weight-average molecular weight predictions are addressed in section 7.4.

7.2 Paper 2

For the styrene and butyl acrylate system, experimental homo- and copolymerization data were well predicted by the simulator. Unlike the conversion and cumulative copolymer composition data, which were not significantly affected by the varying amount of solvent, the cumulative weight-average molecular weight decreased with an increase in solvent concentration. An increase in the Sty:BA ratio resulted in an increase in the cumulative copolymer composition, and a decrease in the conversion. Cumulative weight-average molecular weight data were inconsistent, but seemed to indicate a slight decrease in $\overline{M}_w$ values with a corresponding increase in the Sty:BA ratio. Improvements to the $\overline{M}_w$ predictions are addressed in section 7.4.

The glass transition temperature (T_g) model study was inclusive because the amount of solvent present in the reaction mixture proved to be too large to allow diffusion control to occur fully. To better compare the copolymer T_g, the reaction conditions should be changed. Smaller quantities of solvent should be used, or the runs could be conducted in bulk. Another alternative would be to allow the reaction to continue for a much longer period.

The glass transition of a polymer takes place over a small range, rather than a specific temperature, partly due to the dependence of T_g on the polymer chain length. In this study, this effect is deemed to be negligible; however, this could be a factor for future study.

7.3 BA/MMA/VAc terpolymerization

The MMA/VAc copolymerization was examined, followed by the BA/MMA/VAc terpolymerization. Both systems behaved similarly in that a double rate phenomenon was observed. At low conversions for the terpolymerization, there was a virtual solution copolymerization of BA and MMA monomers, with the vinyl acetate acting as the solvent. After the near depletion of the acrylic monomers, the remaining vinyl acetate polymerized and exhibited its own auto-acceleration. The homopolymer database, as well as the copolymerization reactivity ratios, provided good model predictions.

The simulator showed good agreement with the experimental data at low conversions, but it was unable to continue once the auto-acceleration began. The ODE solver was unable to cope with the excessive stiffness of the system. An alternative is proposed in section 7.5.1.

7.4 Molecular weight predictions

Additional experimental runs need to be carried out to obtain more accurate transfer rate constants, especially in the case of transfer to solvent and to chain transfer agent (CTA). This set of runs should be designed so that the rate constant for transfer to monomer is first well defined, i.e. no solvent or CTA in the reaction mixture. Then, separate runs, each using solvent and CTA individually, should follow. This approach will reduce the number of simultaneous parameters to be defined. Along with parameter estimation, experiments designed to obtain more accurate values for the chain transfer parameters would likely allow better model predictions of the $\overline{M}_w$ data.

The polymer is assumed to be linear. In some systems, transfer to polymer is possible, which would result in branching. If branching did occur along the polymer backbone, $\overline{M}_w$ values would be offset. The addition of the appropriate equations[105] to the model would allow the simulator to account for polymer branching, and perhaps result in better fits to the $\overline{M}_w$ data.

7.5 Simulator

7.5.1 Simulator speed

Simulation running times were found to vary considerably, depending on the monomer system and the simulation settings. Using the simplest of conditions, simulations could run in the range of 10-20 seconds. Since most of the simulation time is spent on converging to a stable solution by the ODE solver, adding more ingredients to the reaction mixture increased the running time because each ingredient provides its own ODE. Also, a more viscous reaction medium resulted in earlier diffusion-controlled

kinetics. Therefore, the addition of solvent, which decreases the viscosity of the medium, decreases the running time, despite adding a corresponding ODE. In the more viscous cases, with more ingredients, simulation times could reach 30 minutes. And in extreme cases, such as systems containing MMA/VAc, the `Stifbs` ODE solver was unable to converge to a solution. It should be noted that the simulation running time is also dependent on the computer speed.

As mentioned in section 2.4.3, the major drawback in using Java™ is its performance. Throughout the development of the simulator, many changes were made to accelerate the progress of simulations. With more knowledge of Java™ and its intricacies, perhaps further shortcuts could be implemented.

Because polymerizations typically exhibit numerical stiffness, many iterations are required for the ODE solver to converge to a stable solution. Therefore, using a different ODE solver, one which minimizes the number of iterations, can significantly reduce the computation time. From a theoretical point of view, the VODE solver shows promise.

VODE was developed at the Lawrence Livermore National Laboratory in the early 1990s. It comes from a family of ODE solvers written in the FORTRAN programming language, which started in the early 1970s with the GEAR package.[106] It was observed that the GEAR solver was unable to function with certain chemical kinetics problems that have frequent and abrupt time variations. The EPISODE solver was then developed, which used a variable-coefficient form of the BDF method. Major changes included the coefficient evaluation and the estimation and control of the local error. VODE is an extension of the EPISODE solver, which provides some minor (yet important) internal improvements, as well as a standardized format

The solution methods included in VODE are multi-step methods, which means they use information from previous steps in performing the numerical integration. Starting with user-defined initial conditions, ODEs are replaced with difference equations, and solved step by step. The VODE solver uses the implicit Adams-Moulton method in the non-stiff case, and the backwards differentiation formula in the stiff case. In both cases, the maximum order is limited by stability characteristics.

In both cases, a predictor-corrector scheme is applied. An explicit Adams-Bashforth method is used as a predictor, which generates initial estimates of the solution.

Following the predictor step, either implicit method corrects the initial guess iteratively using a Newton-Raphson iteration technique until convergence, providing a reasonable approximation to the true solution.

The BDF method exhibits stiff stability[107], meaning that its step size is not constrained to small values once the rapid components are negligible. The step size is only restricted by the accuracy imposed by the numerical solution. To satisfy accuracy requirements, the BDF method uses small step sizes in regions where the most rapid exponentials are active, but outside these regions, larger step sizes may be used.

In both the non-stiff and stiff cases, the methods used in VODE allow the step size and the order to vary throughout the integration. These are key features in the efficient use of linear multi-step methods.

The reader is referred to [108] for a detailed mathematical description of the methods used in LSODE (a relative of VODE), and [109] for details on the new features incorporated by VODE.

It is important to note than under some peripheral conditions, the `Stifbs` solver was unable to converge to a solution. Due to the nature of the VODE solver, it is believed that VODE would be more stable in extreme conditions, e.g. when the polymerization is highly diffusion-controlled.

7.5.2 Sensitivity analysis

Once a model has been proposed to describe certain polymer properties, the unknown parameters can be estimated by fitting the model to the data. However, lack of information about the precision of the parameter estimates can lead to erroneous conclusions. Conducting a sensitivity analysis is therefore important to determine which model parameters are more sensitive to small fluctuations in the process variables. A highly sensitive parameter will cause the response to fluctuate greatly even when subjected to small process variations. Thus, results of a sensitivity analysis will help guide the researcher in conducting optimal experiments that could yield the most information about the process with minimal effort.

7.5.3 Simulator interface

Although steps were taken to document the running procedure properly, several changes would be useful in making the simulator more user-friendly. The entire simulator should be prepared into an executable file. It is more straightforward to click a file rather than open a DOS window and type commands. Also, the use of Windows instead of DOS as the interface would further simplify interactions with the simulator, rendering it more intuitive. Database manipulations, simulation progress, inputs and outputs could all be controlled through Windows-based interfaces.

References

105. Dubé, M.A.; Soares, J.B.P.; Penlidis, A.; Hamielec, A.E. *Ind. Eng. Chem. Res.*, **36**(4), 966 (1997).
106. Hindmarsh, A.C. Lawrence Livermore National Laboratory Report UCID-30001, Rev. 3, December 1974.
107. Gear, C.W. *Numerical Initial Value Problems in Ordinary Differential Equations*, Prentice Hall, Englewood Cliffs (NJ), 1971.
108. Radhakrishnan, K.; Hindmarsh, A.C. *Description and Use of LSODE, the Livermore Solver for Ordinary Differential Equations*, Lawrence Livermore National Laboratory, Report UCRL-ID-113855, 1993.
109. Brown, P.N.; Byrne, G.D.; Hindmarsh, A.C. *VODE, SIAM Journal on Scientific and Statistical Computing*, **10**(5), 1038 (1989).

Appendix A: Component Database

Following are the databases for various components. It should be noted that only the components used are listed. The actual databases, each in their respective TXT file, contain more components.

Table A.1: Physical properties of the polymers studied

	poly BA	poly MMA	poly Sty	poly VAc	
MW_i	1.2817E+02	1.0012E+02	1.0412E+02	8.6090E+01	g/mol
A_i	1.2120E+00	1.1950E+00	1.0840E+00	1.2145E+00	g/cm^3
B_i	8.4500E-04	3.3000E-04	6.0500E-04	8.7493E-04	g/cm^3 °C
$C_{p,i}$	4.0000E-01	4.0000E-01	4.0000E-01	3.1810E-01	cal/(g K)
$T_{g,i}$	2.1800E+02	3.8700E+02	3.7800E+02	3.0300E+02	K
$V_{F,0,i}$	2.5000E-02	2.5000E-02	2.5000E-02	2.5000E-02	L
α_i	4.8000E-04	4.8000E-04	4.8000E-04	4.8000E-04	L/K
$k_{fP,ij}$ (pre-exp.)	0.0000E+00	0.0000E+00	0.0000E+00	4.2549E+06	L/(mol min)
$k_{fP,ij}$ (act. en.)	0.0000E+00	0.0000E+00	0.0000E+00	8.9470E+03	cal/mol

Table A.2: Physical properties of the initiators studied

	AIBN	BPO	
MW_i	1.6421E+02	2.4223E+02	g/mol
A_i	0.0000E+00	0.0000E+00	g/cm^3
B_i	0.0000E+00	0.0000E+00	g/cm^3 °C
$C_{p,i}$	0.0000E+00	0.0000E+00	cal/(g K)
$k_{d,i}$ (pre-exp.)	6.2300E+16	6.4290E+15	L/(mol min)
$k_{d,i}$ (act. en.)	3.0704E+04	3.0100E+04	cal/mol
$eff_{0,i}$ (pre-exp.)	2.4700E-02	7.5000E-01	—
$eff_{0,i}$ (act. en.)	-2.1660E+03	0.0000E+00	cal/mol
$V_{F,crit,f,i}$ (pre-exp.)	6.3654E-01	1.5000E-01	L
$V_{F,crit,f,i}$ (act. en.)	1.3688E+03	0.0000E+00	cal/mol
C	6.8500E-01	2.5000E-01	L
$k_{f,P,ij}$ (pre-exp.)	0.0000E+00	0.0000E+00	L/(mol min)
$k_{f,P,ij}$ (act. en.)	0.0000E+00	0.0000E+00	cal/mol

Table A.3: Physical properties of the monomers studied

	BA	MMA	Sty	VAc	
MW_i	1.2817E+02	1.0012E+02	1.0412E+02	8.6090E+01	g/mol
A_i	9.1910E-01	9.6647E-01	9.2400E-01	9.5741E-01	g/cm^3
B_i	1.0120E-03	1.1640E-03	9.1800E-04	1.2713E-03	g/cm^3 °C
$C_{p,i}$	4.3000E-01	4.1110E-01	4.3000E-01	4.7160E-01	cal/(g K)
$k_{p,0,ij}$ (pre-exp.)	1.6646E+11	2.9520E+07	1.3020E+09	7.8000E+10	L/(mol min)
$k_{p,0,ij}$ (act. en.)	9.6300E+03	4.3530E+03	7.7592E+03	8.4035E+03	cal/mol
$\Delta H_{p,i}$	-1.8400E+04	-1.3810E+04	-1.7000E+04	-2.0895E+04	cal/mol
$T_{g,i}$	1.8515E+02	1.6710E+02	1.8500E+02	1.0915E+02	K
$V_{F,crit,p,j}$ (pre-exp.)	1.0000E-02	7.4080E-01	3.1105E-01	6.0000E-02	L
$V_{F,crit,p,j}$ (act. en.)	1.4436E+03	1.5896E+03	1.6718E+03	0.0000E+00	cal/mol
$V_{F,0,i}$	2.5000E-02	2.5000E-02	2.5000E-02	2.5000E-02	L
α_i	1.0000E-03	1.0000E-03	1.0000E-03	1.0000E-03	L/K
$k_{t,0,ij}$ (pre-exp.)	7.0000E+07	5.8800E+09	4.9200E+11	9.8400E+11	L/(mol min)
$k_{t,0,ij}$ (act. en.)	8.7300E+02	7.0100E+02	3.4713E+03	3.4014E+03	cal/mol
γ (pre-exp.)	7.0000E-01	1.6093E+00	0.0000E+00	0.0000E+00	—
γ (act. en.)	0.0000E+00	4.4013E+02	0.0000E+00	0.0000E+00	cal/mol
B_j	5.0000E-01	1.0000E+00	1.0000E+00	1.0000E+00	—
δ	1.0000E-03	1.0000E-03	1.0000E-03	1.0000E-03	L/g
$n_{M\,in\,P} = j_c$	2.0000E+02	4.7000E+01	1.7400E+02	1.0000E+02	—
$l_0 = a$	6.5400E-09	6.9000E-09	7.4000E-09	7.5000E-09	dm
σ	6.2000E-09	5.8500E-09	6.5000E-09	6.0000E-09	dm
K_3^* (pre-exp.)	2.0000E-02	5.6300E-01	9.4400E+00	5.0000E-01	L/(mol min)
K_3^* (act. en.)	-1.2109E+04	-8.9000E+03	-3.8329E+03	-7.0656E+03	cal/mol
m	5.0000E-01	5.0000E-01	5.0000E-01	5.0000E-01	—
n	1.7500E+00	1.7500E+00	1.7500E+00	1.7500E+00	—
A	1.3100E+00	1.1100E+00	3.4800E-01	8.0000E-01	—
$k_{f,M,ij}$ (pre-exp.)	9.3436E+05	9.3435E+04	6.5789E+08	1.1170E+07	L/(mol min)
$k_{f,M,ij}$ (act. en.)	7.4751E+03	7.4751E+03	1.3427E+04	9.8950E+03	cal/mol
$k_{ptdb,ij}$ (pre-exp.)	0.0000E+00	0.0000E+00	0.0000E+00	2.7289E+07	L/(mol min)
$k_{ptdb,ij}$ (act. en.)	0.0000E+00	0.0000E+00	0.0000E+00	5.5099E+03	cal/mol
$k_{pidb,ij}$ (pre-exp.)	0.0000E+00	0.0000E+00	0.0000E+00	0.0000E+00	L/(mol min)
$k_{pidb,ij}$ (act. en.)	0.0000E+00	0.0000E+00	0.0000E+00	0.0000E+00	cal/mol

Table A.4: Physical properties of the solvents studied

	benzene	toluene	
MW_i	7.8120E+01	9.2140E+01	g/mol
A_i	8.7600E-01	8.8300E-01	g/cm^3
B_i	0.0000E+00	9.1600E-04	g/cm^3 °C
$C_{p,i}$	4.1470E-01	4.0480E-01	cal/(g K)
$T_{g,i}$	1.7100E+02	1.1300E+02	K
$V_{F,0,i}$	2.5000E-02	2.5000E-02	L
α_i	1.0000E-03	1.0000E-03	L/K
$k_{f,S,ij}$ (pre-exp.)	2.9800E+10	1.2368E+07	L/(mol min)
$k_{f,S,ij}$ (act. en.)	1.5753E+04	1.1408E+04	cal/mol

Table A.5: Physical properties of the CTA studied

	n-dodecyl mercaptan	
MW_i	2.0200E+02	g/mol
A_i	0.0000E+00	g/cm^3
B_i	0.0000E+00	g/cm^3 °C
$C_{p,i}$	0.0000E+00	cal/(g K)
$k_{f,CTA,ij}$ (pre-exp.)	2.7181E+12	L/(mol min)
$k_{f,CTA,ij}$ (act. en.)	1.2976E+04	cal/mol

Table A.6: Cross-termination factor [—] between radicals ending in monomer *i* and monomer *j*

i \ *j*	BA	MMA	Sty	VAc
BA	1	0	30	0
MMA	0	1	14	0
Sty	30	14	1	1
VAc	0	0	1	1

Table A.7: Glass transition temperature of the alternating copolymer [K]

i \ *j*	BA	MMA	Sty	VAc
BA	218	350	291	350
MMA	350	387	363	355
Sty	291	363	378	355
VAc	350	355	355	303

Appendix B: Source Code

The complete source code developed for the polymerization simulator can be obtained by request to:

Dr. Marc A. Dubé
Dept. of Chemical Engineering, University of Ottawa